

Dissertation zur Erlangung des Doktorgrades
der Fakultät für Chemie und Pharmazie
der Ludwig-Maximilians-Universität München



**Novel mechanisms of flavopiridol:
protection against inflammation-induced endothelium-leukocyte
interactions *in vivo* and *in vitro***

Erklärung:

Diese Dissertation wurde im Sinne von §13 Abs. 3 bzw. 4 der Promotionsordnung vom 29. Januar 1998 von Frau Prof. Dr. Angelika M. Vollmar betreut.

Ehrenwörtliche Versicherung:

Diese Dissertation wurde selbstständig, ohne unerlaubte Hilfe erarbeitet.

München, 20. Mai 2010

Ulrike Schmerwitz

Dissertation eingereicht am: 20. Mai 2010

1. Gutachter: Frau Prof. Dr. Angelika M. Vollmar

2. Gutachter: Herr Prof. Dr. Christian Wahl-Schott

Mündliche Prüfung am: 28. Juni 2010

dedicated to my family

1 Contents

1	Contents	I
2	Introduction	1
2.1	Background and aim of the study	2
2.2	Inflammation.....	4
2.2.1	The endothelium	4
2.2.2	Leukocytes	5
2.2.3	Leukocyte-endothelial cell interactions.....	6
2.2.4	The selectin family.....	8
2.2.5	Integrins and the immunoglobulin (Ig) superfamily of CAMs	8
2.2.6	Regulation of VCAM-1 and ICAM-1	8
2.2.7	The nuclear factor-kappa B (NF- κ B) transcription factor	9
2.2.8	The NF- κ B signaling pathway	10
2.3	Cyclin dependent kinases	12
2.3.1	Cell cycle Cdks.....	12
2.3.2	Transcriptional Cdks.....	13
2.4	The Cdk9-cyclin T1 complex.....	14
2.4.1	Function of the P-TEFb complex.....	15
2.5	Cyclin dependent kinase inhibitors.....	16
2.5.1	Flavopiridol (Alvocidib)	16
2.5.2	Flavopiridol in clinical trials.....	18
2.6	Cdk inhibitors as anti-inflammatory approach	18
3	Materials and Methods.....	20
3.1	Materials	21
3.1.1	Flavopiridol.....	21
3.1.2	Biochemicals, inhibitors, dyes, and cell culture reagents	21
3.1.3	Technical equipment	23
3.2	Cell culture	24
3.2.1	Isolation and cultivation of human umbilical vein endothelial cells	24

3.2.2	Isolation and cultivation of neutrophils.....	25
3.3	Cytotoxicity assays.....	26
3.3.1	CellTiter-Blue™ cell viability assay	26
3.3.2	Quantification of DNA fragmentation by PI staining (Nicoletti method)	26
3.4	Concanavalin A-induced liver injury model.....	28
3.4.1	Procedures.....	28
3.4.2	Hematoxylin and eosin (H&E) staining	28
3.4.3	Granulocyte staining.....	28
3.4.4	Myeloperoxidase (MPO) activity.....	29
3.5	Cremaster muscle preparation and intravital microscopy	29
3.5.1	Surgical procedure	29
3.5.2	Intravital microscopy.....	30
3.6	Cell adhesion assay.....	30
3.7	Flow cytometry.....	31
3.7.1	Determination of cell surface expression of adhesion molecules	31
3.7.2	Determination of cell surface expression of CD11b	31
3.7.3	Determination of oxidative stress in neutrophils	31
3.8	Quantitative RT-PCR.....	32
3.8.1	Isolation of RNA of tissue sections.....	32
3.8.2	Isolation of RNA of HUVECs	32
3.8.3	Reverse transcription	33
3.8.4	Quantitative Real-Time PCR	33
3.9	Immunocytochemistry.....	34
3.10	Western blot analysis	35
3.10.1	Preparation of samples	35
3.10.2	Protein quantification: bicinchoninic protein assay	36
3.10.3	SDS-PAGE.....	36
3.10.4	Electroblotting	37
3.10.5	Protein detection	38
3.10.6	Unspecific protein staining of gels and membranes	39
3.11	Transfer of nucleic acids into HUVECs.....	40

3.11.1	Transfection of siRNA	40
3.11.2	Experimental procedure	41
3.11.3	Application of shRNA via adenoviral vectors.....	41
3.11.4	Dual Luciferase [®] Reporter assay system	41
3.12	Electrophoretic mobility shift assay.....	42
3.12.1	Extraction of nuclear proteins.....	42
3.12.2	Protein quantification: Bradford assay.....	43
3.12.3	Electrophoretic Mobility Shift Assay	43
3.13	<i>In vitro</i> IKKβ kinase activity assay	44
3.14	Kinome array (PepChip)	45
3.15	Protein Kinase Assay (³³PanQinase[®] Activity Assay).....	45
3.16	Statistical Analysis	46
4	Results	47
4.1	Anti-inflammatory effects of flavopiridol <i>in vivo</i>.....	48
4.1.1	Concanavalin A-induced liver injury model.....	48
4.1.1.1	Flavopiridol protects against concanavalin A-induced liver injury	48
4.1.1.2	Liver necrosis is reduced by flavopiridol	49
4.1.1.3	Flavopiridol inhibits the infiltration of neutrophils into the liver	50
4.1.1.4	Flavopiridol reduces levels of ICAM-1 and E-selectin in the liver	51
4.1.2	Cremaster muscle model	52
4.1.2.1	Flavopiridol reduces leukocyte-endothelium interactions <i>in vivo</i>	52
4.1.2.2	Microvascular parameters in cremaster muscle venules	53
4.1.2.3	Motility of interstitially migrating leukocytes	54
4.1.2.4	Flavopiridol inhibits ICAM-1 expression in cremaster muscle tissue ...	55
4.2	Cell viability and apoptosis.....	56
4.2.1	Effects of flavopiridol on endothelial cell viability	56
4.2.2	Effects of flavopiridol on apoptosis	57
4.3	Anti-inflammatory actions of flavopiridol <i>in vitro</i>	58
4.3.1	Flavopiridol reduces neutrophil-endothelium interactions.....	58
4.3.2	Influence of flavopiridol on leukocyte activation	59
4.3.3	Flavopiridol reduces the expression of cell adhesion molecules	60

4.4	Effects of flavopiridol on NF-κB signaling	62
4.4.1	Flavopiridol reduces NF- κ B promoter activity.....	62
4.4.2	Flavopiridol has no effect on IKK α/β and I κ B α	63
4.4.3	Flavopiridol has no influence on p65.....	64
4.5	Analysis of kinome alterations by flavopiridol	66
4.5.1	The influence of LIMK1, JNK, CK2 and PKC θ on ICAM-1 expression	67
4.6	Involvement of Cdks in inflammatory events	69
4.6.1	IC ₅₀ profiling of flavopiridol	69
4.6.2	Effect of a specific Cdk4/6 inhibitor on ICAM-1	70
4.6.3	ICAM-1 expression in the absence of Cdk8	71
4.6.4	The loss of Cdk9 has a strong effect on ICAM-1 expression.....	72
5	Discussion	73
5.1	Flavopiridol protects against inflammatory actions	74
5.1.1	The impact of flavopiridol on concanavalin A induced liver injury.....	74
5.1.2	Flavopiridol reduces leukocyte-endothelium interactions <i>in vivo</i>	75
5.1.3	Flavopiridol reduces leukocyte-endothelium interactions <i>in vitro</i>	75
5.2	The underlying mechanisms of the anti-inflammatory properties of flavopiridol	77
5.2.1	Flavopiridol has no effect on the NF- κ B activation cascade.....	77
5.2.2	Flavopiridol affects LIMK1, CK2, JNK, and PKC θ	78
5.2.3	LIMK1, CK2, JNK, and PKC θ do not influence inflammatory actions	79
5.3	Cdks in inflammation-induced processes	80
5.3.1	Cdk4 and 6 in inflammation-induced processes.....	81
5.3.2	Cdk8 in inflammation-induced processes.....	81
5.3.3	The importance of Cdk9 in inflammation	81
5.3.4	Complexity of gene regulatory network: P-TEFb and NF- κ B.....	82
5.4	Conclusion	83
6	Summary	84
7	References	87

8	Appendix.....	97
8.1	Abbreviations	98
8.2	Publications.....	101
8.2.1	Original publication.....	101
8.2.2	Oral communication	101
8.3	Curriculum vitae.....	102
8.4	Acknowledgements	103

2 Introduction

2.1 Background and aim of the study

The endothelium functions as the barrier between blood and tissue and thus regulates blood cell trafficking and plays an important role in vascular homeostasis (1). Therefore, the loss of proper endothelial function is associated with a number of pathological processes (2). The loss of proper endothelial function is related to an immense variety of diseases, including diabetes, hypertension, atherosclerosis, and other chronic inflammatory diseases. In acute and chronic inflammation, leukocyte-endothelial cell interactions are early and critical events.

An enormous issue is the repression of inflammation, therefore anti-inflammatory agents are extensively used clinically. However, anti-inflammatory compounds such as non-steroidal anti-inflammatory drugs (NSAIDs), corticosteroids and chemotherapeutic agents, are often characterized by limited efficacy and severe side-effects. Hence, there exists a great need for new targets and potent blockers of the inflammatory response (3).

Flavopiridol, a synthetic flavonoid, is a pan-specific cyclin dependent kinase (Cdk) inhibitor. Flavopiridol was the first Cdk inhibitor to undergo clinical trials (4) and in a panel of 60 human cancer cell lines flavopiridol was proven to be a potent inhibitor of cell growth (5, 6). Currently, flavopiridol is tested as single agent as well as in combination with other agents in numerous clinical trials as drug against hematologic and solid cancers (<http://www.clinicaltrials.gov>). In the ongoing clinical trials against cancer, flavopiridol shows good compliance with limited toxicities at plasma concentrations up to 10-fold higher than those necessary to inhibit cell cycle progression *in vitro* (7).

Recently, Cdk inhibitors were suggested to play relevant roles not only in cancer diseases but also in processes regarding immune response and inflammation. A few studies exist which suggest Cdk inhibitors as potential anti-inflammatory agents because of their ability to influence the apoptosis of neutrophils and therefore the resolution of inflammation (8, 9). It was reported, that flavopiridol was effective to inhibit synovial hyperplasia in collagen-induced arthritis in mice (10) and to suppress IL-6-inducible hepatic acute phase response proteins (11). Due to findings in cancer cell lines, where flavopiridol inhibited the activity of NF- κ B, a proinflammatory transcription factor, flavopiridol was suggested to might have an influence on inflammation (12).

Hitherto, no studies exist that focus on the impact of Cdk inhibitors in general and of flavopiridol in particular on the inflammation-activated endothelium.

Thus, it was the aim of the present work

- 1. to investigate the impact of flavopiridol on the interaction of leukocytes and the inflammation-activated endothelium *in vivo* and *in vitro* and**
- 2. to characterize the signaling mechanisms underlying the anti-inflammatory actions of flavopiridol**

2.2 Inflammation

Inflammation is part of the beneficial anti-microbial, immune defense system that has been honed and conserved by evolution over millions of years (13). Ideally, following prompt detection of a micro-organism by immune mechanisms, an inflammatory reaction should contain and destroy the organism before it multiplies, spreads, becomes established, or causes harm. Self-regulation and limitation are the key, final components of the response as the system must actively drive resolution of inflammation to restore tissue homeostasis (3). Nonresolution of inflammation can lead to atherosclerosis, obesity, cancer, chronic obstructive pulmonary disease, asthma, inflammatory bowel disease, or rheumatoid arthritis (14).

Because of the importance of deleterious inflammatory responses in human disease, anti-inflammatory agents are extensively used clinically. Early anti-inflammatory agents were used long before their targets were known, such as non-steroidal anti-inflammatory drugs (NSAIDs) as well as corticosteroids. More recently, successful anti-inflammatory agents were introduced whose targets were identified in advance, such as cytokines $\text{TNF}\alpha$ or $\text{IL-1}\beta$. However, anti-inflammatory agents have often limited efficacy and severe side-effects and, therefore, the extensive search for new anti-inflammatory agents possessing mechanisms of action different from those of marketed drugs holds on.

2.2.1 The endothelium

The endothelium is a thin monocellular layer that covers all the inner surface of the blood vessels with a surface area of approximately 350 m^2 . It separates the circulating blood from the tissues and is responsible for the exchange of materials between blood and tissues. Therefore, the endothelium is critically involved in vital functions of the cardiovascular system, including regulation of perfusion, fluid and solute exchange, homeostasis and coagulation, vasculogenesis, angiogenesis, and inflammatory responses. The endothelial lining of blood vessels in different organs differs with respect to morphology and permeability and is classified as 'continuous', 'fenestrated', or 'discontinuous'. Furthermore, the release of mediators, antigen presentation, or stress responses of endothelial cells varies between species, different organs and vessel classes. Excessive or prolonged increases in

permeability of the endothelial monolayer, as in cases of chronic inflammation, may lead to tissue edema/swelling. The loss of proper endothelial function, or endothelial dysfunction, respectively is a hallmark for vascular diseases (13, 15).

2.2.2 Leukocytes

Leukocytes are derived from hematopoietic stem cells and are distinguished in two main types: granulocytes and agranulocytes (Figure 2.1).

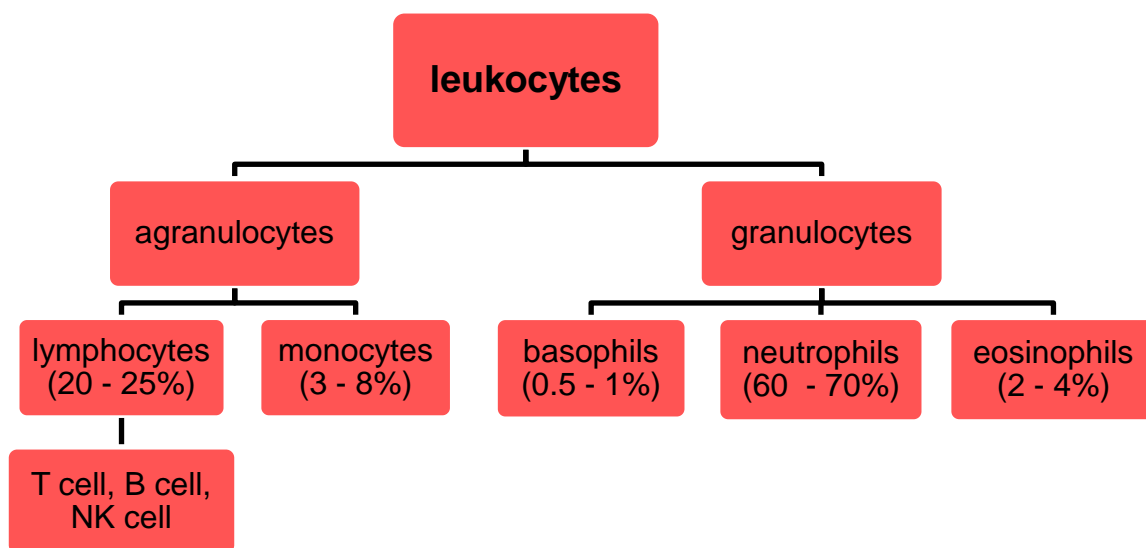


Figure 2.1: Types of leukocytes.

Granulocytes (polymorphonuclear leukocytes, PMNs) are eosinophils, basophils and neutrophils and are named for the numerous granules within their cytoplasm. Each of these granules contains a range of toxic products such as proteases, lysozyme, and lactoferrin (8). Basophils are responsible for allergic response (releasing histamine), while neutrophils and eosinophils are key players in the immune response against bacteria, fungi and parasites. They are attracted by and are believed to follow a concentration gradient of chemotactic stimuli released by invading pathogens or tissues under challenge. Neutrophils are recruited to the site of injury within minutes following trauma and are the hallmark of acute inflammation.

Agranulocytes (mononuclear leukocytes) include lymphocytes, monocytes and macrophages. Lymphocytes are common in the lymphatic system. There are three types of lymphocytes: B cells, T cells, and natural killer (NK) cells. Monocytes are important for antibody response and once monocytes move from the bloodstream out

into the body tissues, they differentiate allowing phagocytosis and become tissue macrophages.

Leukocytes contribute to the inflammatory response by secreting cytotoxic and pro-inflammatory compounds, by phagocytic activity, and by targeted attack on foreign agents.

2.2.3 Leukocyte-endothelial cell interactions

Interactions of leukocytes with endothelial cells are early events in immune surveillance of tissues, wound repair, and acute and chronic inflammation. Inflammatory responses in all tissue compartments require the emigration of leukocytes from the microvasculature through endothelial cells into the respective microenvironment (16). The leukocyte adhesion cascade to stimulated endothelial cells includes slow rolling, adhesion strengthening, intraluminal crawling, paracellular and transcellular migration, and migration through the basement membrane (Figure 2.2).

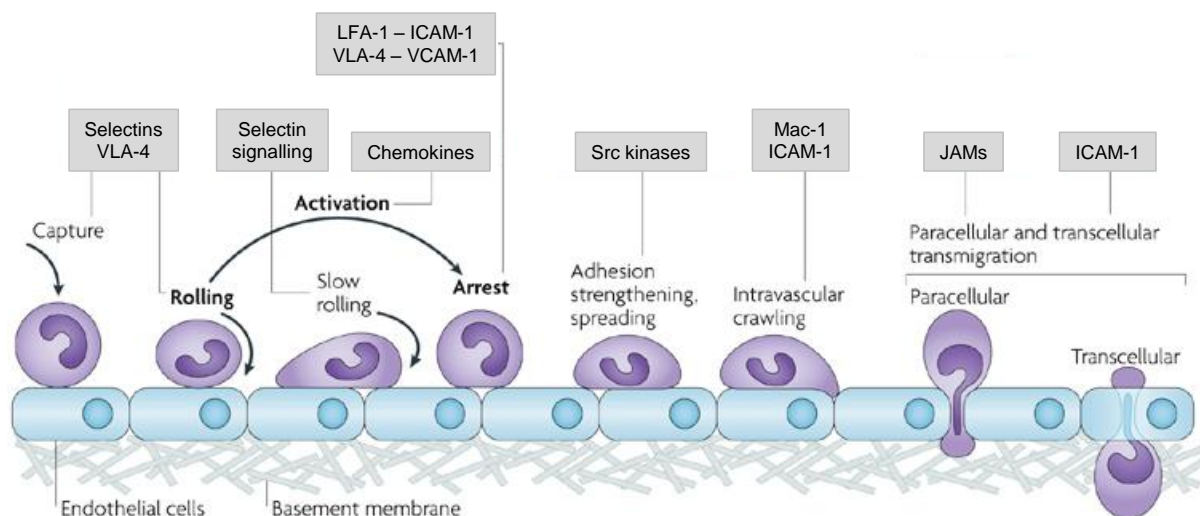


Figure 2.2: The leukocyte-endothelium adhesion cascade.

The initial interaction of leukocytes with the endothelium lining the vessel wall is termed tethering, and the subsequent rotational movement along the vessel wall is termed rolling. These events are dependent on the family of the selectins and their counterreceptors. Chemokines trigger leukocytes to adhere and activate integrins to mediate binding to immunoglobulin superfamily members resulting in arrest. Adhesion strengthening and intravascular crawling are two steps which ultimately contribute to efficient emigration out of the vasculature. Numerous proteins, including JAMs, ICAM-1, and other molecules, have been implicated in the final step, the emigration process, including paracellular and transcellular transmigration. Key molecules involved are ICAM-1, intercellular adhesion molecule 1; JAM, junctional adhesion molecule; LFA-1, lymphocyte function-associated antigen 1; Mac-1, macrophage antigen 1, VCAM-1, vascular cell-adhesion molecule 1, VLA-4, very late antigen 4. The image is adapted from Ley et al. (17).

The first contact between neutrophils and the endothelium of postcapillary venules is known as capture or tethering and is mediated by selectins and their counter receptors (17, 18). Selectin binding and the presentation of chemokines by endothelial cells induce activation of signaling pathways in neutrophils that cause changes in integrin conformation (inside-out signaling). The endothelium has an active role in the rolling of leukocytes. Integrins participate in slow rolling and mediate arrest, e.g. slow rolling of neutrophils along the wall of inflamed venules is mediated by the β 2-integrins, specifically LFA-1 and Mac-1 (19). *In vitro* and *in vivo* studies have established that leukocyte arrest during rolling is rapidly triggered by chemokines or other chemoattractants and is mediated by the binding of leukocyte integrins to immunoglobulin superfamily members, such as ICAM-1 and VCAM-1, expressed by endothelial cells (20, 21). The initial leukocyte-facilitated clustering of ICAM-1 requires Src-dependent phosphorylation of the actin-binding protein cortactin (22). Upon arrest, integrins bound to their ligands can signal into the neutrophil (outside-in signaling), stabilize the adhesion (postadhesion strengthening), activate different signaling pathways, and initiate transmigration. Transmigration through venular walls is the final step in the process of leukocyte emigration into inflamed tissues and can occur with minimal disruption to the complex structure of vessel walls. Some endothelial junctional molecules actively mediate leukocyte transendothelial migration, such as ICAM-1 and JAMs.

2.2.4 The selectin family

The selectin family of cell adhesion molecules (CAMs) consists of three members which all mediate rolling of leukocytes along the endothelium (23). P-selectin is stored in granules in endothelial cells and platelets and translocates rapidly to the cell surface in response to several inflammatory stimuli. E-selectin is present exclusively in endothelial cells and its expression is regulated by increased transcription after stimulation by inflammatory cytokines such as $\text{TNF}\alpha$ and $\text{IL-1}\beta$. The third selectin molecule L-selectin is expressed on many subclasses of leukocytes and is rapidly discarded from the surface of the leukocyte after activation (24).

2.2.5 Integrins and the immunoglobulin (Ig) superfamily of CAMs

Integrins are expressed constitutively on leukocytes and many other cell types. Integrins are activated rapidly from a low-affinity to a high-affinity state following cell activation and ligand binding. Integrins mediate adhesion of cells to matrix proteins, cellular counterreceptors and many other substrates (25, 26). The interaction between integrins and CAMs of the Ig superfamily is particularly important in inflammation. The Ig superfamily of CAMs consists of large proteins that are expressed on many different cell types, including endothelial cells where the expression of some of these molecules is upregulated by inflammatory cytokines. In leukocyte recruitment, interactions between $\beta 2$ integrins on the surface of leukocytes and ICAM-1 on endothelial cells are important mechanisms in leukocyte firm arrest on the endothelium and their transendothelial migration to sites of inflammation as well as their function as costimulatory molecules for T cell activation.

2.2.6 Regulation of VCAM-1 and ICAM-1

Intercellular adhesion molecule-1 (ICAM-1, CD54) and vascular cell adhesion molecule-1 (VCAM-1, CD106) are inducible cell adhesion glycoproteins of the immunoglobulin supergene family. VCAM-1 is not constitutively expressed in most tissues but is upregulated through de novo synthesis after stimulation with $\text{TNF}\alpha$ and $\text{IL-1}\beta$. ICAM-1 and VCAM-1 are involved in firm adhesion of leukocytes to the apical surface of endothelial cells through interactions with leukocyte CD11a/CD18 (LFA-1)

and/or CD11b/CD18 (Mac-1) and CD49a/CD29, respectively (22). VCAM-1 clustering has been observed in the steps leading to transmigration.

ICAM-1 is constitutively expressed on the cell surface and is overexpressed by proinflammatory mediators in a wide variety of cell types, including fibroblasts, leukocytes, endothelial cells, and epithelial cells (27). These stimuli increase ICAM-1 expression primarily through activation of ICAM-1 gene transcription. The architecture of the ICAM-1 promoter is complex (Figure 2.3), containing a large number of binding sites for inducible transcription factors, the most important of which is NF- κ B. NF- κ B acts in concert with other transcription factors or transcriptional coactivators which facilitate the assembly of distinct stereospecific transcription complexes on the ICAM-1 promoter. These transcription complexes presumably mediate the induction of ICAM-1 expression in different cell types and in response to different stimuli (28).

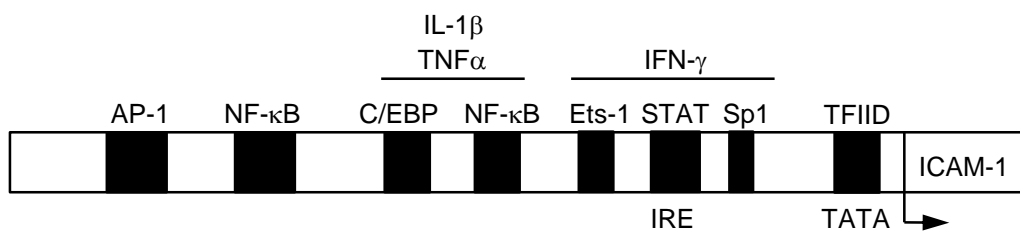


Figure 2.3: Schematic structure of the ICAM-1 promoter.

The ICAM-1 promoter contains a number of binding sites for inducible transcription factors (including NF- κ B, AP-1, Ets-1, C/EBP, Sp-1), that mediate various activation signals elicited at the cell surface. Upstream of each initiation site is a consensus TATA element that binds the general transcription factor IID (TFIID). The C/EBP site cooperates with the neighboring NF- κ B site to mediate the TNF α and IL-1 β induction of ICAM-1. The IFN- γ response is mediated by STAT binding to the IFN- γ response element (IRE).

2.2.7 The nuclear factor-kappa B (NF- κ B) transcription factor

The nuclear factor-kappa B (NF- κ B) transcription factor plays a critical role in diverse cellular processes associated with proliferation, apoptosis, inflammation, as well as innate and adaptive immune responses (29, 30). This pleiotropic transcription factor can be activated by a diverse spectrum of modulating stimuli, linking NF- κ B with an ever-increasing array of genetic targets (31).

The NF- κ B family of transcription factors consists of five members, p50, p52, p65 (RelA), c-Rel, and RelB. NF- κ B dimers bind to κ B sites within the promoters/enhancers of target genes and regulate transcription through the

recruitment of coactivators and corepressors. In untreated cells NF- κ B belongs to its inactive state where NF- κ B dimers are associated with one of three typical I κ B proteins, I κ B α , I κ B β , or I κ B ϵ , or the precursor proteins p100 and p105. These I κ Bs maintain NF- κ B dimers in the cytoplasm and are crucial for signal responsiveness. By contrast, in human cancers and leukemias NF- κ B is often constitutively activated (32).

2.2.8 The NF- κ B signaling pathway

NF- κ B is controlled by distinct regulatory pathways, the canonical, noncanonical and atypical pathways. The most frequently observed is the canonical, or classical pathway, which is induced in response to various inflammatory stimuli (Figure 2.4), the other pathways are induced by RNA virus infection or lymphokines.

In the canonical pathway, the IKKs, which form a complex composed of two catalytic subunits, IKK α and IKK β , and a regulatory subunit, IKK γ /NEMO, are responsible for activation of the NF- κ B transcription factor (33). Inducing stimuli trigger IKK activation by phosphorylating IKK α/β . Activated IKK β leads to phosphorylation, ubiquitylation, and degradation of I κ B α . I κ B α is rapidly degraded through the 26S proteasome, thereby freeing multiple NF- κ B dimers, although the p65:p50 heterodimer is likely the primary target of I κ B α . Phosphorylation of p65 on a number of Ser residues is required for transcriptional activation; Ser276 and Ser536 are thought to be the most important phosphorylation sites in regulating transcriptional activity. Inducible phosphorylation of p65 at Ser276 by protein kinase A (PKA) has been demonstrated to be crucial for NF- κ B transcriptional activity downstream of I κ B α degradation (34) and promotes the interaction of p65 with the transcriptional coactivators CBP (CREB-binding protein) and p300 (35). Released NF- κ B dimers are further activated through various posttranslational modifications and translocate to the nucleus where they bind to specific DNA sequences and promote transcription of target genes (36).

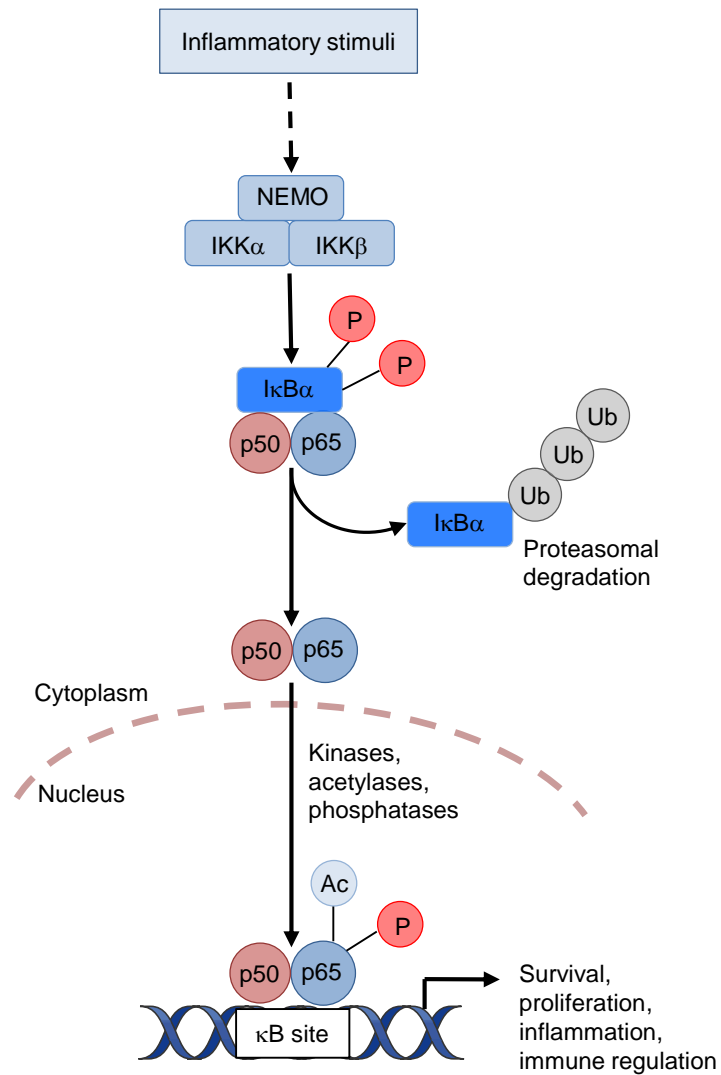


Figure 2.4: Relevant regulatory steps in the canonical NF- κ B pathway.

The canonical NF- κ B pathway is induced by inflammatory stimuli, such as TNF α , and is dependent on activation of IKK β . This activation results in the phosphorylation (P) of I κ B α at Ser32 and Ser36, leading to its ubiquitination (Ub) and subsequent degradation. Released NF- κ B dimers translocate to the nucleus and bind κ B sites in the promoters or enhancers of target genes, which leads to their transcription.

2.3 Cyclin dependent kinases

The cyclin dependent kinases (Cdks) are serine/threonine kinases and part of the diverse protein kinase family. They are essential facilitators of life at the molecular level via their ubiquitous phosphorylation reactions (37). The majority of Cdks identified rely on binding partners called cyclins for their activation. In all, there are 13 Cdks and 25 identified cyclins known so far and although there is a high level of sequence and structural homology between them, Cdks can be classified in two groups based on their roles in cell cycle, including Cdk1, Cdk2, Cdk3, Cdk4, Cdk6, and Cdk7 and those responsible for transcriptional regulation, including Cdk5, Cdk7, Cdk8, Cdk9, Cdk10, Cdk11, Cdk12, and Cdk13 (38, 39).

2.3.1 Cell cycle Cdks

The Cdks have been traditionally described as key regulators of the cell cycle, whereby different Cdks become activated during cell-cycle progression when complexed with their associated cyclin partners (39). Three interphase Cdks (Cdk2, Cdk4, and Cdk6), a mitotic Cdk (Cdk1), and ten cyclins that belong to four different classes (the A-, B-, D- and E-type cyclins) regulate the cell cycle (Figure 2.5).

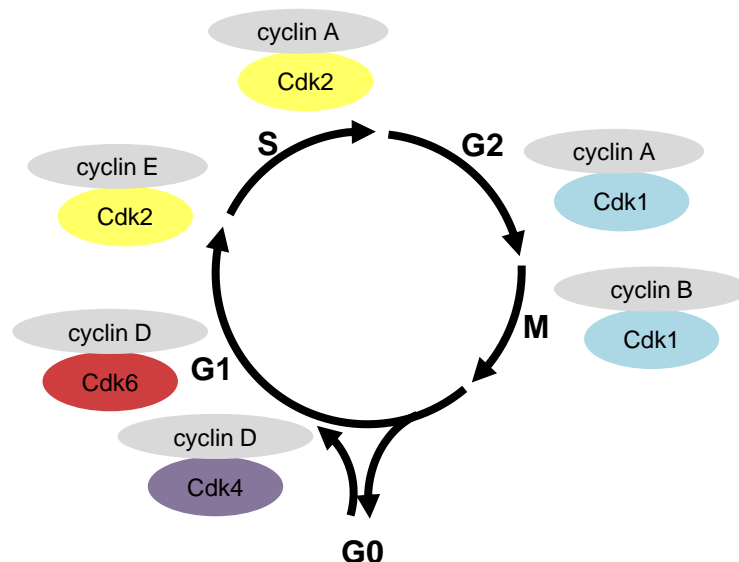


Figure 2.5: The stages of the cell cycle and the regulatory Cdk/cyclin complexes.

The transition from one cell cycle phase to another is regulated by different cellular proteins. Key regulatory proteins are the Cdks, which become activated at specific points of the cell cycle. Cdk4 and Cdk6 associated with cyclin D together with Cdk2 associated with cyclin E control G1 phase progression as well as G1/S transition. In early S phase, Cdk2/cyclin A complexes promote DNA replication and cell cycle progression, whereas cyclin A and cyclin B in complexes with Cdk1 control the G2/M transition. Cdk1 complexed with cyclin B drives cell division.

Apart from the binding to proper cyclin, Cdks undergo an activating phosphorylation by Cdk7/cyclin H also named CAK, Cdk-activating kinase (Figure 2.6). CAK itself is a trimeric complex consisting of the catalytic component Cdk7, a regulatory subunit cyclin H, and a RING finger assembly factor called ménage a trois (MAT1) (40, 41).

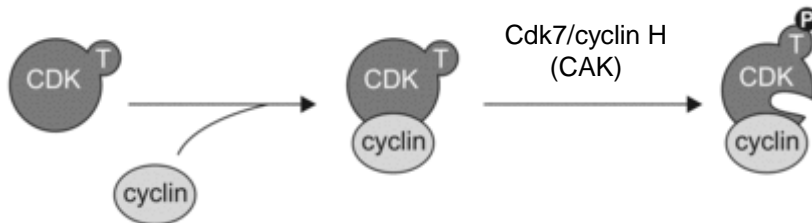


Figure 2.6: Function of CAK, Cdk activating kinase.

Activation of human Cdks is a multistep process. It starts with binding to cyclins, followed by specific phosphorylation (P) within the activation loop (T-loop) by Cdk7/cyclin H (CAK), which leads to uncovering of the active site. The image is adapted from Wesiersky and Gadek (42).

2.3.2 Transcriptional Cdks

Only a certain subset of Cdk-cyclin complexes is directly involved in driving the cell cycle. Cdk7 complexed with cyclin H provides a direct link between regulation of cell cycle and transcription because it is both CAK and a constituent of the basal transcription factor TFIIF. Transcriptional kinases, such as Cdk8 with cyclin C and Cdk9 with cyclin T, constitute a second nonoverlapping group of Cdks. The transcriptional Cdks promote initiation and elongation of nascent RNA transcripts by phosphorylation of the largest subunit of RNA polymerase II (Pol II) (42, 43). RNA Pol II is subjected to a tight control at various steps during the transcription cycle, including the recruitment of transcription preinitiation complex (PIC) to DNA, transcription initiation, promoter clearance, promoter-proximal pausing, elongation, termination, and re-initiation (44). In the process of gene activation, RNA Pol II is phosphorylated by the preinitiation complex subunit TFIIF at Ser5 within the carboxy terminal domain (CTD) coinciding with transcription initiation and promoter clearance (40, 45). Cdk9 is one of the major CTD kinases that phosphorylates RNA Pol II at Ser2 and signifies productive transcription elongation (Figure 2.7). Moreover, Cdk9 does not only phosphorylate CTD of RNA Pol II but also other proteins bound to the transcriptional complex. For example, the negative elongation factors NELF (negative elongation factor) and DRB-sensitivity inducing factor (DSIF), which repress transcriptional elongation, are phosphorylated and thus inactivated by Cdk9 (43).

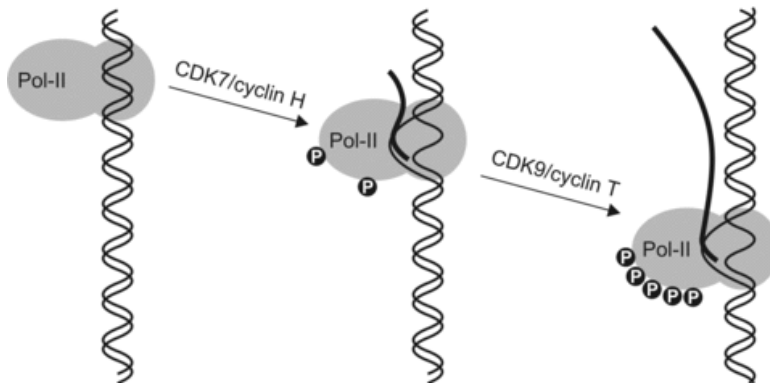


Figure 2.7: Phosphorylation of the C-terminal domain of the RNA polymerase II.

The C-terminal domain of the RNA polymerase II is hypophosphorylated when initially recruited to genes, and undergoes sequential phosphorylation at Ser5 by Cdk7/cyclin H and at Ser2 at Cdk9/cyclin T at the start of elongation. The image is adapted from Wesiersky and Gadek (42).

2.4 The Cdk9-cyclin T1 complex

Cdk9 associates with each of four cyclins (T1, T2a, T2b and K), forming distinct positive transcription elongation factors (P-TEFb). The majority of Cdk9 is complexed with cyclin T1 in nuclear speckles and a small fraction of Cdk9 is found in an apparently uncomplexed form in the cytoplasm. Studies have shown that nuclear P-TEFb exists in two functionally distinct complexes. Half of nuclear P-TEFb is found as an inactive complex associated with HEXIM1 and 7SK snRNA (46). Transcriptionally active P-TEFb associates with the bromodomain containing protein, Brd4 (Figure 2.8) (47).

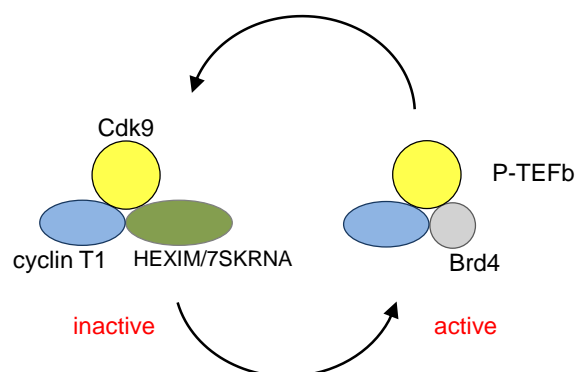


Figure 2.8: Nuclear states of P-TEFb in the resting cell.

Approximately half of nuclear P-TEFb is in inactive state associated with HEXIM1 and 7SK snRNA. The component that is actively involved in RNA Pol II dependent transcription is associated with Brd4.

2.4.1 Function of the P-TEFb complex

The P-TEFb complex is widely implicated in the control of basal gene expression, where it is involved in transitioning paused RNA Pol II to enter productive transcriptional elongation mode by phosphorylating Ser2 in the CTD of the RNA Pol II (Figure 2.7) (48). Moreover, P-TEFb integrates mRNA synthesis with histone modification, pre-mRNA processing, and mRNA export (49). P-TEFb function relies on Cdk9 protein kinase activity (50). RNA Pol II transcriptional regulation is an essential process for guiding eukaryotic gene expression. In complex organisms, elongation control is critical for the regulated expression of most genes. In those organisms, the function of P-TEFb is influenced negatively by HEXIM proteins and 7SK snRNA and positively by a variety of recruiting factors (51). P-TEFb is required for transcription of most genes, including heat shock and c-Myc genes and also promotes efficient transcription of the full-length HIV genome (52).

P-TEFb plays a key role in cellular activation, proliferation, and differentiation. Thus, it inherits a central role in normal and disease states. P-TEFb has recently been shown to be involved in cancers, AIDS, cardiac hypertrophy, and inflammation (53, 54).

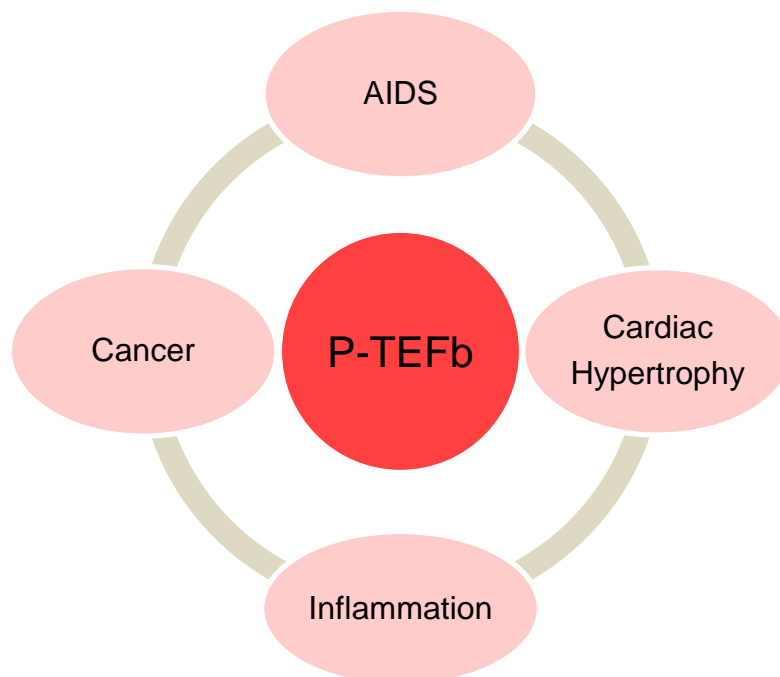


Figure 2.9: Role of P-TEFb in various diseases.

2.5 Cyclin dependent kinase inhibitors

The activity of Cdk-cyclin complexes is regulated by the phosphorylation of Cdks, and also by the association with the members of two endogenous inhibitor families (CKIs) (55, 56). The INK4 (inhibitor of Cdk4) family includes p16^{INK4a}, p15^{INK4b}, p18^{INK4c}, and p19^{INK4d}, which bind to and inhibit Cdk4 and Cdk6. The Cip/Kip families include p21^{CIP1}, p27^{KIP1} and p57^{KIP2}, which bind to all the Cdk-cyclin complexes and inhibit their activities (57). In malignant cells, altered expression of Cdks and their modulators, including overexpression of cyclins and loss of expression of Cdk inhibitors, results in deregulated Cdk activity, providing a selective growth advantage (58). Cell cycle deregulation is one of the first steps that transform normal cells into tumor cells. For this reason, targeting Cdks by specific inhibitors may slow growth or induce apoptosis. Because of their critical role in cell cycle progression and cellular transcription, as well as the association of their activities with apoptotic pathways, the Cdks comprise an attractive set of targets for novel anticancer drug development. The first generation of Cdk-cyclin inhibitors are low-molecular weight molecules, composed as ATP-competitive inhibitors, such as flavopiridol and roscovitine, which are currently involved in a large number of clinical trials (59). Further, the development of ATP-noncompetitive Cdk-cyclin inhibitors has been launched.

2.5.1 Flavopiridol (Alvocidib)

Flavopiridol (Alvocidib) is a currently synthetically produced flavonoid, although its chemical structure is identical to a product obtained from the stem bark of *Dysoxylum binectariferum*, a plant used in India as herbal medicine (60).

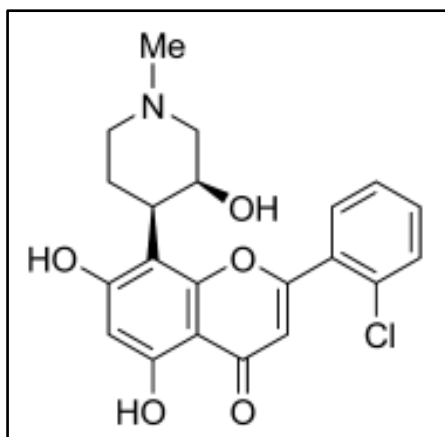


Figure 2.10: Structure of flavopiridol.

Flavopiridol has been found to have strong activity against multiple Cdks. In addition, flavopiridol is active to a lesser degree on tyrosine kinases, such as the epidermal growth factor receptor (EGFR) and protein kinase C (PKC) (Table 2.1) (6). Flavopiridol has a high potency to inhibit the proliferation of a broad range of human tumor cell lines after prolonged exposure time and inhibits *in vivo* the growth of human tumors, such as leukemias and lymphomas (61). Flavopiridol is also proposed as potential antiviral drug because it blocks HIV-1 replication.

Interestingly, flavopiridol interferes with the cell cycle at two points, it arrests the cell cycle at the G2/M phase and delays the G1 to S phase progression (6). Structure-activity studies have shown that flavopiridol interferes with binding of ATP to the adenine-binding pocket of Cdks, such as Cdk2 (62). Flavopiridol modulates transcriptional processes by the potent inhibition of P-TEFb, resulting in suppressed transcription and decreased phosphorylation of RNA Pol II (63). The transcripts that are most sensitive to Cdk9 inhibition are those with short half-lives because their levels decrease when initiation and elongation of transcription are inhibited. Thus, this transcriptional inhibition leads to a decrease in levels of proteins, such as cyclin D1, VEGF and Mcl-1 essential for cell cycling and survival (64, 65).

Table 2.1: Activity of flavopiridol on cellular kinases.

Family	Kinase	IC₅₀ (μM)
EGFR family	EGFR	21-25
Signal transducing kinases	PKA	122-145
	PKC	6
Cyclin dependent kinases (direct inhibition)	Cdk1/cyclin B	0.03-0.4
	Cdk2/cyclin A	0.1
	Cdk2/cyclin E	0.1
	Cdk4/cyclin D	0.02-0.04
	Cdk6/cyclin D	0.06
	Cdk7/cyclin H	0.11-0.3
	Cdk9/cyclin T	0.003

2.5.2 Flavopiridol in clinical trials

In preclinical studies, flavopiridol was active in diverse hematopoietic cell lines (66, 67) and induced G1 and G2/M arrest in many exponentially growing tumor cell types. Flavopiridol was the first Cdk inhibitor to enter clinical trials and is currently in clinical trials for the treatment of different cancers (phase I/II) (68, 69).

Clinical tumor responses could be observed on different types of progressive tumors refractory to conventional treatment, such as non-Hodgkin's lymphoma, human neoplasms and renal, colon, and prostate cancers. The beneficial effects with flavopiridol were based on the inhibition of Cdks to prevent and/or treat abnormalities in the cell cycle and concentrations between 300 and 500 nM were achieved safely (4). Especially in poor-risk acute myelogenous leukemia (AML) and in chronic lymphocytic leukemia (CLL) some encouraging responses were noted with flavopiridol as single agent or in combinations with chemotherapy (70, 71). Recent findings revealed that binding to human plasma proteins reduces free flavopiridol concentration and makes continuous intravenous infusion dosing ineffective. However, flavopiridol, when administered by a 30-min intravenous bolus followed by a 4-hour continuous intravenous infusion, is effective in high-risk, refractory chronic lymphocytic leukemia (72). A recently developed liposomal formulation of the drug ought to increase the drug's half-life and perhaps its efficacy (73).

2.6 Cdk inhibitors as anti-inflammatory approach

The Cdk inhibitors play an integral role in the regulation of the cell cycle and transcriptional regulation and have also been suggested as potential anti-inflammatory agents that can influence the resolution of inflammation (8).

Apoptosis of inflammatory cells and their subsequent clearance by macrophages are key mechanisms in successful resolution of inflammation. Cdk inhibitors have been used for the selective induction of apoptosis in actively proliferating cancer cell lines for several years (74). The induction of apoptosis by Cdk inhibitors seems to be mediated by the modulation of Bcl-2 family members and to be executed in a caspase-dependent manner (75). A panel of Cdk inhibitor drugs have been shown to promote neutrophil apoptosis in a concentration- and time-dependent manner. Apoptosis of neutrophils ensures that toxic neutrophil granule contents are securely packaged in apoptotic bodies and expedites phagocytosis occurs by macrophages.

Effects on other cell types including lymphocytes and fibroblasts have also been demonstrated with Cdk inhibitor drugs indicating that they may have pleiotropic anti-inflammatory, pro-resolution activity (8). Cdk inhibitor drugs have been reported to be efficacious in resolving established animal models of neutrophil-dominant and lymphocyte-driven inflammation. Neutrophils have functional Cdks, are transcriptionally active and demonstrate augmented apoptosis in response to Cdk inhibitor drugs, while lymphocyte proliferation and secretory function are inhibited. Recently, it was reported, that specific inhibitors of Cdks facilitate resolution of inflammation by augmenting neutrophil apoptosis (9).

3 Materials and Methods

3.1 Materials

3.1.1 Flavopiridol

Flavopiridol was provided from the National Cancer Institute. Flavopiridol was solubilized in DMSO at 10 mM and stored at -20°C. For experiments, flavopiridol was freshly diluted in growth medium to 10 µM and further diluted to the indicated concentrations.

3.1.2 Biochemicals, inhibitors, dyes, and cell culture reagents

Reagent	Producer
Accustain [®] formaldehyde	Sigma-Aldrich, Taufkirchen, Germany
Amphotericin B	PAA Laboratories, Pasching, Austria
BC Assay reagent	Interdim, Montulocon, France
Bradford Reagent [™]	Bio-Rad, Munich, Germany
Calyculin	Millipore, Schwabach/Ts., Germany
CellTiter Blue [™]	Promega, Madison, WI, USA
Collagen A/G	Biochrome AG, Berlin, Germany
Collagenase G	Biochrome AG, Berlin, Germany
Complete [®]	Roche diagnostics, Penzberg, Germany
Dianisidine-hydrochlorid	Sigma-Aldrich, Taufkirchen, Germany
Dihydrorhodamine-123 (DHR)	Invitrogen, Karlsruhe, Germany
DMSO	Sigma-Aldrich, Taufkirchen, Germany
Endothelial Cell Growth Medium (ECGM)	Provitro, Berlin, Germany
FCS gold	PAA Laboratories, Pasching, Austria
fMLP	Sigma-Aldrich, Taufkirchen, Germany
Formaldehyde, 16% ultrapure	Polysciences Europe GmbH, Eppelheim, Germany
M199 Medium	PAA Laboratories, Pasching, Austria
Myristoylated PKC θ pseudosubstrate inhibitor	Calbiochem, Darmstadt, Germany
NaF	Merck, Darmstadt, Germany
Na ₃ VO ₄	ICN Biomedicals, Aurora, Ohio, USA

Reagent	Producer
Page Ruler™ Prestained Protein Ladder	Fermentas, St. Leon-Rot, Germany
Penicillin	PAA Laboratories, Pasching, Austria
Propidium iodide	Sigma-Aldrich, Taufkirchen, Germany
PermaFluor mounting medium	Beckman Coulter, Krefeld, Germany
PMSF	Sigma-Aldrich, Munich, Germany
RNAlater	Ambion, Austin, TX, USA
SP600125	Enzo Life Sciences, Lörrach, Germany
Streptomycin	PAA Laboratories, Pasching, Austria
TBB	Tocris Bioscience, Bristol, UK
Tumor necrosis factor (TNF)- α	PeproTech GmbH, Hamburg, Germany
Triton X-100	Merck, Darmstadt, Germany

PBS (pH 7.4)		PBS+ Ca²⁺/Mg²⁺ (pH 7.4)	
NaCl	132.2 mM	NaCl	137 mM
Na ₂ HPO ₄	10.4 mM	KCl	2.68 mM
KH ₂ PO ₄	3.2 mM	Na ₂ HPO ₄	8.10 mM
H ₂ O		KH ₂ PO ₄	1.47 mM
		MgCl ₂	0.25 mM
		CaCl ₂	0.50 mM
		H ₂ O	

3.1.3 Technical equipment

Name	Device	Producer
AB7300 RT-PCR	Real-time PCR system	Applied Biosystems, Foster City, CA, USA
Axioskop	Upright microscope	Zeiss, Jena, Germany
Culture flasks, plates, dishes	Disposable cell culture material	TPP, Trasadingen, Switzerland
Curix 60	Tabletop film processor	Agfa, Cologne, Germany
Cyclone	Storage Phosphor Screens	Canberra-Packard, Schwadorf, Austria
FACSCalibur	Flow cytometer	Becton Dickinson, Heidelberg, Germany
ibidi slides	Microscope slide	ibidi GmbH, Munich, Germany
LSM 510 Meta	Confocal laser scanning microscope	Zeiss, Jena, Germany
Mikro 22R	Table centrifuge	Hettich, Tuttlingen, Germany
Nanodrop [®] ND-1000	Spectrophotometer	Peqlab, Wilmington, DE, USA
Nucleofector II	Electroporation device	Lonza GmbH, Cologne, Germany
Odyssey 2.1	Infrared Imaging System	LI-COR Biosciences, Lincoln, NE, USA
Orion II Microplate Luminometer	Luminescence	Berthold Detection Systems, Pforzheim, Germany
Polytron PT1200	Ultrax homogenizer	Kinematica AG, Lucerne, Switzerland
SpectraFluor Plus [™]	Microplate multifunction reader	Tecan, Männedorf, Austria
Sunrise [™]	Microplate absorbance reader	Tecan, Männedorf, Austria
Vi-Cell [™] XR	Cell viability analyzer	Beckman Coulter, Fullerton, CA, USA

3.2 Cell culture

3.2.1 Isolation and cultivation of human umbilical vein endothelial cells

Human umbilical cords were kindly provided by Klinikum München Pasing, Frauenklinik Dr. Wilhelm Krüsmann, and Rotkreuzklinikum München. Primary human umbilical vein endothelial cells (HUVECs) were isolated by collagenase treatment of umbilical cords (76). Experiments were performed using cells at passage 3. Cells were cultivated on 0.001% collagen G-coated flasks, plates, or dishes in growth medium. For splitting and seeding (1:3), cells were washed twice with pre-warmed PBS before incubation with T/E for 1-2 minutes at 37°C. The digest was terminated by adding approximately 20 ml stopping medium. Next, cells were centrifuged for 5 minutes at 1,000 rpm to remove the T/E. The pellet was resuspended in pre-warmed growth medium and cells were plated.

Growth medium		Stopping medium	
ECGM	500 mL	M199	500 mL
Supplement	23.5 mL	FCS	50 mL
FCS	50 mL		
Antibiotics	3.5 mL		
Trypsin/EDTA (T/E)			
Trypsin	0.05%		
EDTA	0.20%		
PBS			

3.2.2 Isolation and cultivation of neutrophils

Human neutrophil granulocytes were separated from heparinized peripheral blood of healthy volunteers. CD15 MicroBeads (Mini-Macs, Miltenyi Biotec GmbH, Bergisch Gladbach, Germany) were added to the whole blood for 30 minutes at 4°C, which labeled the neutrophils magnetically. Using whole blood columns, CD15⁺ cells were directly separated from whole blood and collected in neutrophil isolation medium. Cells were counted and kept at room temperature in HEPES buffer or neutrophil growth medium until use (usually < 30 min). Assays using neutrophils were performed at 37°C.

HEPES buffer (pH 7.4)

NaCl	125 mM
KCl	3 mM
NaH ₂ PO ₄	1.25 mM
CaCl ₂	2.5 mM
MgCl ₂	1.5 mM
Glucose	10 mM
Hepes	10 mM
H ₂ O	

Neutrophil isolation medium

PBS	500 mL
BSA	2.5 mL
EDTA	2 mM

Neutrophil growth medium

M199	500 mL
FCS	10 mL
Antibiotics	3.5 mL

3.3 Cytotoxicity assays

3.3.1 CellTiter-Blue™ cell viability assay

Cell viability in HUVECs was analyzed via measuring the reduction of resazurin to resorufin (CellTiter-Blue™). 2.5×10^4 cells/well were seeded into 96-well plates and treated with flavopiridol for 24 and 48 hours. Resazurin was added to the medium and after two hours of incubation the conversion of resazurin to resorufin was determined. The assay was performed as described in the provided protocol of CellTiter-Blue™ Cell Viability Assay. The reduction of resazurin was determined by calculating the ratio of fluorescence at 530/590 nm in a SpectraFluor Plus plate reader.

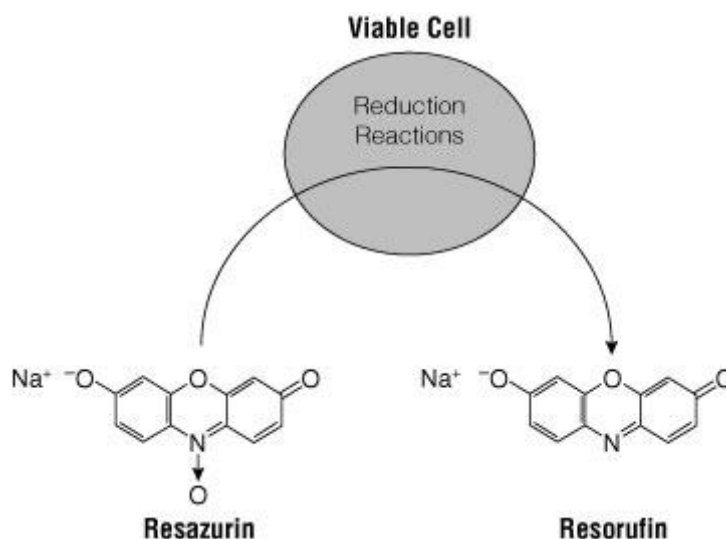


Figure 3.1: CellTiter-Blue™ cell viability assay.

Conversion of resazurin to resorufin by metabolically active cells. The image is adapted from www.promega.com.

3.3.2 Quantification of DNA fragmentation by PI staining (Nicoletti method)

During the apoptotic process endogenous endonucleases become activated and cause the fragmentation of nuclear DNA into oligonucleosomal-size fragments. A widely used assay to quantify apoptotic cell death is the counting of nuclei with subdiploid DNA content after staining with propidium iodide (PI). Quantification of apoptosis was carried out according to Nicoletti et al (77). Cells were permeabilized in a buffer containing PI and fluorescence was measured by flow cytometry. The whole DNA content of cells is stained independently from their viability or membrane integrity. Most cells of normal untreated cell populations are in G₀/G₁ phase with

diploid DNA content and emit a homogenous fluorescence after binding of PI to DNA. DNA fragments of apoptotic cells or apoptotic bodies respectively have a lower fluorescence and thus appear “left” to the G0/G1 peak in the FL2 histogram. Confluent HUVECs were treated for 24 and 48 hours with increasing concentrations of flavopiridol. After stimulation, cell culture supernatants containing apoptotic cells were collected. Cells were washed, trypsinized, resuspended in the supernatant, and centrifuged 10 minutes at 600 x g at 4°C. After another washing step with PBS, cells were resuspended in a buffer (0.1% sodium citrate and 0.1% Triton X-100 in PBS) containing 2 mg/ml PI and incubated protected from light overnight at 4°C. The fluorescence intensity of PI was measured in the logarithmic mode of the fluorescence channel 2 (FL2, λ_{em} 585 nm) using a flow cytometer. Nuclei left to the G1 peak containing hypodiploid DNA were considered as apoptotic.

FACS buffer (pH 7.37)

NaCl	8.12 g
KH ₂ PO ₄	0.26 g
Na ₂ HPO ₄	2.35 g
KCl	0.28 g
Na ₂ EDTA	0.36 g
LiCl	0.43 g
NaN ₃	0.20 g
H ₂ O	ad 1.0 L

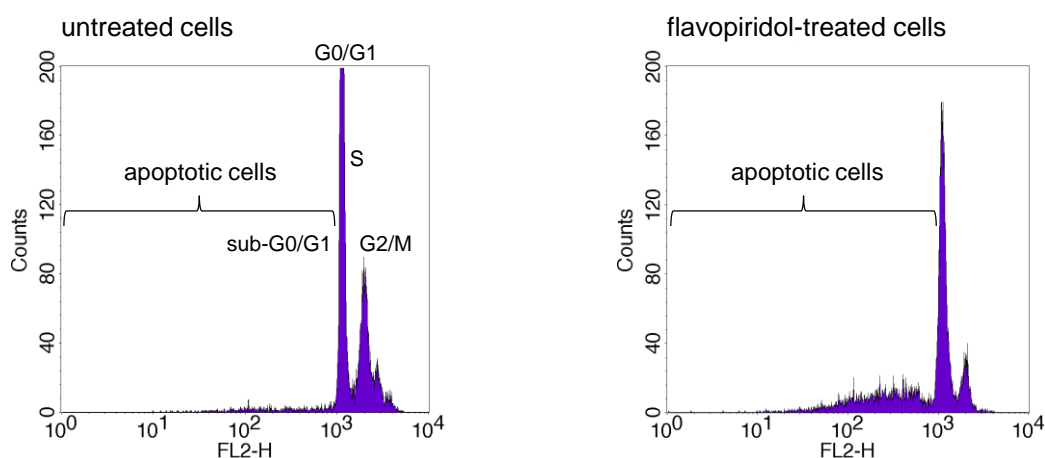


Figure 3.2: Determination of DNA fragmentation by PI staining (Nicoletti method).

Representative examples of apoptotic analysis of either control cells (left panel) or 500 nM flavopiridol-treated cells (right panel) are displayed. Sub-G0/G1 peaks are considered as apoptotic cells.

3.4 Concanavalin A-induced liver injury model

The concanavalin A-induced liver injury model was performed in collaboration with PD Dr. Gabriele Sass and Prof. Dr. Gisa Tiegs from the Division of Experimental Immunology and Hepatology of the University Medical Center Hamburg-Eppendorf, Hamburg, Germany.

3.4.1 Procedures

Male C57Bl/6 mice (6-8 weeks; weight range: 18-22 g) were obtained from the animal facilities of the University Medical Center Hamburg-Eppendorf, Hamburg, Germany. Concanavalin A (ConA; dissolved in pyrogen-free saline) was purchased from Sigma-Aldrich (Taufkirchen, Germany). It was administered to mice intravenously at 15 mg/kg. Flavopiridol (44 ng in 250 μ l PBS; bolus sufficient to reach 100 nM plasma concentration) was administered intravenously 15 minutes prior to ConA administration. Mice were sacrificed eight hours after ConA application.

Liver damage was assessed by measuring plasma enzyme activity of alanine aminotransferase (ALT) and aspartate aminotransferase (AST) (78), using an automated procedure with the COBAS MIRA[®] (Roche, Basel, Suisse).

3.4.2 Hematoxylin and eosin (H&E) staining

Liver tissue was fixed in 4% phosphate-buffered formaldehyde and embedded into paraffin. Paraffin sections of 3 μ m were cut and stored at room temperature until use. Routine histology [hematoxylin and eosin (H&E) staining] was performed in order to evaluate basic histomorphological features.

3.4.3 Granulocyte staining

Paraffin sections of 5 μ m were cut and stained for chloroacetate esterase, an enzyme usually considered specific for cells of granulocytic lineage. A naphthol AS-D chloroacetate esterase kit (Sigma-Aldrich) was used according to the manufacturer's protocol and the intensity of staining was evaluated by microscope.

3.4.4 Myeloperoxidase (MPO) activity

Myeloperoxidase (MPO) activity in the tissue and the number of present neutrophils are directly proportional (79). Therefore, to measure the accumulation of neutrophils in liver tissue, the activity of MPO is determined. Liver tissues, 80 mg each, were crushed and homogenized on ice in phosphate buffer (pH 6.0) containing 1% of hexadecyltrimethyl ammonium bromide (HTAB). After lysis by sonication, the suspension was centrifuged for 30 minutes at 12,000 rpm at 4°C. MPO activity of the supernatants was determined by agitating equal volumes of the supernatants and the substrate solution [0.06% dianisidine and 0.0009% H₂O₂ in phosphate buffer (pH 6.0)]. MPO activity was measured by determination of the absorbance at 540 nm with a SpectraFluor Plus plate reader.

Phosphate buffer (pH 6.0)

KH ₂ PO ₄	9.08 g/L
Na ₂ HPO ₄	11.88 g/L
H ₂ O	

3.5 Cremaster muscle preparation and intravital microscopy

The open cremaster muscle preparation and intravital microscopy was performed in collaboration with Dr. Alexander Khandoga and Prof. Dr. Fritz Krombach from the Walter Brendel Center of Experimental Medicine, Munich, Germany.

3.5.1 Surgical procedure

Male C57Bl/6 mice (6-8 weeks; Charles River, Sulzfeld, Germany) were anaesthetized by an intraperitoneal injection of ketamine (100 mg/kg) and xylazine (10 mg/kg). Surgical preparation of cremaster muscles and intravital microscopy were performed as described previously (80). Inflammatory stimulation was achieved by intrascrotal injection of 300 ng of recombinant murine TNF α (R&D Systems) diluted in 400 μ l PBS, 4 h prior to intravital microscopic observation. At the same time, flavopiridol (11 ng in 250 μ l PBS; bolus sufficient to reach 25 nM plasma concentration) was injected intravenously. The control group received intravenous administration of PBS (250 μ l).

3.5.2 Intravital microscopy

In each animal, at least five single unbranched postcapillary venules with diameters of 17.5 to 35 μm were analyzed. During a 15 min observation period, leukocyte rolling, adhesion, and transendothelial migration were assessed by near-infrared reflected light oblique transillumination microscopy. Videotaped images were evaluated off-line using CAPIMAGE software (Zeintl). Leukocyte rolling flux fraction is defined as the flux of rolling leukocytes in percent of total leukocyte flux. The total number of adherent leukocytes was determined for each venule segment (100 μm) and is expressed per $10^4 \mu\text{m}^2$ of venule surface area. Emigrated cells were counted in an area reaching out 75 μm to each side of a vessel over a distance of 100 μm vessel length and are presented per $10^4 \mu\text{m}^2$ tissue area. Centerline blood flow velocity was measured by using intraarterially administered microspheres (0.96 μm ; FluoSpheres; Invitrogen). The wall shear rate [s^{-1}] was estimated as $8 \times [V_b/d]$, where V_b refers to the mean blood flow velocity and d to the diameter of the vessel. Mean blood flow velocity, V_b , was approximated by multiplying the centerline blood flow velocity with 0.625 (81). The number of leukocytes in whole blood was determined at the end of each experiment using Coulter A^CT Counter (Coulter Corp., Miami).

3.6 Cell adhesion assay

Confluent HUVECs in 24-well plates were stimulated 30 minutes with flavopiridol (100nM) prior to $\text{TNF}\alpha$ (10 ng/ml) activation for 24 hours. Freshly isolated neutrophils ($10^6/\text{ml}$, 100 $\mu\text{l}/\text{well}$) were coincubated with HUVECs for 30 minutes. The suspension was centrifuged for 3 minutes at 800 x g at room temperature. After incubation for 30 minutes at 37°C, nonadherent cells were removed by washing twice with prewarmed PBS+ $\text{Ca}^{2+}/\text{Mg}^{2+}$.

Adhered neutrophils were quantified by a MPO assay. MPO activity was assessed photometrically at a wavelength of 450 nm with a substrate solution (see 3.4.4). A standard curve of MPO activity with an increasing number of neutrophils has been performed in parallel with each assay.

3.7 Flow cytometry

Table 3.1: Antibodies used for flow cytometry.

Specificity	Format	Isotype	Dilution	Provider
CD11b	FITC	Monoclonal antibody	1:20	AbD Serotec
E-selectin	PE	Monoclonal antibody	1:20	Tebu-bio
ICAM-1	FITC	Monoclonal antibody	1:25	BIOZOL
VCAM-1	FITC	Monoclonal antibody	1:20	BD Pharmingen

3.7.1 Determination of cell surface expression of adhesion molecules

Confluent HUVECs in 24-well plates were treated 30 minutes with increasing concentrations of flavopiridol prior to activation with $\text{TNF}\alpha$ (10 ng/ml) for 6 hours (E-selectin) or 24 hours (ICAM-1, VCAM-1). Then, cells were washed twice with pre-warmed PBS, removed by careful trypsinization, and fixed in formaldehyde 4%. After one washing step with PBS, cells were centrifuged (1000 rpm, 5 minutes, RT). The supernatant was removed and the pellet was incubated with antibodies against human ICAM-1, E-selectin, or VCAM-1 for 45 minutes at room temperature. Afterwards, cells were analyzed by flow cytometry (FACSCalibur, BD Biosciences, Heidelberg, Germany).

3.7.2 Determination of cell surface expression of CD11b

Neutrophils ($10^6/\text{ml}$, 100 μl) were incubated with flavopiridol 30 minutes before 15 minutes activation with fMLP (10^{-7} M). Then, cells were fixed with 4% formaldehyde and washed with PBS followed by incubation with saturating concentrations of FITC-labeled antibody against CD11b for 45 minutes at room temperature. Cells were washed once with PBS, resuspended in PBS and analyzed by flow cytometry. At least 5,000 events were acquired.

3.7.3 Determination of oxidative stress in neutrophils

Oxidative stress in neutrophils was assessed by measuring the intracellular oxidation of dihydrorhodamine (DHR) to rhodamine. Neutrophils ($10^6/\text{ml}$, 100 μl) in suspension

were primed with DHR (1 μ M) for 10 minutes at 37°C. Cells were pretreated for 30 minutes with 100 nM flavopiridol and activated with fMLP (10^{-7} M) for 15 minutes. The reaction was stopped on ice and the cells were analyzed by flow cytometry. At least 5,000 events were acquired.

3.8 Quantitative RT-PCR

3.8.1 Isolation of RNA of tissue sections

Total mRNA from liver tissues from the concanavalin A model was isolated using the RNeasy Mini Kit (Qiagen, Hilden, Germany). The tissues, each about 20 mg, were homogenized in 300 μ l RLT buffer (provided with the RNeasy Mini Kit) using a homogenizer. Then, procedures were followed as default by the RNeasy Mini Kit protocol. Finally, RNA was eluted with RNase-free water and amounts were quantified by measuring the absorption at 260 nm (A260) and 280 nm (A280) (NanoDrop, Wilmington, DE, USA). On an agarose gel the intensity ratio of ribosomal 28S and 18S RNA was used for evaluation of RNA integrity.

RNA was isolated from RNAlater-stored cremaster muscle tissues using the RNeasy Fibrous Tissue Kit (Qiagen, Hilden, Germany). Tissue was homogenized as described above for liver tissues and following procedures were performed as described by the RNeasy Fibrous Tissue Kit protocol.

Samples were stored at -85°C until used for reverse transcription.

3.8.2 Isolation of RNA of HUVECs

Total RNA was extracted using the RNeasy mini Kit (Qiagen GmbH, Hilden, Germany) according to the manufacturer's instructions. Cells were cultured in 6-well plates and were treated as indicated. Thereafter, cells were lysed and homogenized in the presence of RLT buffer and procedures were followed as default by the RNeasy Mini Kit protocol. The purified RNA was eluted with RNase-free water and quantification of the samples was performed using NanoDrop (see 3.8.1). Verification of RNA integrity was determined and samples were stored at -85°C until used for reverse transcription.

3.8.3 Reverse transcription

Reverse transcription was performed with the High Capacity cDNA Reverse Transcription Kit (Applied Biosystems, Foster City, DA, USA) according to the manufacturer's manual. Equal amounts of total RNA, 500 ng for liver and cremaster muscle tissues or 1500 ng for HUVECs were re-transcribed for 2 hours at 37°C. The cDNA was stored at -20° C until used for quantitative RT-PCR.

3.8.4 Quantitative Real-Time PCR

All primers and probes were designed using the Primer Express[®] 2.0 software (Applied Biosystems) and were obtained from biomers.net (Ulm, Germany). The probe oligonucleotide sequence was labeled with the reporter dye 6-carboxyfluorescein (FAM) at the 5' end and the quencher dye tetramethyl-6-carboxyrhodamine (TAMRA) at the 3' end. In Table 3.2 sequences of forward as well as reverse primers and probe are displayed.

Table 3.2: Primer and probe sequences.

<i>ICAM-1</i>		
forward	mouse	5'-CTG CTG CTT TTG AAC AGA ATG G-3'
reverse	mouse	5'-TCT GTG ACA GCC AGA GGA AGT G-3'
probe	mouse	5'-AGA CAG CAT TTA CCC TCA G-3'
forward	human	5'-GCA GAC AGT GAC CAT CTA CAG CTT-3'
reverse	human	5'-CTT CTG AGA CCT GTG GCT TCG T-3'
probe	human	5'-CCG GCG CCC AAC GTG ATT CT-3'
<i>E-selectin</i>		
forward	mouse	5'-CAA CGT CTA GGT TCA AAA CAA TCA G-3'
reverse	mouse	5'-TTA AGC AGG CAA GAG GAA CCA-3'
probe	mouse	5'-CAC AAA TGC ATC GTG GGA-3'

GAPDH

forward	mouse	5'-TGC AGT GGC AAA GTG GAG AT-3'
reverse	mouse	5'-TGC CGT GAG TGG AGT CAT ACT-3'
probe	mouse	5'-CCA TCA ACG ACC CCT TCA TTG-3'
forward	human	5'-GGG AAG GTG AAG GTC GGA GT-3'
reverse	human	5'-TCC ACT TTA CCA GAG TTA AAA GCA G-3'
probe	human	5'-ACC AGG CGC CCA ATA CGA CCA A-3'

Quantitative RT-PCR was performed using the AB 7300 RealTime PCR system, together with the TaqMan Gene Expression Master Mix (Applied Biosystems) according to the manufacturer's instructions. PCR on GAPDH was used as internal reference and serial dilution of cDNA served as standard curves. Fluorescence-development was analyzed using the AB 7300 system software and calculation of relative mRNA content was done according to a mathematical model for relative quantification of real time PCR products (82).

3.9 Immunocytochemistry

HUVECs were seeded on 8-well ibiTreat μ -slides (ibidi GmbH, Munich, Germany). After stimulation, cells were washed once with ice-cold PBS+ $\text{Ca}^{2+}/\text{Mg}^{2+}$ and fixed in 4% formaldehyde for 10-15 minutes. After one PBS washing step, cells were permeabilized by 0.2% Triton X-100 in PBS for exactly 2 minutes. Then, cells were washed three times for 5 minutes with PBS, unspecific binding was blocked by incubation with 0.2% BSA in PBS for 60 minutes. Cells were incubated with the primary antibody against p65 (Santa-Cruz Biotechnology Inc., 1:200 in 0.2% BSA/PBS) for 60 minutes. After three washes with PBS for 5 minutes, cells were incubated with the Alexa Fluor[®] 488-conjugated secondary antibody (Invitrogen, 1:400 in 0.2% BSA/PBS) for 60 minutes. Afterwards, cells were washed again three times with PBS, and covered with PermaFluor mounting medium (VWR, Darmstadt, Germany). Images were obtained with a Zeiss LSM 510 Meta confocal laser scanning microscope (Zeiss, Jena, Germany).

3.10 Western blot analysis

Western blot analysis is an extensively used technique to identify specific proteins in various protein mixtures, e.g. cell lysates or tissue homogenates. It includes the electrophoretic separation of proteins according to their molecular weights, their transfer to a membrane (“blotting”), and their visualization by immunodetection.

3.10.1 Preparation of samples

HUVECs were treated as indicated and washed twice with ice-cold PBS. The PBS was removed completely and cells were lysed by adding RIPA buffer (for non-phosphorylated proteins) or lysis buffer (to sustain phosphorylated status of proteins) followed by freezing at -80°C . Cells were thawed on ice, scratched from the plate/dish and transferred to 1.5 ml reaction tubes. Cellular debris was removed by centrifugation (14,000 rpm, 10 min, 4°C). Supernatants were transferred to a new reaction tube and aliquots were taken for protein quantification using the bicinchoninic protein assay (BCA).

RIPA buffer		Lysis buffer	
Tris/HCl	50 mM	Tris/HCl	50 mM
NaCl	150 mM	NaCl	150 mM
Nonidet NP 40	1%	Nonidet NP 40	1%
Deoxycholic acid	0.25%	Deoxycholic acid	0.25%
SDS	0.10%	SDS	0.10%
<u>add before use:</u>		<u>add before use:</u>	
Complete [®]	4.0 mM	Complete [®]	4.0 mM
PMSF	1.0 mM	PMSF	1.0 mM
Na ₃ VO ₄	1.0 mM	Na ₃ VO ₄	0.3 mM
NaF	1.0 mM	NaF	1.0 mM
H ₂ O	ad 100 mL	β-Glycerophosphate	3.0 mM
		Pyrophosphate	10 mM
		H ₂ O ₂	600 μM
		H ₂ O	ad 100 mL

3.10.2 Protein quantification: bicinchoninic protein assay

Bicinchoninic protein assay (BCA) was performed as described previously (83). Protein samples (10 μ l) were incubated with 200 μ l BCA reagent for 30 minutes at 37°C. Absorbance of the complex was measured photometrically at 550 nm. Protein standards were obtained by diluting a stock solution of BSA (2 mg/ml). Linear regression was used to determine the actual protein concentration of each sample. 5x SDS-sample buffer was added to the lysates, which were boiled for 5 minutes at 95°C for inactivation. Protein samples were kept at -20°C until use.

5x SDS-sample buffer

Tris/HCl	3.125 M, pH 6.8
Glycerol	10 mL
SDS	5%
DTT	2%
Pyronin Y	0.025%
H ₂ O	ad 20 mL

3.10.3 SDS-PAGE

Proteins were separated by discontinuous SDS-polyacrylamid gel electrophoresis (SDS-PAGE) according to Laemmli (84) using Power Tec™ HC from Bio-Rad (Munich, Germany). Prior to loading the samples, the apparatus was assembled as described by the producer and the chamber was filled with ice-cold electrophoresis buffer.

Protein concentrations of the probes were unified by adding the required volume of 1x SDS sample buffer. Then, probes were boiled for 5 minutes at 95°C before loading the samples on the SDS gel. Empty slots were filled with an appropriate volume of 1x SDS-sample buffer. The molecular weight of proteins was determined by loading the Page Ruler™ Prestained Protein Ladder on the gel.

Electrophoresis was carried out at 100 V for 21 min for protein stacking and 200 V for 45 min for protein separation.

Stacking gel		Separating gel (10%)	
PAA solution 30%	1.275 mL	PAA solution 30%	5.0 mL
1.25 M Tris/HCl, pH 6.8	0.75 mL	1.5 M Tris/HCl, pH 8.8	3.75 mL
SDS 10%	75 μ L	SDS 10%	150 μ L
H ₂ O	5.25 mL	H ₂ O	6.1 mL
APS	75 μ L	APS	75 μ L
TEMED	20 μ L	TEMED	20 μ L

Electrophoresis buffer	
Tris base	3.0 g
Glycine	14.4 g
SDS	1.0 g
H ₂ O	ad 1.0 L

3.10.4 Electroblotting

After separating on the SDS-PAGE, proteins were electrophoretically transferred to a nitrocellulose membrane (Hybond ECL™, Amersham Biosciences, NJ, USA) using a Trans-Blot® SD Semi-Dry Transfer Cell from Bio-Rad. Prior to blotting, the membrane was incubated for at least 30 min in anode buffer on a shaking platform. For semi-dry transfer, the gel-membrane sandwich is placed between carbon plate electrodes. Therefore, one sheet of thick blotting paper (Whatman, Schleicher & Schüll, Dassel, Germany) was soaked with anode buffer and rolled onto the anode. Subsequently, the membrane and the gels were added. Finally the stack was covered with another sheet of thick blotting paper soaked with cathode buffer. The transfer cell was closed and transfer was carried out at 15 V for 1 h.

Anode buffer		Cathode buffer	
Tris	12 mM	Tris	12 mM
CAPS	8 mM	CAPS	8 mM
Methanol	15%	SDS	0.1%
H ₂ O		H ₂ O	

3.10.5 Protein detection

Prior to the immunological detection of the relevant proteins, unspecific protein binding sites were blocked with PBS containing 5% skimmed milk powder (blotto 5%) for 2 hours at room temperature. Afterwards, detection of the proteins was performed by incubating the membrane with the respective primary antibody at 4°C overnight. After four washing steps with PBS containing 0.1% Tween (PBS-T), the membrane was incubated with the secondary antibody, followed by 4 additional washing steps. All steps regarding the incubation of the membrane were performed under gentle agitation.

In order to visualize the proteins, two different methods have been used depending on the labels of secondary antibodies.

Antibodies directly labeled with infrared (IR) fluorophores

Secondary antibodies coupled to IRDye™ 800 and Alexa Fluor® 680 with emission at 800 and 700 nm, respectively, were used. Membranes were incubated for 2 hours with the secondary antibody before three washing steps with PBS-T and one time washing with PBS to remove the interfering Tween 20. After washing, membranes were scanned and analyzed using the Odyssey infrared imaging system version 2.1. After scanning the membrane with two-color detection, bands were quantified using Odyssey software.

Antibodies coupled to horseradish peroxidase (HRP)

Proteins were detected with ECL (enhanced chemiluminescence) when the secondary antibody was conjugated to HRP (horseradish peroxidase). Membranes were incubated for 2 hours with the secondary antibody prior to four washing steps with PBS-T. Then, the membrane was gently agitated in ECL Plus™ Western Blotting detection reagent (Amersham Bioscience) for 1 minute protected from light, and layered between two plastic sheets afterwards. Chemiluminescence was detected by exposing the membranes to an X-ray film for the appropriate time period in a darkroom. X-ray films were developed in a table processor (Curix 60 Developing System, Agfa-Gevaert AG).

Table 3.3: Primary anti bodies.

Antigen	Isotype	Dilution	in	Provider
β -actin	mouse monoclonal	1:1,000	blotto 1%	Chemicon
Cdk8	goat polyclonal	1:1,000	blotto 1%	Santa Cruz
Cdk9	mouse monoclonal	1:1,000	blotto 1%	Santa Cruz
I κ B α	rabbit polyclonal	1:1,000	blotto 1%	Santa Cruz
IKK α / β phospho	rabbit polyclonal	1:500	BSA 5%	Cell Signaling
LIMK1	rabbit polyclonal	1:1,000	BSA 5%	Cell Signaling
NF- κ B p65	rabbit polyclonal	1:500	blotto 1%	Santa Cruz
NF- κ B p65 phosphoSer536	rabbit polyclonal	1:1,000	BSA 5%	Cell Signaling

Table 3.4: Secondary antibodies.

Antibody	Dilution	in	Provider
Goat anti-mouse IgG ₁ -HRP	1:1,000	blotto 1%	Biozol
Goat anti-mouse IgG _{2b} -HRP	1:1,000	blotto 1%	Southern Biotechnology
Goat anti-rabbit: HRP	1:1,000	blotto 1%	Dianova
Alexa Fluor [®] 680 goat anti-mouse IgG	1:10,000	blotto 1%	Molecular Probes
Alexa Fluor [®] 680 goat anti-rabbit IgG	1:10,000	blotto 1%	Molecular Probes
IRDye [™] 800CW goat anti-mouse IgG	1:20,000	blotto 1%	LI-COR Biosciences
IRDye [™] 800CW goat anti-rabbit IgG	1:20,000	blotto 1%	LI-COR Biosciences

3.10.6 Unspecific protein staining of gels and membranes

To control equal loading of the gel and the performance of the transfer, polyacrylamide gels were stained for 10 minutes with Coomassie staining solution. Afterwards, gels were extensively washed with destaining solution until proteins appeared as blue bands.

After protein detection, membranes were stained with Ponceau solution for 5 minutes and destained with distilled water.

Coomassie staining solution		Coomassie destaining solution	
Coomassie blue G	0.3%		
Glacial acetic acid	10%	Glacial acetic acid	10%
Ethanol	45%	Ethanol	33%
H ₂ O		H ₂ O	

Ponceau solution	
Ponceau S	0.1%
Glacial acetic acid	5%
H ₂ O	

3.11 Transfer of nucleic acids into HUVECs

3.11.1 Transfection of siRNA

For transient transfection with the indicated siRNAs, HUVECs were electroporated using the Nucleofector[®] II device in combination with the HUVEC Nucleofector[®] Kit (both from Lonza Cologne AG, Germany). In order to silence the expression of LIMK1 or Cdk8, HUVECs were transiently transfected with On-TARGETplus Individual Duplexes (LIMK1 siRNA) or On-TARGETplus SMARTpool (Cdk8 siRNA) (Dharmacon, Lafayette, CO, USA). On-Targetplus siCONTROL non-targeting siRNA was used as a control. Each siRNA was suspended in Dharmacon 1x siRNA buffer, aliquoted and stored at -80°C. The concentration of siRNA was confirmed using a NanoDrop (Wilmington, DE, USA).

siRNA	Target sequences	Provider
LIMK1	5'-GAGCAUGACCCUCACGAUA-3' 5'-GCCCAGAUGUGAAGAAUUC-3'	Dharmacon
Cdk8	5'-GGACAGAAUUAUCAAUGUA-3' 5'-GAGCAAGGCAUUUACCAA-3' 5'-AGAAUAGCAUUACUUCGA-3' 5'-CGUCAGAACCAAUUUUUCA-3'	Dharmacon
Non-targeting (nt)	5'-UGGUUUACAUGUCGACUAA-3'	Dharmacon

3.11.2 Experimental procedure

For each transfection, 2×10^6 HUVECs were suspended in 100 μ l HUVEC Nucleofector Solution and added to 3 μ g of the respective siRNA. The mixture of cells and siRNA was transferred to an Amaxa certified cuvette and transfection was performed (program A-034). Immediately after electroporation, 950 μ l of prewarmed growth medium was added to the cells. Afterwards, cells were seeded into 24-well plates (250,000 cells per well) and 24 hours after transfection, cells were stimulated with TNF α for additional 24 hours prepared for flow cytometry analysis. Transfection efficiency was checked by Western blot analysis. For this purpose cells were seeded in 6-well plates (500,000 cells per well).

3.11.3 Application of shRNA via adenoviral vectors

Additionally, we used adenoviral vectors encoding short hairpin RNA (shRNA) for gene function analysis. HUVECs, containing shRNA control and shRNA Cdk9 vectors were purchased from Sirion (Sirion Biotech GmbH, Martinsried, Germany). These cells were seeded into 24-well plates and 72 hours after infection, cells were incubated for additional 24 hours with TNF α and prepared for FACS analysis. Efficient knock-down of Cdk9 was checked by Western blot analysis (cells were seeded in 6-well plates).

3.11.4 Dual Luciferase[®] Reporter assay system

Because of their distinct evolutionary origins, firefly and renilla luciferases have different enzyme structures and substrate requirements. These differences make it possible to selectively discriminate between their respective bioluminescent reactions. Thus, using the Dual Luciferase[®] Reporter (DLR) assay system, the luminescence from the firefly luciferase reaction may be quenched while simultaneously activating the luminescent reaction of Renilla luciferase.

The expression plasmid pGL4.32 [luc2P/NF- κ B-RE/Hygro], a firefly luciferase reporter gene, contains five copies of an NF- κ B response element (NF- κ B-RE). As expression control, pGL4.74 [*hRluc*/TK], a Renilla luciferase was used (Promega, Madison, WI, USA). HUVECs were co-transfected with a ratio of 10:1 of expression plasmid and expression control by electroporation using amaxa[®] HUVEC

Nucleofector[®] kit (Lonza Cologne AG). After transfection, 80,000 cells/ml were seeded in 96-well plates and 24 h later stimulated with increasing concentrations of flavopiridol (1 to 300 nM) for 30 minutes followed by 5.5 hours TNF α -treatment. Subsequently, cells were washed once with PBS+ Ca²⁺/Mg²⁺, completely removed and lysed with 20 μ l Passive Lysis Buffer (1x; diluted 1:5 from 5x Passive Lysis Buffer, Promega, Mannheim, Germany). Following a freezing step, cell lysates were allowed to thaw 15 minutes at room temperature under mild agitation. Luciferase Assay reagent II and Stop & Glo buffer were prepared freshly according to the manufacturer's instructions (DLR Assay System, Promega) and used for injectors 1 and 2, respectively. The luminometer was programmed to perform a 2 sec. measurement delay followed by a 10 sec. measurement read for both luciferase activities. 20 μ l of each sample were transferred into luminometer plates and measured using a luminometer (Berthold Orion II, Berthold Detection Systems, Pforzheim, Germany). Reaction was initiated by injecting 100 μ l of Luciferase Assay reagent II followed by Stop & Glo buffer into each well.

NF- κ B promoter activity was assessed as x-fold change of firefly luciferase activity after normalization for Renilla luciferase activity.

3.12 Electrophoretic mobility shift assay

3.12.1 Extraction of nuclear proteins

For the preparation of nuclei, HUVECs were treated as indicated and washed twice with ice-cold PBS. The PBS was removed completely and cells were lysed by adding 400 μ l nuclear extraction buffer A. Cells were scraped off the plate/dish and transferred to 1.5 ml reaction tubes. Cells were allowed to swell on ice for 15 min. Nonidet P-40 (0.625%) was added, followed by 10 sec. of vigorous vortexing. Probes were centrifuged (14,000 rpm, 1 minute, 4°C), supernatants removed, and pellets incubated for 30 minutes under agitation at 4°C in 40 μ l nuclear extraction buffer B. After centrifugation (14,000 rpm, 5 minutes, 4°C), supernatants were collected and frozen at -80°C. Protein concentrations were determined by Bradford assay.

Extraction buffer A		Extraction buffer B	
HEPES, pH 7.9	10 mM	HEPES, pH 7.9	20 mM
KCl	10 mM	NaCl	0.4 mM
EDTA	0.1 mM	EDTA	0.1 mM
EGTA	0.1 mM	EGTA	0.1 mM
DTT	1.0 mM	DTT	1.0 mM
PMSF	0.5 mM	PMSF	0.5 mM
		Glycerol	25%

3.12.2 Protein quantification: Bradford assay

Bradford assay (Bradford solution, Bio-Rad) was performed as described previously (85). It employs Coomassie Brilliant Blue as a dye, which binds to proteins. 10 μ l protein samples were incubated with 190 μ l Bradford solution (1:5 dilution in water) for 5 min. Thereafter, absorbance was measured photometrically at 592 nm (Tecan Sunrise Absorbance reader, TECAN). Protein standards were obtained by diluting a stock solution of BSA (500 μ g/ml). Linear regression was used to determine the actual protein concentration of each sample.

3.12.3 Electrophoretic Mobility Shift Assay

The oligonucleotide for NF- κ B with the consensus sequence 5'-AGT TGA GGG GAC TTT CCC AGG C-3' was purchased from Promega. Using the T4 polynucleotide kinase the oligonucleotides were 5' end-labeled with [γ - 32 P]-ATP. Equal amounts of nuclear protein were incubated with 2 μ g poly(dIdC) and 3 μ l of freshly prepared reaction buffer for 10 minutes at room temperature. The binding-reaction was started by adding 1 μ l of the radioactive oligonucleotide and carried out for 30 minutes at room temperature. The protein-oligonucleotide complexes were separated by gel electrophoresis (Power TecTM HC, BioRad) with 0.25 x TBE buffer at 100 V for 60 minutes using non-denaturing polyacrylamide gels (5% PAA, 20% glycerol). After electrophoresis, gels were exposed to Cyclone Storage Phosphor Screens (Canberra-Packard, Schwadorf, Austria) for 24 hours, followed by analysis with a phosphor imager station (Cyclone Storage Phosphor System, Canberra-Packard).

5x Binding buffer		Loading buffer	
Tris/HCl	50 mM	Tris/HCl	250 mM
NaCl	250 mM	Glycerol	40%
MgCl ₂	5.0 mM	Bromphenolblue	0.2%
EDTA	2.5 mM		
Glycerol	20%		

Reaction buffer	
5x Binding buffer	90%
Loading buffer	10%
DTT	2.6 mM

TBE 10x	
Tris	890 mM
Boric acid	890 mM
EDTA	20 mM
H ₂ O	

3.13 *In vitro* IKK β kinase activity assay

The effect of flavopiridol on purified IKK β activity was determined using the HTScan[®] IKK β Kinase Assay Kit according to the instructions of the manufacturer (Cell Signaling Technology, Frankfurt/M., Germany). This assay measures the effect of flavopiridol on the phosphorylation of a biotinylated I κ B- α (Ser-32) substrate peptide. A phospho-I κ B- α (Ser-32/36)-specific mouse monoclonal antibody was used to detect the phosphorylated substrate peptide. For assay standardization, the kit provides an active GST-IKK β kinase fusion protein. Purified IKK β kinase was pretreated with different concentrations of flavopiridol (1-300 nM) 5 minutes prior to the treatment of substrate peptide. Each kinase assay was performed in duplicate. IKK β activity was expressed relative to kinase buffer 1x. 100 μ M Staurosporine was used as positive control.

3.14 Kinome array (PepChip)

A kinome array (PepChip) was performed to study the effects of flavopiridol on overall signaling in endothelial cells. PepChip performance and analysis of the results were done as described previously (86, 87) in collaboration with Dr. Jos Joore from Pepscan System BV, Lelystad, The Netherlands. Confluent HUVECs in 4x 100 mm dishes were treated with TNF α for 15 minutes or 30 minutes with 100 nM flavopiridol prior to 15 minutes TNF α incubation. After two washing steps with ice-cold PBS, native protein lysates of these cells were generated by lysing cells with M-PER Mammalian Protein Extraction Reagent (Pierce, Rockford, IL), containing 2.5 mM sodium pyrophosphate, 2 mM sodium β -glycerophosphate, 1 mM Na₃VO₄, and 1 mM NaF. Lysates were centrifuged at 14,000 rpm for 10 minutes at 4°C, and supernatants were frozen immediately in liquid nitrogen. Afterwards, 70 μ l lysates/array was mixed with 10 μ l activation solution (20 μ Ci [γ -³³P] ATP, 50% glycerol, 5 mM DTT, 50 mM MgCl₂, 50 mM MnCl₂, 250 μ g/ml PEG 8000, and 250 μ g/ml BSA) and centrifuged 5 minutes at 14,000 g. Next, 70 μ l of the supernatant was loaded onto the array and incubated for 2 hours at 37°C in saturated humidity. On the PepChip, 1152 different peptides with specific phosphorylation motifs for the respective kinases were spotted in triplicates. Chips were washed in 2 cycles, first 5 minutes in 2 M NaCl containing 1% Triton X-100, followed by 5 minutes in PBS containing 1% Triton X-100. Afterward, chips were rinsed 3 times with distilled water and then air-dried.

Phosphor-storage screens were exposed to the chip for 24 hours to determine and to quantify the phosphorylation status of peptides (i.e., kinase substrates), which gave information about the activity of the associated upstream kinase. The phosphorylation status of the chips was compared spot by spot. The results were ranked by extent of inhibition of phosphorylation.

3.15 Protein Kinase Assay (³³PanQinase[®] Activity Assay)

A radiometric protein kinase assay (³³PanQinase[®] Activity Assay) was used for measuring the kinase activity of 255 protein kinases. The analysis was done in collaboration with Dr. Frank Totzke from ProQinase GmbH, Freiburg, Germany.

All kinase assays were performed in 96-well FlashPlates™ from Perkin Elmer (Boston) in a 50 µl reaction volume. The reaction cocktail was pipetted in 4 steps in the following order: 10 µl of non-radioactive ATP solution (in H₂O), 25 µl of assay buffer/[γ-³³P]-ATP mixture, 5 µl of test sample in 10% DMSO, 10 µl of enzyme/substrate mixture. Flavopiridol was tested at 9 final semi-log assay concentrations in the range from 1 x 10⁻⁰⁵ M to 1 x 10⁻⁰⁹ M with a final DMSO concentration of 1%. The assay for all enzymes contained 60 mM HEPES-NaOH, pH 7.5, 3 mM MgCl₂, 3 mM MnCl₂, 3 µM Na₃VO₄, 1.2 mM DTT, 50 µg/ml PEG20000, 1 µM ATP/[γ-³³P]-ATP (approx. 6 x 10⁰⁵ cpm per well), protein kinase, and substrate. Since 9 distinct concentrations of flavopiridol were tested against each kinase, the evaluation of the raw data resulted in 9 values for residual activities per kinase. Based on each 9 corresponding residual activities, IC₅₀ values were calculated using Prism 5.02 for Windows (GraphPad; www.graphpad.com).

3.16 Statistical Analysis

Statistical analysis was performed with Prism software (version 3.03; GraphPad Software, San Diego, CA). All experiments were performed at least three times unless otherwise indicated in the figure legend.

Data were expressed as mean value ± SEM, and analyzed using One Way ANOVA, Student's t-test, or Mann-Whitney rank sum test. P values < 0.05 were considered as statistically significant.

4 Results

4.1 Anti-inflammatory effects of flavopiridol *in vivo*

4.1.1 Concanavalin A-induced liver injury model

The concanavalin A-induced liver injury model was performed in collaboration with PD Dr. Gabrielle Sass and Prof. Dr. Gisa Tiegs from the Division of Experimental Immunology and Hepatology, University Medical Center Hamburg-Eppendorf, Hamburg.

4.1.1.1 Flavopiridol protects against concanavalin A-induced liver injury

Concanavalin A (ConA) in a dosis of 15 mg/kg bodyweight is widely used as the optimal dose to induce murine hepatitis (88). We pretreated the mice with flavopiridol before intravenous administration of a single dose of ConA (15 mg/kg bodyweight). After eight hours we determined plasma transaminase activities as a pathologically important marker for liver injury. When the mice were pretreated with flavopiridol, ConA-induced hepatitis was greatly suppressed, as proven by a large decrease in the levels of the transaminases ALT and AST (7621 ± 690 U/L vs. 4245 ± 1403 U/L of ALT; 9156 ± 742 U/L vs. 3570 ± 952 U/L of AST) (Figure 4.1).

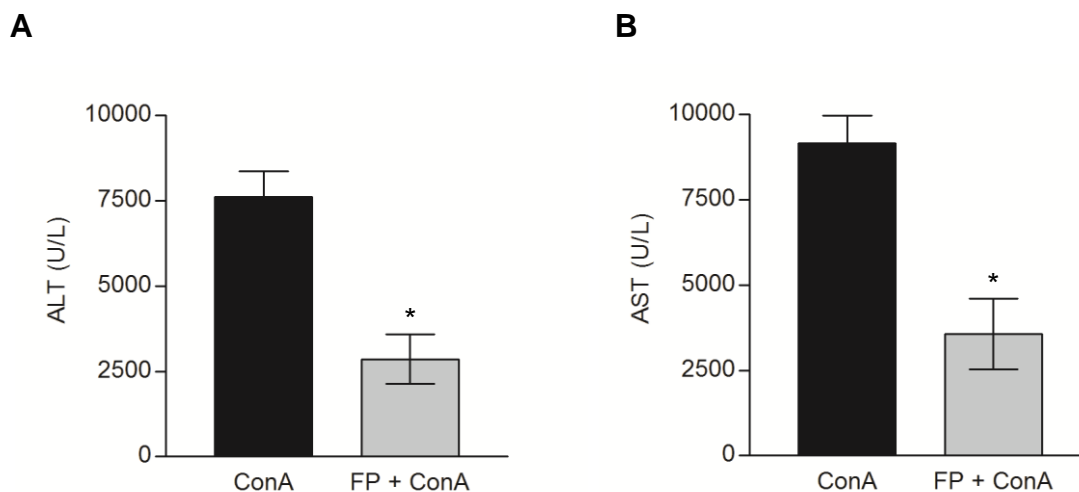


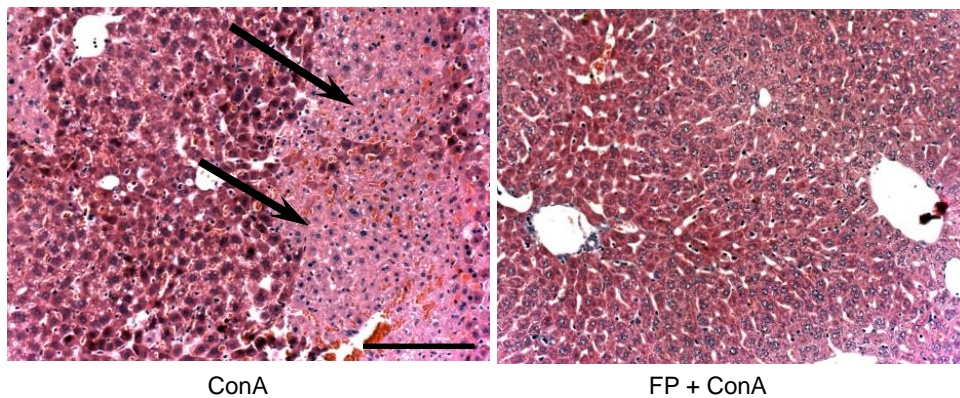
Figure 4.1: Flavopiridol protects against ConA-induced liver injury.

Mice were either treated (i.v.) with flavopiridol (FP, 44 ng in 250 μ l PBS, n = 6) or vehicle (250 μ l PBS, n = 6) 15 minutes prior to ConA injection (15 mg/kg bodyweight). Liver tissues were removed eight hours after ConA administration and plasma transaminase levels of ALT (A) and AST (B) were assessed. *, p < 0.01 vs. ConA, t-test.

4.1.1.2 Liver necrosis is reduced by flavopiridol

Liver damage was analyzed histologically eight hours after injection of ConA. Liver tissue was removed and embedded in paraffin for H&E staining. We observed degenerative changes and necrosis in the histological sections of livers from mice after eight hours of ConA treatment. Mice pretreated with flavopiridol presented decreased liver necrosis resulting in less hepatocyte destruction as shown in Figure 4.2 A. For statistical analysis the liver parenchyma with necrotic injury were calculated (Figure 4.2 B).

A



B

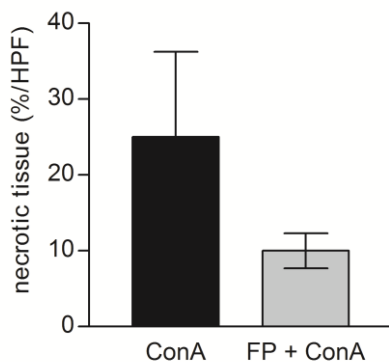


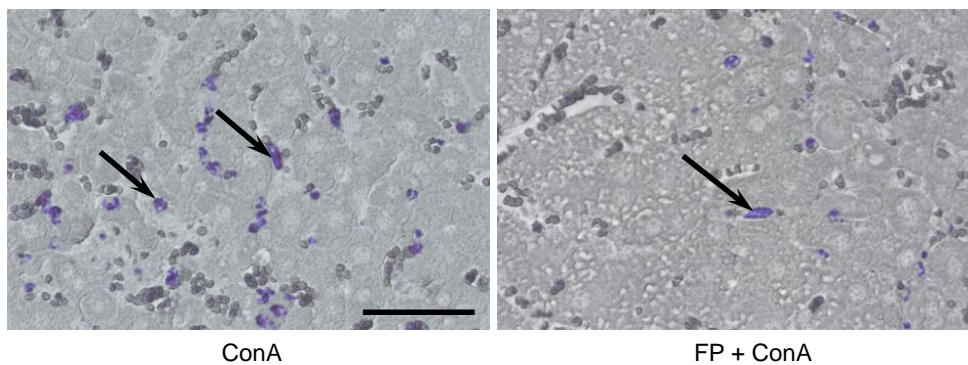
Figure 4.2: Liver necrosis is reduced by flavopiridol.

(A) Representative H&E-stained sections of livers after eight hours ConA treatment with or without pretreatment of flavopiridol (FP, 44 ng in 250 μ l PBS). Original magnification, 200x. Bar, 50 μ m. Arrows indicate necrotic area. (B) The graph represents the quantitative evaluation of liver parenchyma with necrotic injury. HPF (high power field) = original magnification, 200x.

4.1.1.3 Flavopiridol inhibits the infiltration of neutrophils into the liver

Neutrophils are the key initiators of lymphocyte recruitment and liver injury caused by ConA (89). Liver tissue sections were stained for neutrophil naphthol esterase to specify the phenotype of emigrated leukocytes. The number of infiltrated neutrophils in the liver parenchyma was counted around hepatic and portal venules and sinusoids in stained sections. Pretreatment with 100 nM flavopiridol attenuated the ConA-induced transmigration of neutrophils (Figure 4.3 A). In addition, we investigated the myeloperoxidase (MPO) activity of the liver, an index of neutrophil infiltration. Pretreatment with flavopiridol significantly suppressed ConA-induced MPO activity and, therefore, neutrophil infiltration into liver tissue (Figure 4.3 B).

A



B

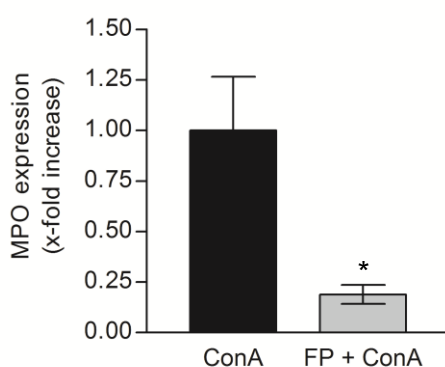


Figure 4.3: Flavopiridol attenuates the infiltration of neutrophils into the liver tissue.

(A) Representative sections of liver tissue demonstrate staining for naphthol AS-D chloroacetate esterase. Arrows indicate extravasated neutrophils. Original magnification, 400x. Bar, 100 μ m. (B) For statistical evaluation of the infiltrated neutrophils MPO activity of liver tissues was measured.

*, $p < 0.01$ vs. ConA, t-test.

4.1.1.4 Flavopiridol reduces levels of ICAM-1 and E-selectin in the liver

Upon ConA injection, a massive induction of hepatic ICAM-1 and E-selectin expression occurs (90). We performed quantitative RT-PCR analysis of liver tissues to assess ICAM-1 and E-selectin mRNA levels. In ConA-induced liver injury samples, we discovered reduced ICAM-1 mRNA levels when mice were pretreated with flavopiridol. In addition, we also found that mRNA levels of the endothelium-specific cell adhesion molecule E-selectin were suppressed with flavopiridol. These results suggest that flavopiridol might also have an impact on liver endothelial cells.

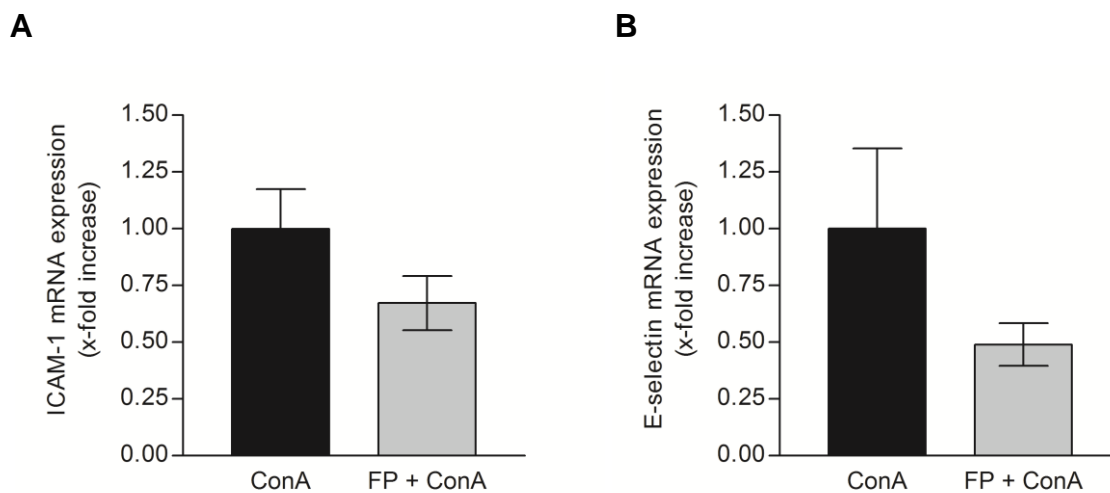


Figure 4.4: Flavopiridol reduces ConA-induced ICAM-1 and E-selectin mRNA levels.

Quantitative RT-PCR analysis of ConA-treated liver tissue. Flavopiridol-pretreated liver tissues showed reduced ICAM-1 (A) and E-selectin mRNA (B) levels. ICAM-1 and E-selectin expression in ConA-treated mice was set as 1.0, respectively. Data are expressed as ratios ICAM-1/GAPDH and E-selectin/GAPDH.

4.1.2 Cremaster muscle model

The surgical preparation of the cremaster muscle and intravital microscopy were performed in collaboration with Dr. Alexander Khandoga and Prof. Dr. Fritz Krombach from the Walter Brendel Center of Experimental Medicine, University of Munich.

4.1.2.1 Flavopiridol reduces leukocyte-endothelium interactions *in vivo*

We studied leukocyte adhesion and transmigration in TNF α -treated cremaster muscle venules using intravital microscopy (IVM). Flavopiridol was administered intravenously before the mice were treated intrascrotally with TNF α for four hours prepared for microscopical analysis. Leukocyte adherence on the venular endothelium was reduced by almost 40%, when mice were treated with flavopiridol (8.7 ± 1.4 n/10 4 μm^2 vs. 12.4 ± 1.8 n/10 4 μm^2) (Figure 4.5 A). The number of extravasated leukocytes was significantly reduced in mice co-treated with flavopiridol in comparison to mice treated with TNF α alone (11.2 ± 0.5 n/10 4 μm^2 vs. 17.5 ± 0.6 n/10 4 μm^2) (Figure 4.5 B).

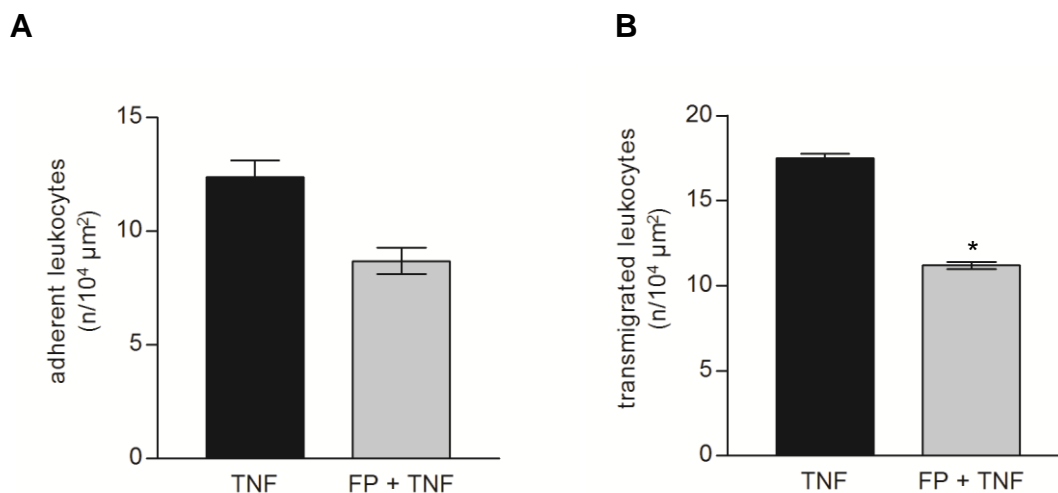


Figure 4.5: Flavopiridol attenuates TNF α -evoked leukocyte-endothelium interaction *in vivo*.

Mice were treated (i.v.) with flavopiridol (FP, 11 ng in 250 μl PBS, n=3) or PBS as control (n=3) followed by intrascrotal injection of TNF α (TNF, 300 ng in 400 μl PBS). The number of adherent (A) and transmigrated (B) leukocytes was quantified in cremasteric venules by intravital microscopy four hours after TNF α -injection. *, p < 0.05 vs. TNF α , Mann-Whitney rank sum test.

4.1.2.2 Microvascular parameters in cremaster muscle venules

Microvascular parameters during the IVM experiments were measured to assure intergroup comparability. Flavopiridol treatment in TNF α activated cremaster muscle venules did not affect parameters like diameters of analyzed microvessels, centerline blood flow velocity, wall shear rate, and systemic white blood counts (Table 4.1).

Table 4.1: Microvascular parameters in cremaster muscle venules.

Mice were treated (i.v.) with flavopiridol (11 ng in 250 μ l PBS, n=3) or PBS as control (n=3) followed by intrascrotal injection of TNF α (300 ng in 400 μ l PBS). In each animal, at least five single unbranched postcapillary venules were analyzed.

Parameter	PBS + TNF α	Flavopiridol + TNF α
vessel diameter (μ m)	26.2 \pm 1.1	25.5 \pm 0.2
white blood cell count (10 ⁶ cells/m)	6.9 \pm 1.8	5.8 \pm 1.0
centerline blood flow velocity (mm/s)	1.56 \pm 0.04	1.52 \pm 0.09
wall shear rate (s ⁻¹)	480.5 \pm 30.0	482.9 \pm 23.1
rolling flux fraction (%)	7.9 \pm 2.2	8.2 \pm 3.1

4.1.2.3 Motility of interstitially migrating leukocytes

We assessed the motility of interstitially migrating leukocytes to further characterize the observed effect of leukocyte-endothelium interactions. No differences were determined between the two groups in the distribution of rolling velocities, i.e., curve-line, and straight-line migration distances (Table 4.2), suggesting that flavopiridol has no influence on the migration of leukocytes.

Table 4.2: Effect of flavopiridol on motility of interstitially migrating leukocytes *in vivo*.

Mice were treated (i.v.) with flavopiridol (11 ng in 250 μ l PBS, n=3) or PBS as control (n=3) followed by intrascrotal injection of TNF α (300 ng in 400 μ l PBS). For single cell tracking of migrated leukocytes, intravital microscopic video recordings were analyzed using the imaging software "Simple PCI" (Hamamatsu Corporation/Compix Inc.). On each side of the analyzed vessel, at least 15 emigrated leukocytes were identified within ROIs and tracked in the perivascular space within a time period of 5 min. Parameters of leukocyte motility, such as curve-line and straight-line velocities were automatically calculated by the software.

Parameter	PBS + TNF α	Flavopiridol + TNF α
Curve-line velocity (μ m/sec)	19.3 \pm 1.8	20.5 \pm 1.4
Curve-line distance (μ m)	96.5 \pm 6.5	102.3 \pm 5.5
Straight-line velocity (μ m/sec)	3.0 \pm 0.7	2.9 \pm 0.4
Straight-line distance (μ m)	14.9 \pm 2.9	14.6 \pm 1.9

4.1.2.4 Flavopiridol inhibits ICAM-1 expression in cremaster muscle tissue

We analyzed the mRNA expression of ICAM-1 to investigate whether flavopiridol has an influence on the cell adhesion molecules of the activated endothelium of the cremaster muscle. We observed a significant decrease of ICAM-1 mRNA expression in flavopiridol treated cremaster muscle tissue (Figure 4.6).

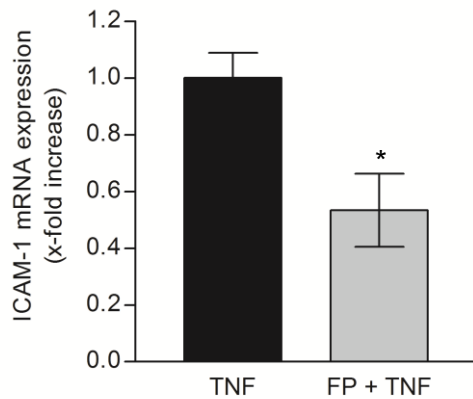


Figure 4.6: Flavopiridol reduces TNF α -evoked ICAM-1 mRNA levels *in vivo*.

Quantitative RT-PCR analysis of cremaster muscle tissue. ICAM-1 mRNA levels are significantly reduced in tissues when mice were treated with flavopiridol (FP; 11 ng in 250 μ l PBS, n=3) before treatment for four hours with TNF α (300 ng in 400 μ l PBS). ICAM-1 expression in cremaster muscle tissue of TNF α -treated mice was set as 1.0. Data are expressed as the ratio ICAM-1/GAPDH.

*, $p < 0.05$ vs. TNF α , t-test.

4.2 Cell viability and apoptosis

To analyze the influence of flavopiridol on inflammatory actions on endothelial cells *in vitro* we firstly excluded the possibility of a cytotoxic effect of flavopiridol on HUVECs. Therefore, we measured the cell viability and apoptotic cell rate up to 48 hours with a focus on the concentration of 100 nM which is used in our experiments.

4.2.1 Effects of flavopiridol on endothelial cell viability

Confluent HUVECs were stimulated with increasing concentrations of flavopiridol for 24 and 48 hours. The cells showed a significant reduction of metabolic activity at a concentration of 200 nM flavopiridol, although about 80% of the cells remained viable. As shown in Figure 4.7, no significant loss of metabolic activity was measured by treatment with 100 nM flavopiridol up to 48 hours, indicating no acute cytotoxicity of 100 nM flavopiridol compared to the controls (100%). We verified that the concentration of flavopiridol used in this study (100 nM) is well-tolerated by HUVECs.

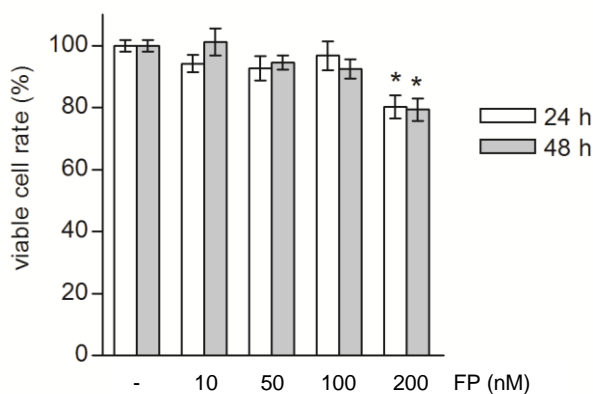


Figure 4.7: Effects of flavopiridol on the viability of HUVECs.

Confluent HUVECs were treated for 24 and 48 hours with increasing concentrations of flavopiridol (FP, 10-200 nM). The viable cell rate was determined by CellTiter-Blue™ assay which is based on the conversion of resazurin to resorufin as an indicator of the metabolic activity. Viable cell rate is expressed as percentage of the control cells (100%). *, $p < 0.01$ vs. control cells, one way ANOVA.

4.2.2 Effects of flavopiridol on apoptosis

In various types of cancer cells, flavopiridol was shown to induce apoptosis (64). By staining the chromatin of endothelial cells with the intercalating agent propidium iodide (PI), we determined DNA fragmentation to exclude apoptotic effects of flavopiridol. HUVECs were treated with flavopiridol (10-200 nM), stained with propidium iodide after 24 and 48 hours, and sub-G0/G1 peaks, adopted widely as one of the reliable biochemical markers of apoptosis, were subsequently assessed by flow cytometry. We found that flavopiridol has no significant effect on apoptosis in confluent HUVECs after 24 and 48 hours (Figure 4.8).

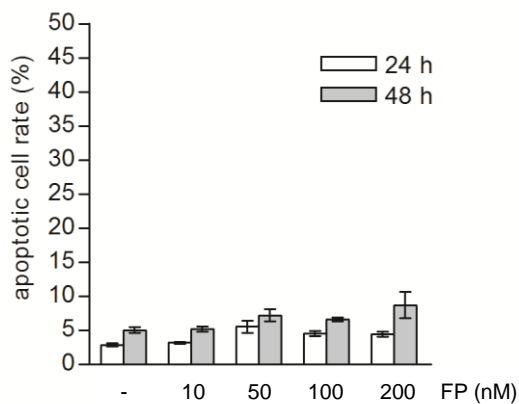


Figure 4.8: Flavopiridol has no influence on apoptosis in endothelial cells.

Confluent HUVECs were treated 24 and 48 hours with increasing concentrations of flavopiridol (FP, 10–200 nM) compared with control cells (-). The apoptotic cell rate was analyzed according to the Nicoletti method by flow cytometry. Sub-G1 peaks are expressed as apoptotic cell rate as percentage. $p > 0.05$ vs. control cells, one way ANOVA.

In summary, we proved that 100nM flavopiridol does not induce apoptosis or affect viability of confluent HUVECs up to 48 hours.

4.3 Anti-inflammatory actions of flavopiridol *in vitro*

Flavopiridol demonstrated strong inhibitory effects on inflammatory actions *in vivo*. Thus, to elucidate anti-inflammatory effects of flavopiridol *in vitro* we analyzed its influence on the leukocyte-endothelium interactions and characterized the impact of flavopiridol to interfere with inflammation-induced events.

4.3.1 Flavopiridol reduces neutrophil-endothelium interactions

The adhesion of human neutrophils to human umbilical vein endothelium cell (HUVEC) monolayers was studied in a static adhesion assay *in vitro*. Neutrophils were activated with fMLP (10^{-7} M) for 30 minutes before they were added to the HUVEC monolayer. We investigated neutrophil adhesion to TNF α -activated HUVECs (24 hours), which were pretreated by flavopiridol (30 minutes). Pretreatment of the endothelium with flavopiridol inhibited the adhesion of neutrophils to the TNF α -activated monolayer by 40% (Figure 4.9). When neutrophils were stimulated 30 minutes with flavopiridol before activation with fMLP, the number of adherent neutrophils was not altered, suggesting that the primary target of flavopiridol are endothelial cells, but not neutrophils.

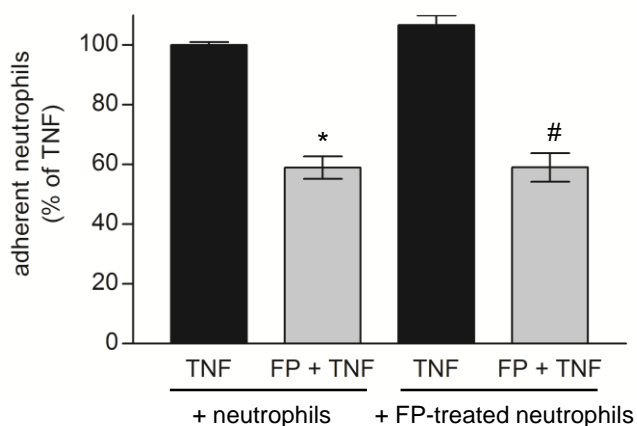


Figure 4.9: Flavopiridol reduces adhesion of neutrophils to HUVEC monolayers.

HUVECs were activated 24 hours by TNF α with or without pretreatment of flavopiridol (FP, 100 nM). Two groups of neutrophils were prepared: one group without treatment and one group with flavopiridol (FP, 100 nM) treatment. The numbers of adherent neutrophils on the TNF α -activated HUVEC monolayer were quantified by analyzing MPO activity. Data are expressed as percentage of TNF α -activated cells. *, $p < 0.05$ compared to TNF α -activated HUVECs, coincubated with neutrophils, t-test; #, $p < 0.05$ compared to TNF α -activated HUVECs, coincubated with flavopiridol-treated neutrophils, t-test. Representative data out of three independent experiments are shown.

4.3.2 Influence of flavopiridol on leukocyte activation

To further exclude that flavopiridol exerts its anti-inflammatory effects via directly targeting neutrophils, the influence of flavopiridol specifically on neutrophils was studied. Therefore, we addressed on the activation marker CD11b and oxidative burst activity.

Neutrophils activated for 15 minutes with fMLP (10^{-7} M) showed a distinct increase of CD11b expression compared with untreated neutrophils. Pretreatment of activated neutrophils with flavopiridol reduced CD11b expression on the neutrophil surface. We found that even with a 10-fold higher concentration of flavopiridol (1 μ M) than that used in our experiments (100 nM) the inhibitory effect on the expression of CD11b was not further affected (Figure 4.10 A). This indicates that flavopiridol has an effect on this cell surface marker, which is not expansible with increasing concentrations. Further investigations about the interactions between flavopiridol and neutrophils are necessary to make a concluding statement.

Polyphenols are known to act as scavenger of reactive oxygen species (ROS) released during the respiratory burst of neutrophils. Human neutrophils were stimulated with fMLP (10^{-7} M) and production of ROS [resulting in dihydrorhodamine (DHR) oxidation] was assessed in the presence or absence of 100 nM and 1 μ M flavopiridol. We observed no influence of flavopiridol on the ROS synthesis in neutrophils (Figure 4.10 B), which also indicates that the polyphenol flavopiridol does not simply act as a ROS scavenger. Due to these results we in the following focused on the action of flavopiridol on endothelial cells.

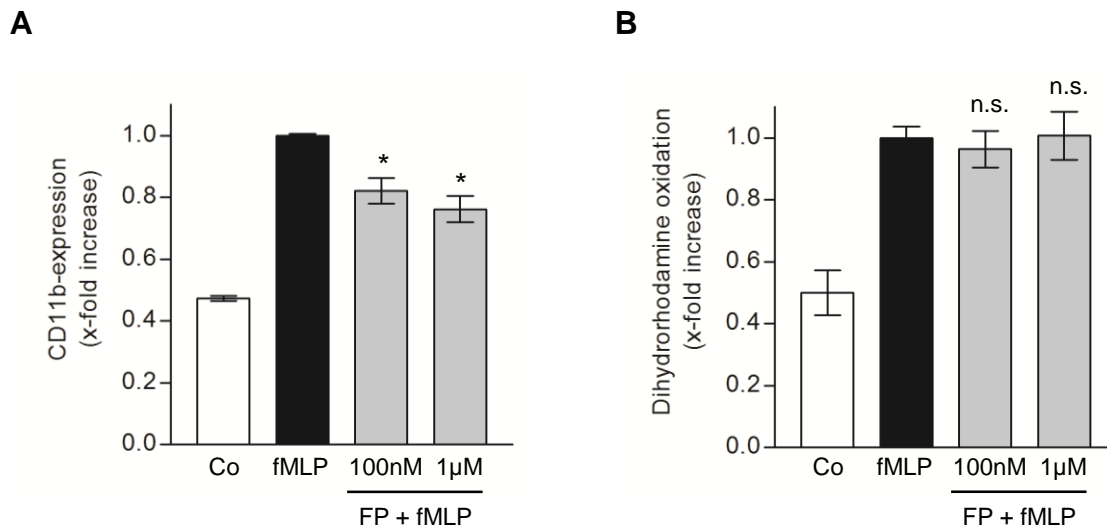


Figure 4.10: Effect of flavopiridol on leukocyte activation.

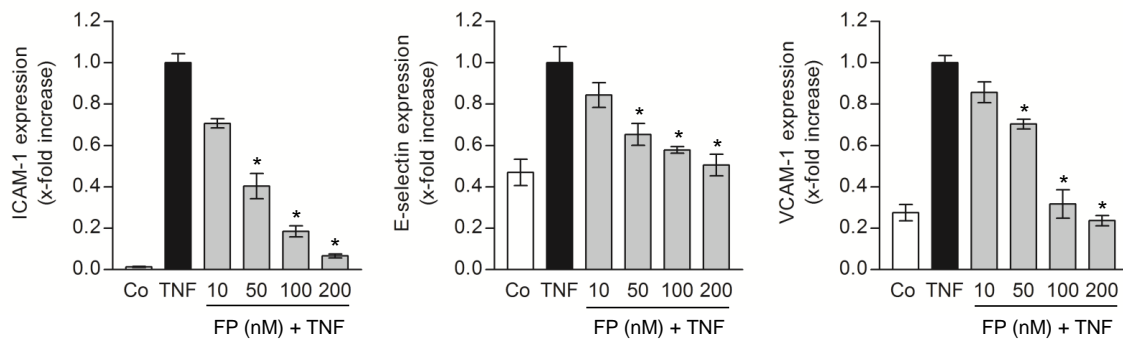
(A) Quantitative evaluation of the expression of the adhesion molecule CD11b. Expression of CD11b markedly increased after 15 minutes fMLP (10^{-7} M) stimulation compared with the control group (Co). Preincubation with flavopiridol attenuated the increase of expression of CD11b. Flavopiridol at a concentration of 100 nM and 1 µM act comparably. *, $p < 0.05$ vs. fMLP, one way ANOVA, $n = 3$.

(B) Isolated neutrophils were loaded with DHR and activated by fMLP (10^{-7} M) for 30 minutes. Some neutrophils were also treated with flavopiridol (100 nM and 1 µM) 30 minutes before activating by fMLP. ROS production of neutrophils was assessed by measuring the intracellular oxidation of DHR in a flow cytometer. n.s., not significant vs. fMLP, one way ANOVA, $n = 3$.

4.3.3 Flavopiridol reduces the expression of cell adhesion molecules

Activation of endothelial cells is characterized by expression of cell surface-adhesion molecules (CAM), such as the intercellular-adhesion molecule (ICAM-1), the vascular cell-adhesion molecule (VCAM-1), and E-selectin. Exposure of cells to $\text{TNF}\alpha$ (10 ng/ml) induced a strong up-regulation of ICAM-1, VCAM-1, or E-selectin surface expression (Figure 4.11 A) as detected by flow cytometry. Pretreatment with flavopiridol (10-200 nM) for 30 minutes inhibited the $\text{TNF}\alpha$ -induced upregulation of ICAM-1 ($\text{IC}_{50} = 27$ nM), VCAM-1 ($\text{IC}_{50} = 74$ nM), and E-selectin ($\text{IC}_{50} = 118$ nM) in a clear concentration-dependent manner. To figure out whether flavopiridol effects transcriptional regulation, we performed quantitative RT-PCR analysis to determine the mRNA levels of ICAM-1. As shown in Figure 4.11 B, $\text{TNF}\alpha$ induced a strong increase of ICAM-1 mRNA that is attenuated up to 70% by pretreatment with 100 nM flavopiridol. Flavopiridol alone did not affect the basal ICAM-1 mRNA expression.

A



B

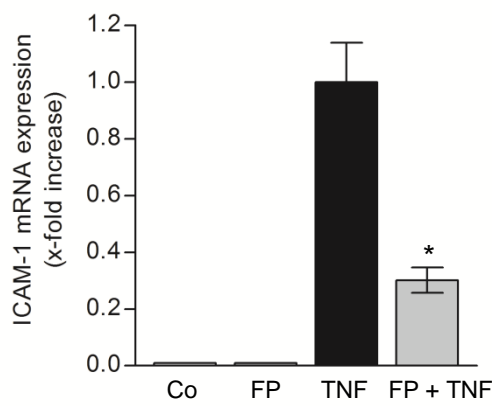


Figure 4.11: Flavopiridol reduces the expression of cell adhesion molecules on HUVECs.

(A) HUVECs were either left untreated (Co, control cells) or treated with $\text{TNF}\alpha$ (TNF, 10 ng/ml) for 24 hours (ICAM-1 and VCAM-1) or six hours (E-selectin). Additionally, cells were preincubated with increasing concentrations of flavopiridol (FP, 10–200 nM) for 30 minutes prior to $\text{TNF}\alpha$. ICAM-1, VCAM-1, and E-selectin expression on the cell surface of HUVECs were assessed by flow cytometry. Data are expressed as x-fold increase of $\text{TNF}\alpha$ activation. *, $p < 0.001$ vs. $\text{TNF}\alpha$, one way ANOVA, $n = 3$. (B) HUVECs were treated with flavopiridol (FP, 100 nM) alone for four hours or 30 minutes preincubation of flavopiridol were followed by four hours $\text{TNF}\alpha$ (10 ng/ml) activation. ICAM-1 mRNA expression was analyzed by quantitative RT-PCR. Data are expressed as ratio of ICAM-1/GAPDH and $\text{TNF}\alpha$ -stimulation (four hours) was set as 1.0. *, $p < 0.001$ vs. $\text{TNF}\alpha$, t-test, $n = 3$.

4.4 Effects of flavopiridol on NF- κ B signaling

4.4.1 Flavopiridol reduces NF- κ B promoter activity

Flavopiridol has the potency to reduce TNF α -induced expression of classical NF- κ B-dependent genes in HUVECs, including the adhesion molecules E-selectin, ICAM-1, and VCAM-1 (Figure 4.11). The promoters of the genes coding for these CAMs contain consensus binding sites for the transcription factor NF- κ B (91). To analyze whether the inhibition was due to reduced transcriptional activation by NF- κ B we used a luciferase-based *in vitro* NF- κ B reporter gene assay. In fact, flavopiridol suppressed TNF α -induced NF- κ B-dependent gene expression dose-dependently (Figure 4.12).

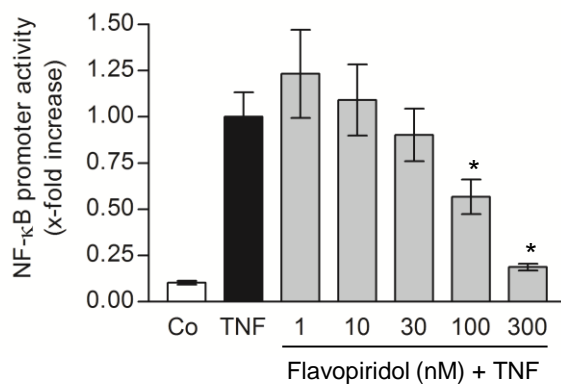


Figure 4.12: Flavopiridol reduces NF- κ B promoter activity.

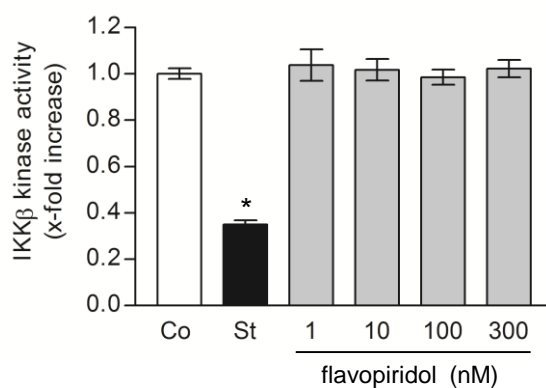
HUVECs were cotransfected with a firefly luciferase reporter vector, containing NF- κ B binding sites and a renilla luciferase reporter vector as control. 24 hours after transfection, HUVECs were preincubated with increasing concentrations of flavopiridol (1-300 nM) 30 minutes before activation by TNF α for 5.5 hours. A Dual Luciferase[®] Reporter assay system was used to assess NF- κ B promoter activities, which are expressed as ratio firefly luciferase/renilla luciferase activities. NF- κ B promoter activity of TNF α -stimulated cells was set as 1.0. *, $p < 0.05$ vs. TNF α , one way ANOVA, $n = 3$.

4.4.2 Flavopiridol has no effect on IKK α/β and I κ B α

We were now interested to investigate which stage of the NF- κ B activation cascade is affected by flavopiridol. TNF α activates NF- κ B via the canonical pathway based on phosphorylation-induced, proteasome-mediated degradation of I κ B α . The key regulatory step in this pathway involves the activation of a high molecular weight I κ B kinase (IKK) complex. In a cell-free kinase activity assay we observed no effect of flavopiridol on recombinant human IKK β kinase (Figure 4.13 A).

We also investigated the influence of flavopiridol on the activation (phosphorylation) of IKK α/β in HUVECs. After 5 minutes treatment with TNF α , phospho-IKK α/β was upregulated, which was not altered by flavopiridol pretreatment (Figure 4.13 B).

A



B

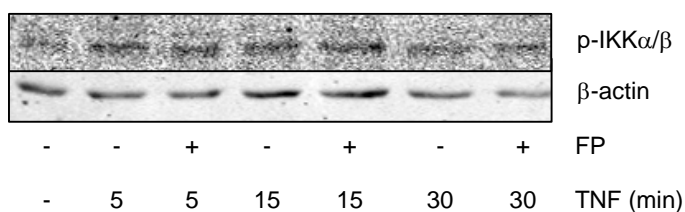


Figure 4.13: Flavopiridol has no influence on IKK α/β .

(A) Influence of increasing concentrations of flavopiridol on IKK β kinase activity was measured by optical density (HTScan[®] IKK β kinase assay). IKK β activity was expressed relative to kinase buffer 1x (Co, control), 100 μ M Staurosporine (St) was used as positive control. *, $p < 0.05$ vs. control, one way ANOVA, $n = 3$. (B) Western blot analysis was performed to investigate the influence of pretreatment with flavopiridol (FP, 100 nM) in TNF α -activated HUVECs on phospho-IKK α/β . The cells were pretreated 30 minutes with the protein phosphatase inhibitor calyculin (100 nM). β -actin was used as a loading control. Representative data out of three independent experiments are shown.

For its activation, NF- κ B has to be released from I κ B α , which is achieved by phosphorylation of I κ B α on two serine residues (Ser32/Ser36) followed by proteasomal degradation. As Western blot data show in Figure 4.14, TNF α induced a rapid degradation of I κ B α within minutes, followed by its reappearance after 60 minutes. Pre-treatment with flavopiridol resulted in no difference of TNF α -mediated I κ B α degradation. Additionally, we analyzed I κ B α at later time points (120–360 min), discovering a better recovering of I κ B α in flavopiridol-pretreated HUVECs.

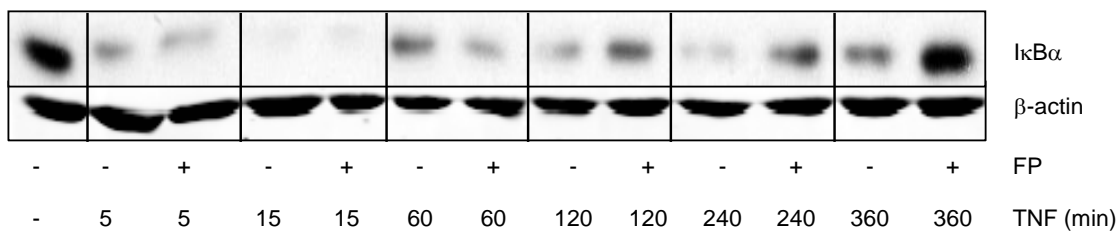


Figure 4.14: Flavopiridol has no influence on degradation of I κ B α .

Western blot analysis was performed to investigate the influence of pretreatment with flavopiridol (FP, 100 nM) in TNF α -activated HUVECs on the degradation of I κ B α . β -actin was used as a loading control.

4.4.3 Flavopiridol has no influence on p65

We tested whether flavopiridol has an effect on the nuclear translocation of p65. In the absence of TNF α , p65 is localized in the cytoplasm and treatment with TNF α increases nuclear translocation of p65 (Figure 4.15 A). Translocation of p65 was not altered when the cells were pretreated with flavopiridol. IKK β is known to phosphorylate p65 at Ser 536 and phospho-p65 (Ser536) is associated with an increased nuclear translocation of NF- κ B. Thus, we investigated whether flavopiridol influences the phosphorylation of p65 at Ser536 in TNF α -activated HUVECs. As shown in Figure 4.15 B, flavopiridol has no effect on TNF α -induced phosphorylation of p65 at Ser536.

In isolated nuclear extracts, incubated with [32 P]-labeled NF- κ B oligonucleotides, flavopiridol does not inhibit TNF α -induced binding activity of NF- κ B to DNA (Figure 4.15 C).

These findings suggest that flavopiridol has no influence on TNF α -mediated p65 translocation, phosphorylation, and NF- κ B DNA-binding activity, although we have shown that flavopiridol inhibits NF- κ B-dependent gene expression.

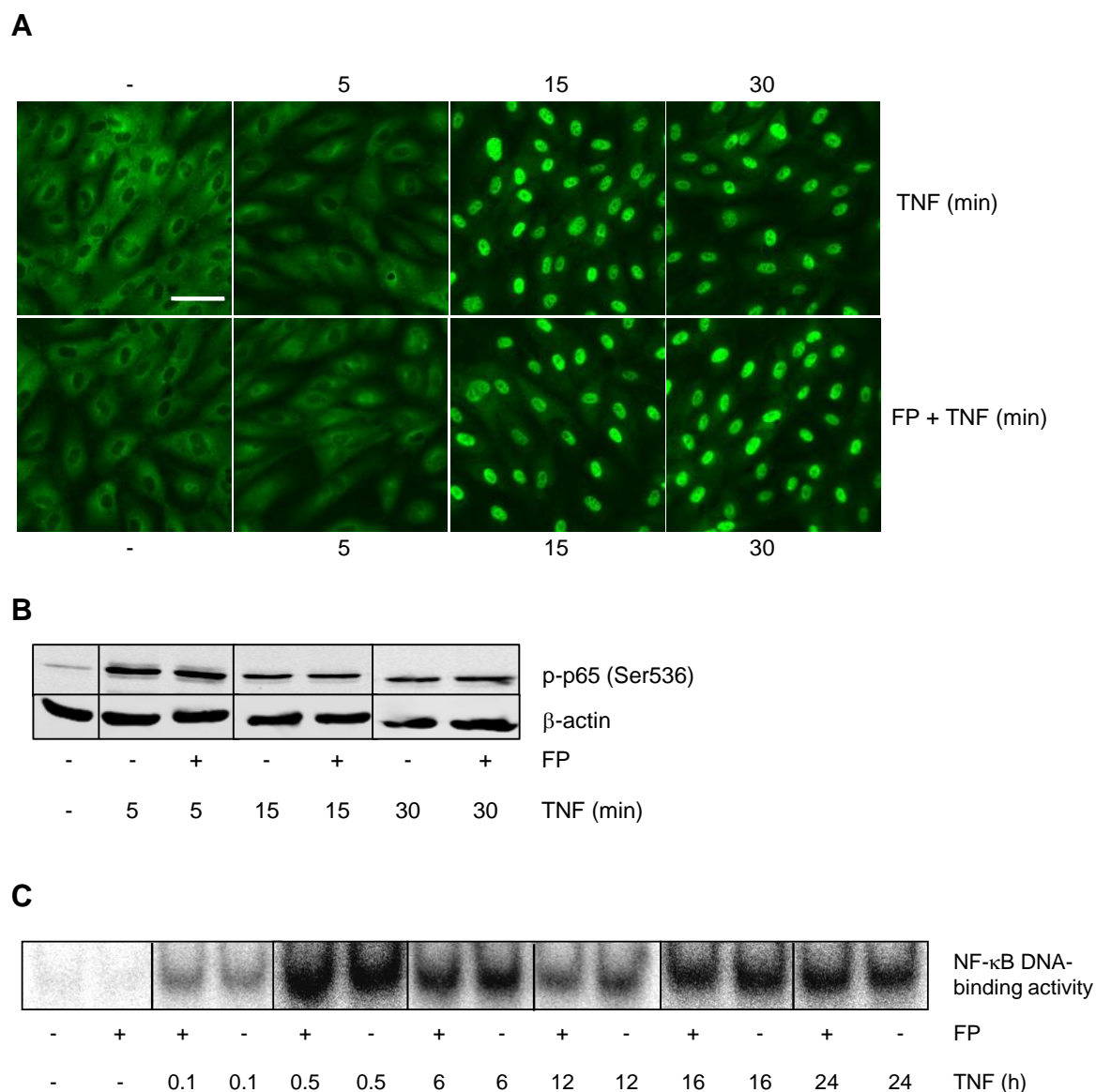


Figure 4.15: Flavopiridol has no influence on TNF α -induced phosphorylation and translocation of p65 as well as on NF- κ B DNA-binding.

(A) Immunofluorescence staining to visualize that 30 minutes pretreatment of flavopiridol (FP, 100 nM) has no effect on the nuclear translocation of the p65 subunit of NF- κ B in TNF α -activated HUVECs. Bar, 50 μ m. (B) Western blot analysis to investigate the influence of 30 minutes pretreatment of flavopiridol (FP, 100 nM) on phospho-p65 (Ser536) in TNF α -activated HUVECs. β -actin was used as a loading control. (C) NF- κ B binding activity was determined in nuclear extracts by electromobility shift assay (EMSA). HUVECs were treated with TNF α for the indicated time points with or without 30 minutes pretreatment of flavopiridol (FP, 100 nM). Representative data out of three independent experiments are shown.

4.5 Analysis of kinome alterations by flavopiridol

Because almost all cellular biochemical pathways are under strict control of reversible phosphorylation by kinases, we assumed that the anti-inflammatory effects of flavopiridol would be reflected in altered activity of these kinases. A major interest was to clarify the molecular mechanisms of the known kinase inhibitor flavopiridol in inflammatory events. Therefore, we performed a global approach using a kinome array (PepChip) containing 1,176 different oligopeptide kinase substrates.

The kinome array compared the phosphorylation patterns of HUVECs treated with TNF α for 15 minutes or treated 30 minutes with 100 nM flavopiridol prior to 15 minutes TNF α incubation. The effects of flavopiridol on rapid signal transduction were examined. Table 4.3 provides the top affected kinases with the highest reduction of activity. Strikingly, an important decrease in LIMK1, JNK1, CK2, and PKC θ was seen.

Table 4.3: Rapid flavopiridol-induced changes of kinome profiles in TNF α -treated HUVECs.

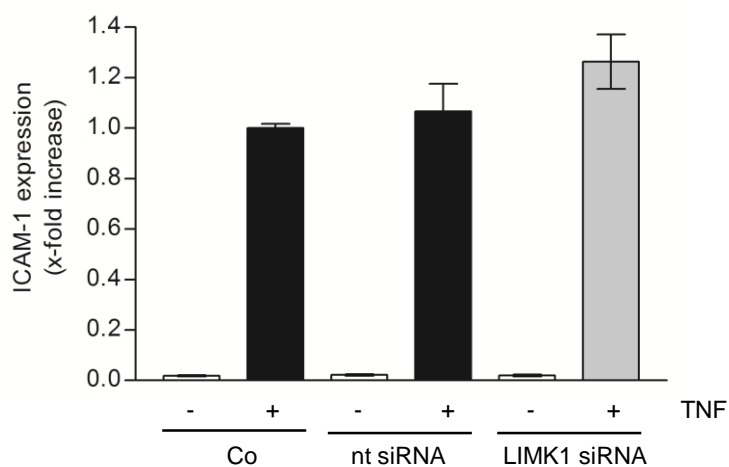
Kinome array (PepChip) data show kinases reduced most in their activity (R.A., residual activity) in lysates prepared from TNF α -activated HUVECs pretreated with flavopiridol (100 nM) compared with TNF α -activated HUVECs.

Kinase	Peptide sequence	R.A.
PKC θ	ESRSGSNRRER	0.61
CK2	QVSSLSESEES	0.46
JNK	APAAPTPAAPA	0.31
LIMK1	MASGVTVNDE	0.10

4.5.1 The influence of LIMK1, JNK, CK2 and PKC θ on ICAM-1 expression

As a next step we investigated whether the inhibition of these kinases is linked to the effect of flavopiridol on ICAM-1 expression to hit on the underlying mechanisms of the anti-inflammatory effects of flavopiridol in HUVECs. TNF α -activated HUVECs lacking LIMK1 show no change in ICAM-1 expression compared with nt siRNA transfected HUVECs (Figure 4.16).

A



B

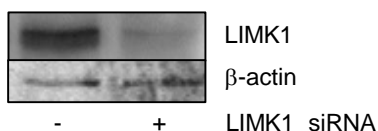


Figure 4.16: Effect of LIMK1 on ICAM-1 protein levels.

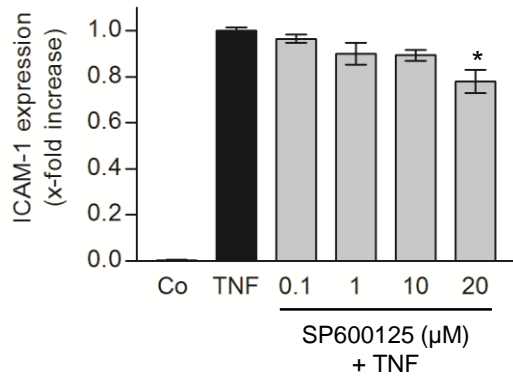
(A) Untransfected HUVECs and HUVECs transfected with LIMK1 siRNA and non-targeting (nt) siRNA were co-incubated with TNF α for 24 h. ICAM-1 expression was assessed by flow cytometry, expressed as x-fold increase of TNF α -activation.

(B) Immunoblotting visualizes sufficient downregulation of LIMK1, β -actin was used as a loading control.

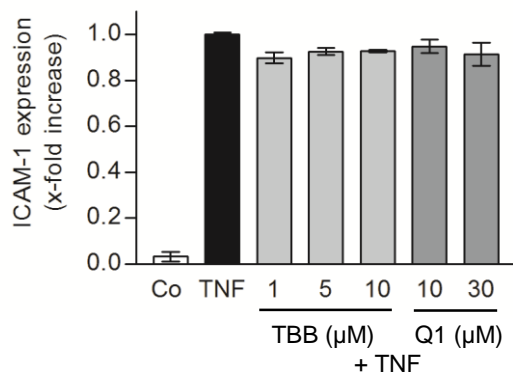
We used specific inhibitors of JNK, CK2, and PKC θ to determine the role of these kinases in the regulation of adhesion molecules induced by TNF α . We tested whether treatment with the JNK inhibitor SP600125, the CK2 inhibitors TBB and quinalizarin (Q1), or the myristoylated PKC θ pseudosubstrate inhibitor (PKC θ inh.) affected the expression of ICAM-1 induced by TNF α . The JNK inhibitor SP600125 only slightly decreased the expression of ICAM-1 by 20% at a concentration of 20 μ M. The CK2 inhibitors and the PKC θ pseudosubstrate inhibitor had no impact on the

TNF α -induced ICAM-1 expression (Figure 4.17 A, B, C). These data suggest that the effects of flavopiridol on ICAM-1 levels are not caused by LIMK1, JNK, CK2, or PKC θ .

A



B



C

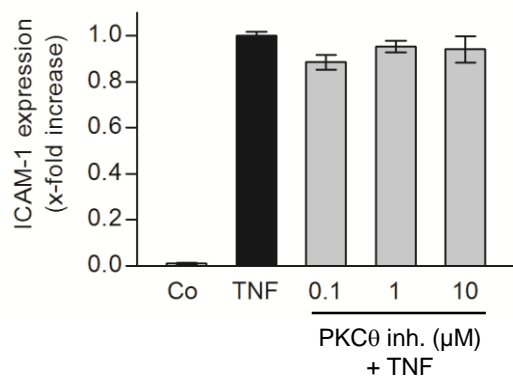


Figure 4.17: Effect of JNK, CK2, and PKC θ inhibitors on ICAM-1 protein levels.

TNF α -activated HUVECs were pretreated with increasing concentrations of the JNK inhibitor SP600125 (0.1-20 μ M) (A), the CK2 inhibitors TBB (1-10 μ M) and quinalizarin (Q1, 10-30 μ M) (B), and the myristoylated PKC θ pseudosubstrate inhibitor (PKC θ inh., 0.1-10 μ M) (C). ICAM-1 expressions were assessed by flow cytometry and expressed as x-fold increase of the TNF α activation. *, $p < 0.05$ vs. TNF α , one way ANOVA, $n = 3$.

4.6 Involvement of Cdks in inflammatory events

4.6.1 IC₅₀ profiling of flavopiridol

Since the kinome array did not cover Cdks, we determined the IC₅₀ profile using 255 protein kinases (³³PanQinase[®] Activity Assay). Flavopiridol appears as an unspecific kinase inhibitor (6), however this IC₅₀ profiling reveals that flavopiridol in low concentrations primarily acts as a Cdk inhibitor. The effects of flavopiridol on Cdks are shown in Table 4.4. We were especially interested in activities of flavopiridol at low nanomolar concentrations to gain information about the responsible actions for the strong inhibition of TNF α induced ICAM-1 levels (IC₅₀ = 27 nM). Only a few Cdks were sensitive to flavopiridol in the 1–100 nM range: Cdk4, Cdk6, Cdk8, and Cdk9.

Table 4.4: IC₅₀ profiling of flavopiridol (³³PanQinase[®] Activity Assay).

The IC₅₀ profile of flavopiridol was determined using 255 protein kinases, the table provides the IC₅₀ values of flavopiridol on Cdks.

Kinase	IC₅₀ (nM)	Kinase	IC₅₀ (nM)
Cdk1/CycA	120	Cdk4/CycD3	19
Cdk1/CycB1	110	Cdk5/p25NCK	480
Cdk1/CycE	96	Cdk5/p35NCK	570
Cdk2/CycA	210	Cdk6/CycD1	36
Cdk2/CycE	260	Cdk7/CycH	440
Cdk3/CycE	280	Cdk8/CycC	21
Cdk4/CycD1	20	Cdk9/CycT	4.9

4.6.2 Effect of a specific Cdk4/6 inhibitor on ICAM-1

The investigation of the effect of Cdk4 and Cdk6 on ICAM-1-expression with the specific Cdk4/6 inhibitor fascaplysin seemed interesting because of the kinase profiling of flavopiridol (Table 4.4). Our data reveal that fascaplysin has no influence on the upregulation of ICAM-1 by $\text{TNF}\alpha$ in HUVECs (Figure 4.18). Thus, we found no correlation between Cdk4/6 and the adhesion molecule ICAM-1.

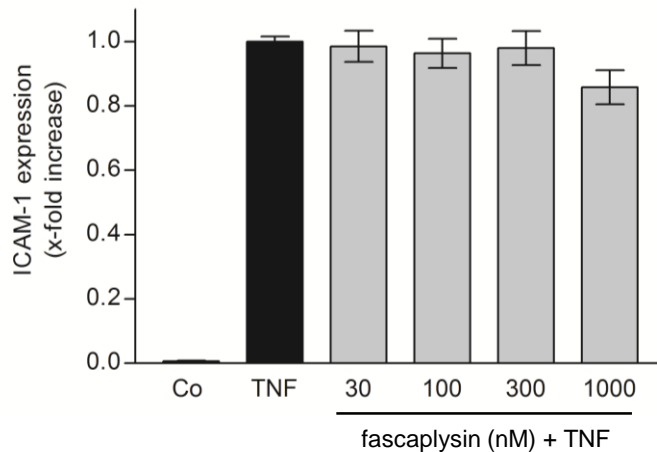


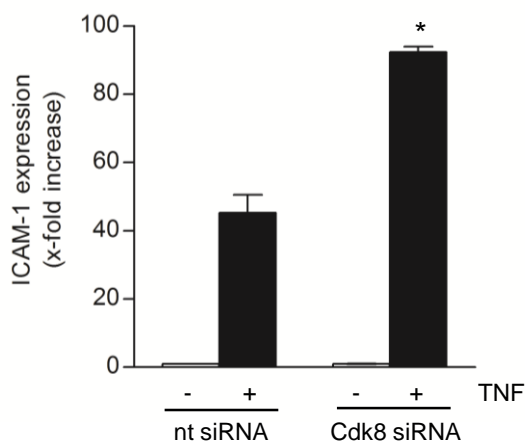
Figure 4.18: Effect of fascaplysin on ICAM-1 cell surface expression.

ICAM-1 expressions of HUVECS treated 30 minutes with the dual Cdk4/6-inhibitor fascaplysin (30-1000 nM) followed by 24 hours treatment of $\text{TNF}\alpha$ were assessed by flow cytometry. Data are expressed as x-fold increase of $\text{TNF}\alpha$ activation, $n = 3$.

4.6.3 ICAM-1 expression in the absence of Cdk8

Another interesting Cdk emerging from the kinase profiling of flavopiridol is Cdk8 (Table 4.4). TNF α -activated HUVECs deficient in Cdk8 show a strong increase in ICAM-1 expression compared with nt siRNA transfected HUVECs (Figure 4.19).

A



B

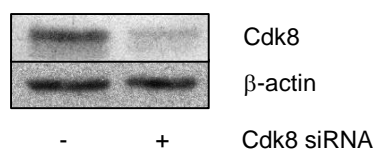


Figure 4.19: ICAM-1 cell surface expression in the absence of Cdk8.

(A) HUVECs transfected with Cdk8 siRNA and non-targeting (nt) siRNA were co-incubated with TNF α for 24 hours. ICAM-1 expressions were assessed by flow cytometry, expressed as x-fold increase of the control cells, respectively. *, $p < 0.05$ vs. nt siRNA transfected HUVECs treated with TNF α , t-test. (B) Immunoblotting visualizes efficient downregulation of Cdk8, β -actin was used as a loading control. Representative data out of three independent experiments are shown.

4.6.4 The loss of Cdk9 has a strong effect on ICAM-1 expression

To study the functional significance of Cdk9 in the regulation of ICAM-1 *in vitro*, we used a shRNA-based strategy to knock down Cdk9 expression. The continuous expression of the Cdk9 shRNA from the adenovirus in the transduced cells has the advantage of a stable knock-down of Cdk9 over a longer period of time. The protein levels of Cdk9 were significantly reduced by the Cdk9 shRNA (Figure 4.20 A). We discovered that TNF α -activated HUVECs transduced with shRNA Cdk9 show a strong reduction of ICAM-1 protein levels compared with cells expressing Cdk9 (Figure 4.20 B). For the Cdk9 shRNA-transduced HUVECs, ICAM-1 expression was reduced by 70% compared with cells infected with the control shRNA. These results strongly suggest that the inhibition of Cdk9 has an impact on TNF α -dependent upregulation of ICAM-1 protein levels in endothelial cells. Cdk9 might represent the target of flavopiridol responsible for ICAM-1 reduction.

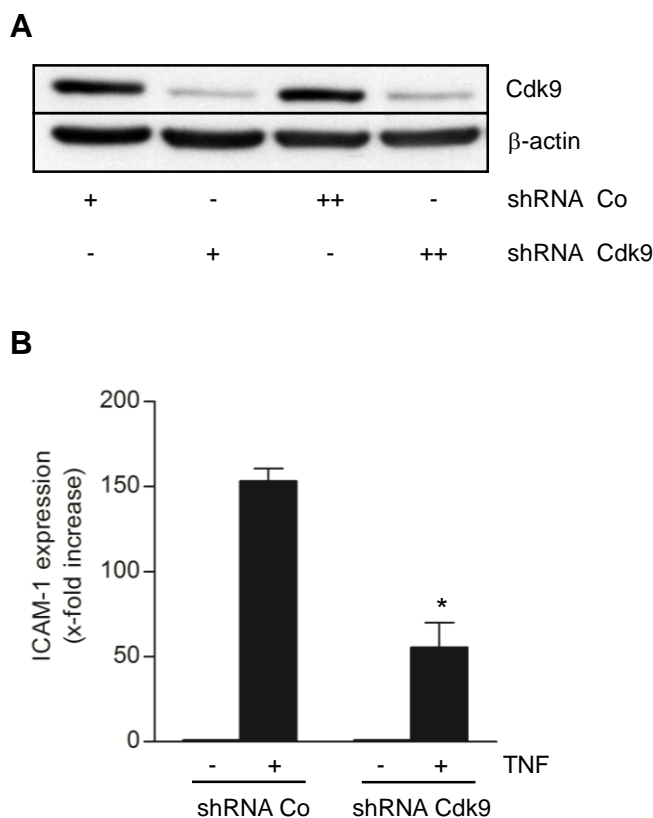


Figure 4.20: The loss of Cdk9 has a strong effect on ICAM-1 cell surface expression.

(A) Detection of Cdk9 in HUVECs transfected with shRNA against Cdk9 (shRNA Cdk9) or a control shRNA (shRNA Co) treated with TNF α 72 hours after transduction (+) and 24 hours later (++) . β -actin was used as a loading control. (B) 72 hours after transduction the cells were treated 24 hours with TNF α . ICAM-1 expression is assessed by flow cytometry, expressed as x-fold increase of the control cells. *, $p < 0.01$ vs. shRNA control transduced HUVECs treated with TNF α , t-test. Representative data out of three independent experiments are shown.

5 Discussion

5.1 Flavopiridol protects against inflammatory actions

Treatment of inflammatory diseases today is largely based on interrupting the synthesis or action of mediators that drive the host's response to injury, such as non-steroidal anti-inflammatory drugs (NSAIDs), steroids, and antihistamines (92). Currently, limited efficacy and severe side-effects of anti-inflammatory agents have encouraged the extensive search for more specific compounds for the inflammatory response (3). Recently, Cdk inhibitors were suggested to play relevant roles in processes regarding immune response. The Cdk inhibitor roscovitine has been shown to promote apoptosis of human neutrophils and enhance the resolution of inflammation (8). The discovery of flavopiridol in inflammatory responses is still in early stages and the key factors and molecular mechanisms that regulate inflammatory gene expression are explored insufficiently.

5.1.1 The impact of flavopiridol on concanavalin A induced liver injury

Acute liver failure induced by intravenous injection of concanavalin A (ConA) is one of the well-known mouse models of T cell-dependent liver injury. This model is characterized by inflammatory infiltration of the liver by neutrophils and simultaneous increase in levels of transaminases in the blood shortly (8–24 h) after ConA challenge (88). The plasma transaminases are important pathological markers and elevated levels are associated with liver cell damage (93). Flavopiridol is effective in attenuating levels of plasma transaminases ALT and AST, which displays its potency in ConA-induced liver injury. Furthermore, flavopiridol protects against a significant increase of infiltrated neutrophils after ConA administration, which is an important effect since neutrophils are the key initiators of lymphocyte recruitment and liver injury caused by ConA (89).

We used flavopiridol at 100 nM and in clinical studies in several tumor types, concentrations between 300 and 500 nM flavopiridol were achieved safely. Phase I/II trials with infusional flavopiridol in combination with standard chemotherapy identified the maximum tolerated doses using flavopiridol daily for 5, 3, and 1 consecutive days with 37.5, 50, and 62.5 mg/m² per day. Plasma flavopiridol concentrations achieved were in the range 1.5–3.5 μM (94).

TNF α has been clearly identified as central mediator of T cell activation-induced acute liver failure. TNF α directly mediates hepatocellular death but also induces the

expression of inflammatory proteins, such as cytokines and adhesion molecules. Hence, ConA injection results in a massive induction of ICAM-1, VCAM-1, and E-selectin in the liver (95). E-selectin is activated by cytokines and initiates neutrophil recruitment in sepsis-induced lung injury (96). We found decreased levels of the cell adhesion molecules ICAM-1 and E-selectin, which may explain the underlying mechanisms for the protective effect of flavopiridol on the ConA-induced liver injury.

5.1.2 Flavopiridol reduces leukocyte-endothelium interactions *in vivo*

For the first time flavopiridol is used in a model of activated cremaster muscle venules, which admits the direct intravital observation of the microcirculation in the cremaster muscle and therefore adhesion and transmigration of leukocytes on the endothelium (97). Leukocytes are recruited locally at the site of inflammation in a series of adhesive steps before transendothelial migration through the interstitial tissue (22). TNF α represents one of the archetypal pro-inflammatory cytokines which is rapidly released upon tissue injury or infection (98). We could show that flavopiridol reduces adherence and transmigration of leukocytes on/through the TNF α -activated endothelium *in vivo*.

The participation of ICAM-1 is relevant for leukocyte crawling *in vivo* (99) and leukocyte crawling is reported as a distinct postarrest step during leukocyte recruitment affecting almost all adherent leukocytes on activated venular endothelium (100). Flavopiridol has a strong influence on the endothelium because of the significant reduction of the ICAM-1 mRNA levels and the leukocyte-endothelium interactions involved.

5.1.3 Flavopiridol reduces leukocyte-endothelium interactions *in vitro*

Studies on flavopiridol in nuclear run-on assays revealed, that 10, 30, and 100 nM have very little effect on global cellular transcription. A totally different result was obtained when cells were treated with 300 nM flavopiridol. Total transcription was dramatically inhibited (64). *In vitro*, we used in our experiments low dosed flavopiridol at 100 nM which is well tolerated by endothelial cells as proven by DNA fragmentation and metabolic activity of the HUVECs. Low dosed flavopiridol allows us to exclude severe effects on cell viability or global transcription.

Neutrophil recruitment at sites of infection or tissue injury is tightly regulated by coordinated expression of adhesion molecules on both neutrophils (e.g. CD11b) and endothelial cells (e.g. ICAM-1, VCAM-1, and E-selectin) and production of cytokines/chemokines (17).

On endothelial cells, flavopiridol reduces in a concentration dependent manner the TNF α -induced upregulation of ICAM-1, VCAM-1, and E-selectin cell surface expression. This result is in accordance with the reduction of adhesion of neutrophils on a TNF α -activated HUVEC monolayer. The impact of flavopiridol on transcriptional regulation of ICAM-1 strongly suggests that flavopiridol interferes already with the transcriptional control of inflammatory proteins.

Although we did not find an effect with flavopiridol on the white blood cell count and the motility of interstitially migrating leukocytes in the cremaster muscle model, *in vitro* flavopiridol has an impact on the CD11b expression. However, the influence of flavopiridol on the CD11b expression on the cell surface of neutrophils is not concentration-dependent. These results suggest that the impact of flavopiridol on leukocytes is not the decisive step in the leukocyte-endothelium interactions discovered *in vivo* and *in vitro*. The inflammatory response encompasses both the production of cytokines and proinflammatory oxidants produced by neutrophils and macrophages. The production of these reactive oxygen species (ROS) is accompanied by a transient increase in oxygen consumption by the cells, called the respiratory burst (101). Polyphenol substances are known to act as potent antioxidants (102). The basic structure of flavopiridol is a polyphenol, therefore we studied the effect of flavopiridol on ROS production. Examination of respiratory burst activity of neutrophils revealed that flavopiridol does not simply act as a ROS scavenger.

Further studies on the underlying mechanisms of flavopiridol-mediated effects on neutrophils might be interesting to establish a concluding statement about the function of flavopiridol on neutrophils.

5.2 The underlying mechanisms of the anti-inflammatory properties of flavopiridol

Previous studies with flavopiridol primarily addressed its effects on diseases linked to several hematologic and solid cancers, like chronic lymphocytic leukemia (103). Furthermore a function on the HIV Tat protein was reported, thus proposing a possible role for flavopiridol in anti-HIV-1 therapy (104).

Hitherto, the association of flavopiridol with inflammatory processes was suggested in two *in vivo* models: flavopiridol is effective in

- 1) treatment of collagen-induced arthritis in mice with suppression of synovial hyperplasia and joint destruction (10) and
- 2) suppression of hepatic acute phase response proteins by disruption of IL-6 signaling in hepatocarcinoma cells (11).

However, the anti-inflammatory mechanisms of action remain unknown.

We showed that treatment with low-dosed flavopiridol decreased cytokine-induced expression of adhesion molecules on protein and mRNA levels at primary endothelial cells, which allowed us to investigate the actions of flavopiridol on endothelial cells in detail. To get insights into the mechanisms causing the anti-inflammatory effects of flavopiridol, we analyzed the underlying molecular pathways of TNF α -induced ICAM-1 regulation.

5.2.1 Flavopiridol has no effect on the NF- κ B activation cascade

Besides its extensive role in regulating the immune response, NF- κ B signaling is critical for the development of various diseases, especially inflammatory diseases and tumors. Thus, the NF- κ B signaling pathway is in the focus for research on pharmacological interventions and numerous therapeutic agents that inhibit either activation or function of NF- κ B (105, 106).

For our work, NF- κ B attracted attention because it is a key regulator of inflammatory responses and NF- κ B sites in the ICAM-1 promoter play an important role in its gene expression (107, 108).

Interestingly, Takada and Aggarwal have shown that flavopiridol suppressed TNF α -induced activation of NF- κ B in a dose and time-dependent manner in several cancer cell lines (Jurkats, A293, HL60), with optimum inhibition occurring upon treatment of

cells with 100 nM flavopiridol for eight hours. The inhibition of NF- κ B activity was linked to suppression of IKK α/β activation, inhibition of I κ B α degradation, blocking of p65 phosphorylation, p65 nuclear translocation, and NF- κ B-dependent reporter gene transcription. Subsequently, they suggested, that flavopiridol inhibited the activation of the proinflammatory transcription factor NF- κ B and NF- κ B-regulated gene expression which could direct flavopiridol to suppress inflammation (12).

However, in endothelial cells short-time preincubation of 100 nM flavopiridol decreased TNF α -induced NF- κ B promoter activity, but had no influence on NF- κ B activation. In HUVECs, TNF α -activated phosphorylation of IKK α/β is not diminished by flavopiridol, as well as phosphorylation and therefore activation of I κ B α . Activation of p65 occurs at several phosphorylation sites, PKAc and MSK1 are known to phosphorylate Ser276, whereas CK2 and IKK α/β phosphorylate Ser529 and Ser536, respectively (39, 109). Moreover, flavopiridol has no influence on the TNF α -activated phosphorylation sites Ser276 and Ser529 (data not shown) as well as Ser536.

After gaining access to the nucleus, NF- κ B must be actively regulated to execute its fundamental function as a transcription factor. Recent studies have highlighted the importance of nuclear signaling in the regulation of NF- κ B transcriptional activity (105). We could demonstrate that flavopiridol does not affect DNA-binding activity of NF- κ B, verified by electro mobility shift assay (EMSA). The EMSA confirms that flavopiridol does not affect the presence of NF- κ B in the nucleus, although a conclusion about transcriptional regulation is not possible, which shows that these data are not inconsistent with the elucidated inhibition of NF- κ B reporter gene expression.

Nevertheless, these data suggest, that the anti-inflammatory effects of flavopiridol in HUVECs are not caused via inhibition of NF- κ B activation.

5.2.2 Flavopiridol affects LIMK1, CK2, JNK, and PKC θ

We performed a global approach via PepChip with flavopiridol-treated HUVECs to gain more insights on the effects of flavopiridol on cellular signaling.

PepChip kinome array is a research tool to investigate the impact of a compound on overall kinase activities in the cellular context using cell lysates. The PepChip array offers proof of both the direct and indirect actions of the respective compound on

kinase activities involved in signal transduction pathways and kinase substrate-dependent interactions (110). This array was supposed to reveal influences of flavopiridol on signaling pathways with relevance to inflammation and to identify a mechanism of action of flavopiridol.

Analyzing kinome profiles of HUVECs treated with flavopiridol identified several involved kinases and revealed four kinases, which are reduced most in their activity: LIMK1, CK2, JNK, and PKC θ .

5.2.3 LIMK1, CK2, JNK, and PKC θ do not influence inflammatory actions

One strategy in the search for anti-inflammatory agents is the analysis of the suppression of individual inflammatory genes or gene products, or specific subsets of genes. In the development of anti-inflammatory drugs little progress has been made toward the goal of modulating the transcription of specific subsets of proinflammatory genes (111). For our work, a major interest was to investigate the interaction of flavopiridol and selective regulation of inflammatory events, in particular the regulation of inducible proinflammatory genes. To figure out whether the kinases, LIMK1, CK2, JNK, and PKC θ revealed by PepChip data, are involved in inflammatory actions, we investigated their effect on the proinflammatory gene ICAM-1.

An important kinase promoting microtubule stability and actin polymerization in human endothelial cells is LIMK1 (112). Genetic deletion of LIMK1 decreased neutrophil infiltration in mouse lungs and was efficacious to decrease ocular inflammation (113, 114). We tested the role of LIMK1 in the regulation of ICAM-1 expression and found that LIMK1 is not involved in inflammatory processes related to ICAM-1.

CK2 is supposed to play an important role in the regulation of expression of genes implicated in inflammation through the control of NF- κ B (115). Already Singh and Ramji (2008) deliberated whether CK2 could be an important regulator of the inflammatory response (115). The specific CK2 inhibitors, TBB and quinalizarin, have no influence on TNF α -upregulated ICAM-1 expression in HUVECs. Although the data of the PepChip suggest a link between CK2 and flavopiridol we also did not identify

an influence of flavopiridol on the CK2 dependent phosphorylation site Ser529 of NF- κ B (data not shown).

Inflammatory cytokines have been shown to stimulate adhesion molecule expression in endothelial cells, in part, by stimulating c-Jun N-terminal kinase (JNK) (116). On HUVECs, the JNK inhibitor SP600125 is approved to exclude unspecific kinase effects at a concentration of 10 μ M (117). By applying SP600125 at a concentration of 10 μ M we discovered no effect on the TNF α -induced ICAM-1 upregulation.

Activation of the PKC/NF- κ B signaling pathway was found to play a major role in the transcriptional induction of the ICAM-1 gene (28). In particular PKC θ plays a key role in T cell activation, proliferation and cytokine production as well as specific activation of AP-1 and NF- κ B (118). No data exists about the function of PKC θ in inflammatory events in endothelial cells. With a PKC θ -selective inhibitor, we found that PKC θ did not alter the TNF α -induced ICAM-1 levels.

5.3 Cdks in inflammation-induced processes

Cdks were initially identified as key components of the cell cycle machinery, but subsequently they have been shown to play roles in cell differentiation, transcription, and inflammation (119). Recent reviews present strong links between cancer and inflammation and that Cdk inhibition plays a key role due to accelerated inflammatory resolution by promoting apoptosis. Currently, the role of Cdks in the resolution of inflammation are unclear but a number of studies have been launched (8).

Interestingly, an IC₅₀ profiling revealed flavopiridol in low concentrations primarily as a Cdk inhibitor. It is noteworthy that concentrations of 100 nM flavopiridol were not sufficient for inhibitory effects on kinases like CK2, IKK β , JNK1, or PKC θ . To gain information about the responsible actions for the strong inhibition of TNF α -induced ICAM-1 levels (IC₅₀ = 27 nM), we were interested in activities of flavopiridol at low nanomolar concentrations. Only a few Cdks were sensitive to flavopiridol in the 1-100 nM range: Cdk4, Cdk6, Cdk8, and Cdk9.

5.3.1 Cdk4 and 6 in inflammation-induced processes

A study evaluated how systemic administration of flavopiridol and a Cdk4/6 selective inhibitor exerted an antiarthritic effect by suppressing proliferation of synovial fibroblasts in collagen-induced arthritis in mice. The results argue that flavopiridol exerted its effects primarily by Cdk4/6 inhibition (10). By using fascaplysin, a Cdk4/6 inhibitor, we have shown for the first time that Cdk4 and 6 are not involved in affecting ICAM-1 levels activated by TNF α . Although reports exist, which predict Cdk4 and 6 to be involved in inflammatory adhesion and cytokine production (120, 121) our data do not support the validation of these assumptions in endothelial cells.

5.3.2 Cdk8 in inflammation-induced processes

Another interesting Cdk emerging from the kinase profiling of flavopiridol is Cdk8, which has been characterized mostly as a transcriptional repressor (122). In comparison with other Cdks little data are known about Cdk8. Recently, Cdk8 was demonstrated to be a positive regulator of AP-1 and early growth response family of oncogenic transcription factors (123). No data exist concerning a link between Cdk8 and inflammation.

We investigated TNF α -activated HUVECs deficient in Cdk8 for ICAM-1 expression. The finding of an increase of ICAM-1 expression in HUVECs, in the absence of Cdk8, excludes Cdk8 as a potential target in anti-inflammatory processes. Cdk8 and its activator cyclin C are components of the RNAPII holoenzyme, where they function as a negative regulator of transcription, resulting in suppression of transcription (124). Thus, it is possible that inhibition of Cdk8 might result in abolishment of suppression of transcription leading to an increase of ICAM-1 expression.

5.3.3 The importance of Cdk9 in inflammation

Already Hou et al (2007) concluded that inhibition of Cdk9 could be a potential therapeutic strategy for inflammatory disease because of the disruption of IL-6 signaling (11).

P-TEFb, a heterodimer of Cdk9 and cyclin T1, is widely implicated in the control of basal gene expression (125). Especially for the P-TEFb complex, flavopiridol showed a strong inhibition in our IC₅₀ profiling with an IC₅₀ value of 4.9 nM. Flavopiridol is the

most potent P-TEFb inhibitor currently identified and exhibits about tenfold selectivity towards P-TEFb compared to other Cdks (126). Disruption of P-TEFb function by the Cdk-inhibitor DRB (5,6-Dichloro-1- β -D-ribofuranosylbenzimidazole) selectively blocked TNF α stimulation of IL-8 mRNA production (127). Most but not all RNA Pol II transcription is sensitive to P-TEFb inhibitors flavopiridol and DRB (128). HUVECs with silenced Cdk9 show strongly decreased ICAM-1 protein and mRNA levels (data not shown). Thus, our results show that Cdk9 is necessary for cytokine-dependent upregulation of ICAM-1. Therefore, we conclude that the anti-inflammatory effect of flavopiridol is primarily achieved by an inhibitory effect on Cdk9.

Caldwell et al. (2006) reported that dnCdk9 repressed the mannose receptor and BMPR2 promoter constructs, but had no effect on the COX-2 promoter in macrophages, implying that Cdk9 does not support transcription of all macrophage genes (129). Therefore it seems plausible that some genes are much less sensitive to pharmacological inhibition of Cdk9 and that the sensitivity may be also cell-type specific (130).

5.3.4 Complexity of gene regulatory network: P-TEFb and NF- κ B

What process is responsible for the decreased NF- κ B promoter activity by flavopiridol?

NF- κ B activates its downstream target genes by pleiotropic mechanisms (131) and interestingly, the complexity of gene regulatory network showed that NF- κ B activation is regulated by Cdks (132). Cdks were found to regulate transcriptional activation by NF- κ B through interactions with the co-activator p300. Nissen and Yamamoto (2000) showed that P-TEFb is differentially recruited to two NF- κ B regulated promoters indicating that P-TEFb is not a global co-regulator of NF- κ B, but appears to be recruited to only a subset of RelA/p50 response elements (133). Recently, it was discovered that a subset of genes, *Gro β* and *IL-8*, were absolutely dependent on phospho-p65 (Ser276) and Cdk9, but others, *I κ B α* , were not. These data suggest that P-TEFb is involved in the activation of a subset of NF- κ B-dependent genes whose mechanism of activation involves Pol II recruitment (125). Baumli et al. (2008) reported that some genes are much less sensitive to pharmacological inhibition of Cdk9 and that the sensitivity may be also cell-type specific (130). In agreement with

these data we show that the recovering and therefore the transcription of I κ B α is not impaired by treatment with low dosed flavopiridol in endothelial cells.

NF- κ B is needed to enhance the efficiency of transcription elongation and pre-mRNA processing (134). In fact, inducible factors, such as NF- κ B, promote acetylation of histones at lysine residues which are then recognized by the protein Brd4. Brd4 recruits P-TEFb, which promotes elongation and pre-mRNA processing by its ability to phosphorylate the C-terminal domain of RNA polymerase II (135). This assumption requires a decrease of functional NF- κ B in the nucleus which results in less acetylation of histones. In our experiments we could show that although the amount of translocated NF- κ B and the NF- κ B DNA-binding activity is not altered the expression of the NF- κ B-dependent gene, *ICAM-1*, is decreased, suggesting that inhibition of Cdk9 is sufficient to reduce *ICAM-1* gene expression.

5.4 Conclusion

In conclusion, the results presented here demonstrate that flavopiridol protects against inflammation-induced endothelial activation *in vivo* and *in vitro*.

For the first time, we investigated the anti-inflammatory potential of flavopiridol on endothelial cells. Flavopiridol inhibits TNF α -induced NF- κ B-dependent gene expression, but did not affect the NF- κ B activation cascade. We found an association between Cdk9 and inflammatory events in endothelial cells. Our findings suggest the inhibition of Cdk9-dependent gene expression as underlying mechanism for the anti-inflammatory effects of flavopiridol.

In conclusion, this study highlights flavopiridol as a novel, promising anti-inflammatory agent, which might reach clinical relevance for the treatment of inflammatory diseases.

6 Summary

Previous studies with flavopiridol primarily addressed its effects on diseases linked to several hematologic and solid cancers, like chronic lymphocytic leukemia (103). Recent reviews present strong links between cancer and inflammation and that Cdk inhibition plays a key role in the resolution of inflammation (8, 119).

Based on these considerations, we hypothesized that flavopiridol could exhibit an anti-inflammatory potential. In a ConA-induced liver injury, flavopiridol greatly suppressed the attenuated levels of transaminases and strongly reduced the infiltration of neutrophils in hepatic tissue. Moreover, ConA injection results in a massive induction of ICAM-1 and E-selectin levels in the liver, which were as well inhibited by flavopiridol. In a second *in vivo* model, flavopiridol significantly reduced leukocyte adhesion and transmigration in TNF α -activated cremaster muscle venules. *In vitro*, we used in our experiments low dosed flavopiridol at 100 nM which is well tolerated by endothelial cells and allows us to exclude severe effects on cell viability and global transcription.

In HUVECs, flavopiridol inhibited cytokine-induced upregulation of cell adhesion molecules and suppressed NF- κ B-dependent gene expression. However, flavopiridol has no effect on the activation of I κ B kinase, on the phosphorylation of I κ B α , and on the nuclear translocation of p65. Taken together, our studies strongly suggest that the anti-inflammatory actions of flavopiridol in endothelial cells are not likely to involve the TNF α -induced activation cascade of NF- κ B.

To gain information about the kinase activities of flavopiridol we performed a kinome array (PepChip) and a kinase panel (IC₅₀ profiling). The kinome array revealed a possible association between the kinases LIMK1, JNK, CK2, and PKC θ and the signaling pathways of flavopiridol. Further investigations showed no correlation between these kinases and inflammatory actions, therefore we conclude that the anti-inflammatory effects of flavopiridol are not caused by LIMK1, JNK, CK2, or PKC θ in endothelial cells. The IC₅₀ profiling highlighted flavopiridol in low concentrations primarily as a Cdk inhibitor and interestingly we found an association between Cdk9 and inflammatory events in endothelial cells.

Therefore we conclude that the anti-inflammatory effect of flavopiridol is primarily achieved by inhibitory effects on Cdk9.

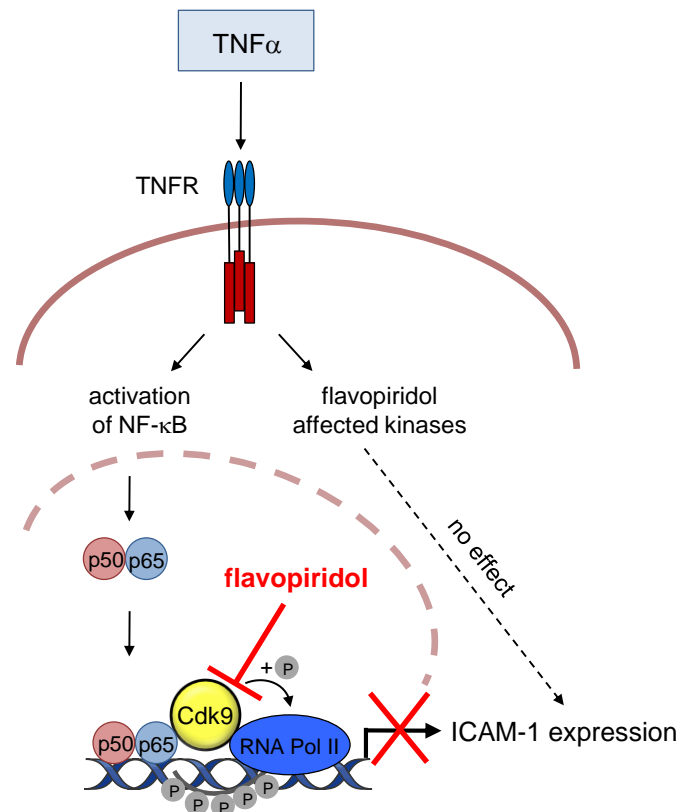


Figure 6.1: Importance of flavopiridol in inflammatory events in endothelial cells.

Upon stimulating endothelial cells with TNF α , NF- κ B translocates from the cytoplasm to the nucleus. There, it binds to its response elements and recruits P-TEFb (Cdk9-cyclin T). The ability of Cdk9 to phosphorylate the C-terminal domain of RNA Pol II stimulates inflammatory gene expression. Flavopiridol inhibits cytokine-induced inflammatory gene expression. Investigations of the underlying mechanisms revealed that the effects are independent of NF- κ B activation and other kinases which are affected by flavopiridol, but due to a strong inhibition of Cdk9.

In summary, we could show for the first time that flavopiridol exerts anti-inflammatory actions and abrogates inflammatory induced leukocyte-endothelium interactions *in vivo* and *in vitro*. We can highlight flavopiridol as a novel, promising anti-inflammatory agent, which might reach clinical relevance for the treatment of inflammatory diseases. Furthermore we revealed Cdk9 as a target with good prospects in inflammatory events.

7 References

1. Galley, H. F., and Webster, N. R. (2004) Physiology of the endothelium. *Br J Anaesth* **93**, 105-113
2. Esper, R. J., Nordaby, R. A., Vilarino, J. O., Paragano, A., Cacharron, J. L., and Machado, R. A. (2006) Endothelial dysfunction: a comprehensive appraisal. *Cardiovasc Diabetol* **5**, 4
3. Lawrence, T., and Gilroy, D. W. (2007) Chronic inflammation: a failure of resolution? *Int J Exp Pathol* **88**, 85-94
4. Senderowicz, A. M. (1999) Flavopiridol: the first cyclin-dependent kinase inhibitor in human clinical trials. *Invest New Drugs* **17**, 313-320
5. Kelland, L. R. (2000) Flavopiridol, the first cyclin-dependent kinase inhibitor to enter the clinic: current status. *Expert Opin Investig Drugs* **9**, 2903-2911
6. Sedlacek, H. H. (2001) Mechanisms of action of flavopiridol. *Crit Rev Oncol Hematol* **38**, 139-170
7. Kouroukis, C. T., Belch, A., Crump, M., Eisenhauer, E., Gascoyne, R. D., Meyer, R., Lohmann, R., Lopez, P., Powers, J., Turner, R., and Connors, J. M. (2003) Flavopiridol in untreated or relapsed mantle-cell lymphoma: results of a phase II study of the National Cancer Institute of Canada Clinical Trials Group. *J Clin Oncol* **21**, 1740-1745
8. Leitch, A. E., Haslett, C., and Rossi, A. G. (2009) Cyclin-dependent kinase inhibitor drugs as potential novel anti-inflammatory and pro-resolution agents. *Br J Pharmacol* **158**, 1004-1016
9. Rossi, A. G., Sawatzky, D. A., Walker, A., Ward, C., Sheldrake, T. A., Riley, N. A., Caldicott, A., Martinez-Losa, M., Walker, T. R., Duffin, R., Gray, M., Crescenzi, E., Martin, M. C., Brady, H. J., Savill, J. S., Dransfield, I., and Haslett, C. (2006) Cyclin-dependent kinase inhibitors enhance the resolution of inflammation by promoting inflammatory cell apoptosis. *Nat Med* **12**, 1056-1064
10. Sekine, C., Sugihara, T., Miyake, S., Hirai, H., Yoshida, M., Miyasaka, N., and Kohsaka, H. (2008) Successful treatment of animal models of rheumatoid arthritis with small-molecule cyclin-dependent kinase inhibitors. *J Immunol* **180**, 1954-1961
11. Hou, T., Ray, S., and Brasier, A. R. (2007) The functional role of an interleukin 6-inducible CDK9/STAT3 complex in human gamma-fibrinogen gene expression. *J Biol Chem* **282**, 37091-37102
12. Takada, Y., and Aggarwal, B. B. (2004) Flavopiridol inhibits NF-kappaB activation induced by various carcinogens and inflammatory agents through inhibition of I-kappaB kinase and p65 phosphorylation: abrogation of cyclin D1, cyclooxygenase-2, and matrix metalloproteinase-9. *J Biol Chem* **279**, 4750-4759
13. Pries, A. R., and Kuebler, W. M. (2006) Normal endothelium. *Handb Exp Pharmacol*, 1-40
14. Nathan, C., and Ding, A. (2010) Nonresolving inflammation. *Cell* **140**, 871-882
15. Pasyk, K. A., and Jakobczak, B. A. (2004) Vascular endothelium: recent advances. *Eur J Dermatol* **14**, 209-213
16. Muller, W. A. (2003) Leukocyte-endothelial-cell interactions in leukocyte transmigration and the inflammatory response. *Trends Immunol* **24**, 327-334
17. Ley, K., Laudanna, C., Cybulsky, M. I., and Nourshargh, S. (2007) Getting to the site of inflammation: the leukocyte adhesion cascade updated. *Nat Rev Immunol* **7**, 678-689
18. Kansas, G. S. (1996) Selectins and their ligands: current concepts and controversies. *Blood* **88**, 3259-3287

19. Dunne, J. L., Ballantyne, C. M., Beaudet, A. L., and Ley, K. (2002) Control of leukocyte rolling velocity in TNF-alpha-induced inflammation by LFA-1 and Mac-1. *Blood* **99**, 336-341
20. Campbell, J. J., Qin, S., Bacon, K. B., Mackay, C. R., and Butcher, E. C. (1996) Biology of chemokine and classical chemoattractant receptors: differential requirements for adhesion-triggering versus chemotactic responses in lymphoid cells. *J Cell Biol* **134**, 255-266
21. Campbell, J. J., Hedrick, J., Zlotnik, A., Siani, M. A., Thompson, D. A., and Butcher, E. C. (1998) Chemokines and the arrest of lymphocytes rolling under flow conditions. *Science* **279**, 381-384
22. Muller, W. A. (2009) Mechanisms of transendothelial migration of leukocytes. *Circ Res* **105**, 223-230
23. Ley, K. (2001) Functions of selectins. *Results Probl Cell Differ* **33**, 177-200
24. Ulbrich, H., Eriksson, E. E., and Lindbom, L. (2003) Leukocyte and endothelial cell adhesion molecules as targets for therapeutic interventions in inflammatory disease. *Trends Pharmacol Sci* **24**, 640-647
25. Takagi, J., and Springer, T. A. (2002) Integrin activation and structural rearrangement. *Immunol Rev* **186**, 141-163
26. Hood, J. D., and Cheresch, D. A. (2002) Role of integrins in cell invasion and migration. *Nat Rev Cancer* **2**, 91-100
27. Roebuck, K. A., and Finnegan, A. (1999) Regulation of intercellular adhesion molecule-1 (CD54) gene expression. *J Leukoc Biol* **66**, 876-888
28. Chen, C. C. (2006) Signal transduction pathways of inflammatory gene expressions and therapeutic implications. *Curr Pharm Des* **12**, 3497-3508
29. Li, Q., and Verma, I. M. (2002) NF-kappaB regulation in the immune system. *Nat Rev Immunol* **2**, 725-734
30. Bonizzi, G., and Karin, M. (2004) The two NF-kappaB activation pathways and their role in innate and adaptive immunity. *Trends Immunol* **25**, 280-288
31. Lenardo, M. J., and Baltimore, D. (1989) NF-kappa B: a pleiotropic mediator of inducible and tissue-specific gene control. *Cell* **58**, 227-229
32. Olivier, S., Robe, P., and Bours, V. (2006) Can NF-kappaB be a target for novel and efficient anti-cancer agents? *Biochem Pharmacol* **72**, 1054-1068
33. Ghosh, S., and Karin, M. (2002) Missing pieces in the NF-kappaB puzzle. *Cell* **109 Suppl**, S81-96
34. Chen, L. F., and Greene, W. C. (2004) Shaping the nuclear action of NF-kappaB. *Nat Rev Mol Cell Biol* **5**, 392-401
35. Zhong, H., Voll, R. E., and Ghosh, S. (1998) Phosphorylation of NF-kappa B p65 by PKA stimulates transcriptional activity by promoting a novel bivalent interaction with the coactivator CBP/p300. *Mol Cell* **1**, 661-671
36. Hayden, M. S., and Ghosh, S. (2008) Shared principles in NF-kappaB signaling. *Cell* **132**, 344-362
37. Morgan, D. O. (1995) Principles of CDK regulation. *Nature* **374**, 131-134
38. Meijer, L., and Raymond, E. (2003) Roscovitine and other purines as kinase inhibitors. From starfish oocytes to clinical trials. *Acc Chem Res* **36**, 417-425
39. Vermeulen, K., Van Bockstaele, D. R., and Berneman, Z. N. (2003) The cell cycle: a review of regulation, deregulation and therapeutic targets in cancer. *Cell Prolif* **36**, 131-149
40. Fisher, R. P. (2005) Secrets of a double agent: CDK7 in cell-cycle control and transcription. *J Cell Sci* **118**, 5171-5180
41. Devault, A., Martinez, A. M., Fesquet, D., Labbe, J. C., Morin, N., Tassan, J. P., Nigg, E. A., Cavadore, J. C., and Doree, M. (1995) MAT1 ('menage a trois')

- a new RING finger protein subunit stabilizing cyclin H-cdk7 complexes in starfish and *Xenopus* CAK. *EMBO J* **14**, 5027-5036
42. Wesierska-Gadek, J., and Krystof, V. (2009) Selective cyclin-dependent kinase inhibitors discriminating between cell cycle and transcriptional kinases: future reality or utopia? *Ann N Y Acad Sci* **1171**, 228-241
 43. Marshall, R. M., and Grana, X. (2006) Mechanisms controlling CDK9 activity. *Front Biosci* **11**, 2598-2613
 44. Fuda, N. J., Ardehali, M. B., and Lis, J. T. (2009) Defining mechanisms that regulate RNA polymerase II transcription in vivo. *Nature* **461**, 186-192
 45. Glover-Cutter, K., Larochele, S., Erickson, B., Zhang, C., Shokat, K., Fisher, R. P., and Bentley, D. L. (2009) TFIIH-associated Cdk7 kinase functions in phosphorylation of C-terminal domain Ser7 residues, promoter-proximal pausing, and termination by RNA polymerase II. *Mol Cell Biol* **29**, 5455-5464
 46. Li, Q., Price, J. P., Byers, S. A., Cheng, D., Peng, J., and Price, D. H. (2005) Analysis of the large inactive P-TEFb complex indicates that it contains one 7SK molecule, a dimer of HEXIM1 or HEXIM2, and two P-TEFb molecules containing Cdk9 phosphorylated at threonine 186. *J Biol Chem* **280**, 28819-28826
 47. Jang, M. K., Mochizuki, K., Zhou, M., Jeong, H. S., Brady, J. N., and Ozato, K. (2005) The bromodomain protein Brd4 is a positive regulatory component of P-TEFb and stimulates RNA polymerase II-dependent transcription. *Mol Cell* **19**, 523-534
 48. Marshall, N. F., Peng, J., Xie, Z., and Price, D. H. (1996) Control of RNA polymerase II elongation potential by a novel carboxyl-terminal domain kinase. *J Biol Chem* **271**, 27176-27183
 49. Bres, V., Yoh, S. M., and Jones, K. A. (2008) The multi-tasking P-TEFb complex. *Curr Opin Cell Biol* **20**, 334-340
 50. Michels, A. A., and Bensaude, O. (2008) RNA-driven cyclin-dependent kinase regulation: when CDK9/cyclin T subunits of P-TEFb meet their ribonucleoprotein partners. *Biotechnol J* **3**, 1022-1032
 51. Peterlin, B. M., and Price, D. H. (2006) Controlling the elongation phase of transcription with P-TEFb. *Mol Cell* **23**, 297-305
 52. Zhou, Q., and Yik, J. H. (2006) The Yin and Yang of P-TEFb regulation: implications for human immunodeficiency virus gene expression and global control of cell growth and differentiation. *Microbiol Mol Biol Rev* **70**, 646-659
 53. Sano, M., Abdellatif, M., Oh, H., Xie, M., Bagella, L., Giordano, A., Michael, L. H., DeMayo, F. J., and Schneider, M. D. (2002) Activation and function of cyclin T-Cdk9 (positive transcription elongation factor-b) in cardiac muscle-cell hypertrophy. *Nat Med* **8**, 1310-1317
 54. He, N., Jahchan, N. S., Hong, E., Li, Q., Bayfield, M. A., Maraia, R. J., Luo, K., and Zhou, Q. (2008) A La-related protein modulates 7SK snRNP integrity to suppress P-TEFb-dependent transcriptional elongation and tumorigenesis. *Mol Cell* **29**, 588-599
 55. Park, M. T., and Lee, S. J. (2003) Cell cycle and cancer. *J Biochem Mol Biol* **36**, 60-65
 56. Sharma, P. S., Sharma, R., and Tyagi, R. (2008) Inhibitors of cyclin dependent kinases: useful targets for cancer treatment. *Curr Cancer Drug Targets* **8**, 53-75
 57. Sherr, C. J., and Roberts, J. M. (1999) CDK inhibitors: positive and negative regulators of G1-phase progression. *Genes Dev* **13**, 1501-1512

58. Hall, M., and Peters, G. (1996) Genetic alterations of cyclins, cyclin-dependent kinases, and Cdk inhibitors in human cancer. *Adv Cancer Res* **68**, 67-108
59. Senderowicz, A. M. (2003) Small-molecule cyclin-dependent kinase modulators. *Oncogene* **22**, 6609-6620
60. Klasa, R. J., List, A. F., and Cheson, B. D. (2001) Rational approaches to design of therapeutics targeting molecular markers. *Hematology Am Soc Hematol Educ Program*, 443-462
61. Arguello, F., Alexander, M., Sterry, J. A., Tudor, G., Smith, E. M., Kalavar, N. T., Greene, J. F., Jr., Koss, W., Morgan, C. D., Stinson, S. F., Siford, T. J., Alvord, W. G., Klabansky, R. L., and Sausville, E. A. (1998) Flavopiridol induces apoptosis of normal lymphoid cells, causes immunosuppression, and has potent antitumor activity In vivo against human leukemia and lymphoma xenografts. *Blood* **91**, 2482-2490
62. De Azevedo, W. F., Jr., Mueller-Dieckmann, H. J., Schulze-Gahmen, U., Worland, P. J., Sausville, E., and Kim, S. H. (1996) Structural basis for specificity and potency of a flavonoid inhibitor of human CDK2, a cell cycle kinase. *Proc Natl Acad Sci U S A* **93**, 2735-2740
63. Chao, S. H., Fujinaga, K., Marion, J. E., Taube, R., Sausville, E. A., Senderowicz, A. M., Peterlin, B. M., and Price, D. H. (2000) Flavopiridol inhibits P-TEFb and blocks HIV-1 replication. *J Biol Chem* **275**, 28345-28348
64. Chao, S. H., and Price, D. H. (2001) Flavopiridol inactivates P-TEFb and blocks most RNA polymerase II transcription in vivo. *J Biol Chem* **276**, 31793-31799
65. Melillo, G., Sausville, E. A., Cloud, K., Lahusen, T., Varesio, L., and Senderowicz, A. M. (1999) Flavopiridol, a protein kinase inhibitor, down-regulates hypoxic induction of vascular endothelial growth factor expression in human monocytes. *Cancer Res* **59**, 5433-5437
66. Byrd, J. C., Shinn, C., Waselenko, J. K., Fuchs, E. J., Lehman, T. A., Nguyen, P. L., Flinn, I. W., Diehl, L. F., Sausville, E., and Grever, M. R. (1998) Flavopiridol induces apoptosis in chronic lymphocytic leukemia cells via activation of caspase-3 without evidence of bcl-2 modulation or dependence on functional p53. *Blood* **92**, 3804-3816
67. Decker, R. H., Dai, Y., and Grant, S. (2001) The cyclin-dependent kinase inhibitor flavopiridol induces apoptosis in human leukemia cells (U937) through the mitochondrial rather than the receptor-mediated pathway. *Cell Death Differ* **8**, 715-724
68. Schwartz, G. K., Ilson, D., Saltz, L., O'Reilly, E., Tong, W., Maslak, P., Werner, J., Perkins, P., Stoltz, M., and Kelsen, D. (2001) Phase II study of the cyclin-dependent kinase inhibitor flavopiridol administered to patients with advanced gastric carcinoma. *J Clin Oncol* **19**, 1985-1992
69. Shapiro, G. I., Supko, J. G., Patterson, A., Lynch, C., Lucca, J., Zaccarola, P. F., Muzikansky, A., Wright, J. J., Lynch, T. J., Jr., and Rollins, B. J. (2001) A phase II trial of the cyclin-dependent kinase inhibitor flavopiridol in patients with previously untreated stage IV non-small cell lung cancer. *Clin Cancer Res* **7**, 1590-1599
70. Fathi, A. T., Grant, S., and Karp, J. E. (2010) Exploiting cellular pathways to develop new treatment strategies for AML. *Cancer Treat Rev* **36**, 142-150
71. Byrd, J. C., Lin, T. S., Dalton, J. T., Wu, D., Phelps, M. A., Fischer, B., Moran, M., Blum, K. A., Rovin, B., Brooker-McEldowney, M., Broering, S., Schaaf, L. J., Johnson, A. J., Lucas, D. M., Heerema, N. A., Lozanski, G., Young, D. C., Suarez, J. R., Colevas, A. D., and Grever, M. R. (2007) Flavopiridol

- administered using a pharmacologically derived schedule is associated with marked clinical efficacy in refractory, genetically high-risk chronic lymphocytic leukemia. *Blood* **109**, 399-404
72. Christian, B. A., Grever, M. R., Byrd, J. C., and Lin, T. S. (2007) Flavopiridol in the treatment of chronic lymphocytic leukemia. *Curr Opin Oncol* **19**, 573-578
 73. Yang, X., Zhao, X., Phelps, M. A., Piao, L., Rozewski, D. M., Liu, Q., Lee, L. J., Marcucci, G., Grever, M. R., Byrd, J. C., Dalton, J. T., and Lee, R. J. (2009) A novel liposomal formulation of flavopiridol. *Int J Pharm* **365**, 170-174
 74. Schang, L. M. (2004) Effects of pharmacological cyclin-dependent kinase inhibitors on viral transcription and replication. *Biochim Biophys Acta* **1697**, 197-209
 75. Hallett, J. M., Leitch, A. E., Riley, N. A., Duffin, R., Haslett, C., and Rossi, A. G. (2008) Novel pharmacological strategies for driving inflammatory cell apoptosis and enhancing the resolution of inflammation. *Trends Pharmacol Sci* **29**, 250-257
 76. Jaffe, E. A., Nachman, R. L., Becker, C. G., and Minick, C. R. (1973) Culture of human endothelial cells derived from umbilical veins. Identification by morphologic and immunologic criteria. *J Clin Invest* **52**, 2745-2756
 77. Nicoletti, I., Migliorati, G., Pagliacci, M. C., Grignani, F., and Riccardi, C. (1991) A rapid and simple method for measuring thymocyte apoptosis by propidium iodide staining and flow cytometry. *J Immunol Methods* **139**, 271-279
 78. Bergmeyer, H. U. (1984) Methods of enzymatic analysis Vol. 82 pp. 416-456, Verlag Chemie, Weinheim
 79. Allan, G., Bhattacharjee, P., Brook, C. D., Read, N. G., and Parke, A. J. (1985) Myeloperoxidase activity as a quantitative marker of polymorphonuclear leukocyte accumulation into an experimental myocardial infarct--the effect of ibuprofen on infarct size and polymorphonuclear leukocyte accumulation. *J Cardiovasc Pharmacol* **7**, 1154-1160
 80. Mempel, T. R., Moser, C., Hutter, J., Kuebler, W. M., and Krombach, F. (2003) Visualization of leukocyte transendothelial and interstitial migration using reflected light oblique transillumination in intravital video microscopy. *J Vasc Res* **40**, 435-441
 81. Wegmann, F., Petri, B., Khandoga, A. G., Moser, C., Khandoga, A., Volkery, S., Li, H., Nasdala, I., Brandau, O., Fassler, R., Butz, S., Krombach, F., and Vestweber, D. (2006) ESAM supports neutrophil extravasation, activation of Rho, and VEGF-induced vascular permeability. *J Exp Med* **203**, 1671-1677
 82. Pfaffl, M. W. (2001) A new mathematical model for relative quantification in real-time RT-PCR. *Nucleic Acids Res* **29**, e45
 83. Smith, P. K., Krohn, R. I., Hermanson, G. T., Mallia, A. K., Gartner, F. H., Provenzano, M. D., Fujimoto, E. K., Goeke, N. M., Olson, B. J., and Klenk, D. C. (1985) Measurement of protein using bicinchoninic acid. *Anal Biochem* **150**, 76-85
 84. Laemmli, U. K. (1970) Cleavage of structural proteins during the assembly of the head of bacteriophage T4. *Nature* **227**, 680-685
 85. Bradford, M. M. (1976) A rapid and sensitive method for the quantitation of microgram quantities of protein utilizing the principle of protein-dye binding. *Anal Biochem* **72**, 248-254
 86. Diks, S. H., Kok, K., O'Toole, T., Hommes, D. W., van Dijken, P., Joore, J., and Peppelenbosch, M. P. (2004) Kinome profiling for studying

- lipopolysaccharide signal transduction in human peripheral blood mononuclear cells. *J Biol Chem* **279**, 49206-49213
87. van Baal, J. W., Diks, S. H., Wanders, R. J., Rygiel, A. M., Milano, F., Joore, J., Bergman, J. J., Peppelenbosch, M. P., and Krishnadath, K. K. (2006) Comparison of kinome profiles of Barrett's esophagus with normal squamous esophagus and normal gastric cardia. *Cancer Res* **66**, 11605-11612
 88. Xu, X., Wei, H., Dong, Z., Chen, Y., and Tian, Z. (2006) The differential effects of low dose and high dose concanavalin A on cytokine profile and their importance in liver injury. *Inflamm Res* **55**, 144-152
 89. Bonder, C. S., Ajuebor, M. N., Zbytniuk, L. D., Kubes, P., and Swain, M. G. (2004) Essential role for neutrophil recruitment to the liver in concanavalin A-induced hepatitis. *J Immunol* **172**, 45-53
 90. Jaeschke, H. (1997) Cellular adhesion molecules: regulation and functional significance in the pathogenesis of liver diseases. *Am J Physiol* **273**, G602-611
 91. Collins, T., Read, M. A., Neish, A. S., Whitley, M. Z., Thanos, D., and Maniatis, T. (1995) Transcriptional regulation of endothelial cell adhesion molecules: NF-kappa B and cytokine-inducible enhancers. *FASEB J* **9**, 899-909
 92. Flower, R. J. (1974) Drugs which inhibit prostaglandin biosynthesis. *Pharmacol Rev* **26**, 33-67
 93. Tiegs, G., Hentschel, J., and Wendel, A. (1992) A T cell-dependent experimental liver injury in mice inducible by concanavalin A. *J Clin Invest* **90**, 196-203
 94. Senderowicz, A. M. (2003) Novel direct and indirect cyclin-dependent kinase modulators for the prevention and treatment of human neoplasms. *Cancer Chemother Pharmacol* **52 Suppl 1**, S61-73
 95. Wolf, D., Hallmann, R., Sass, G., Sixt, M., Kusters, S., Fregien, B., Trautwein, C., and Tiegs, G. (2001) TNF-alpha-induced expression of adhesion molecules in the liver is under the control of TNFR1--relevance for concanavalin A-induced hepatitis. *J Immunol* **166**, 1300-1307
 96. Tsokos, M. (2003) Immunohistochemical detection of sepsis-induced lung injury in human autopsy material. *Leg Med (Tokyo)* **5**, 73-86
 97. Khandoga, A., Huettinger, S., Khandoga, A. G., Li, H., Butz, S., Jauch, K. W., Vestweber, D., and Krombach, F. (2009) Leukocyte transmigration in inflamed liver: A role for endothelial cell-selective adhesion molecule. *J Hepatol* **50**, 755-765
 98. Karin, M., Lawrence, T., and Nizet, V. (2006) Innate immunity gone awry: linking microbial infections to chronic inflammation and cancer. *Cell* **124**, 823-835
 99. Frommhold, D., Kamphues, A., Hepper, I., Pruenster, M., Lukic, I. K., Socher, I., Zablotskaya, V., Buschmann, K., Lange-Sperandio, B., Schymeinsky, J., Ryschich, E., Poeschl, J., Kupatt, C., Nawroth, P. P., Moser, M., Walzog, B., Bierhaus, A., and Sperandio, M. (2010) RAGE and ICAM-1 cooperate in mediating leukocyte recruitment during acute inflammation in vivo. *Blood*
 100. Phillipson, M., Heit, B., Colarusso, P., Liu, L., Ballantyne, C. M., and Kubes, P. (2006) Intraluminal crawling of neutrophils to emigration sites: a molecularly distinct process from adhesion in the recruitment cascade. *J Exp Med* **203**, 2569-2575
 101. D'Alessandro, T., Prasain, J., Benton, M. R., Botting, N., Moore, R., Darley-Usmar, V., Patel, R., and Barnes, S. (2003) Polyphenols, inflammatory

- response, and cancer prevention: chlorination of isoflavones by human neutrophils. *J Nutr* **133**, 3773S-3777S
102. Galati, G., Sabzevari, O., Wilson, J. X., and O'Brien, P. J. (2002) Prooxidant activity and cellular effects of the phenoxyl radicals of dietary flavonoids and other polyphenolics. *Toxicology* **177**, 91-104
103. Christian, B. A., Grever, M. R., Byrd, J. C., and Lin, T. S. (2009) Flavopiridol in chronic lymphocytic leukemia: a concise review. *Clin Lymphoma Myeloma* **9 Suppl 3**, S179-185
104. Canduri, F., Perez, P. C., Caceres, R. A., and de Azevedo, W. F., Jr. (2008) CDK9 a potential target for drug development. *Med Chem* **4**, 210-218
105. Wan, F., and Lenardo, M. J. (2010) The nuclear signaling of NF-kappaB: current knowledge, new insights, and future perspectives. *Cell Res* **20**, 24-33
106. Gilmore, T. D., and Herscovitch, M. (2006) Inhibitors of NF-kappaB signaling: 785 and counting. *Oncogene* **25**, 6887-6899
107. Ledebur, H. C., and Parks, T. P. (1995) Transcriptional regulation of the intercellular adhesion molecule-1 gene by inflammatory cytokines in human endothelial cells. Essential roles of a variant NF-kappa B site and p65 homodimers. *J Biol Chem* **270**, 933-943
108. Whitley, M. Z., Thanos, D., Read, M. A., Maniatis, T., and Collins, T. (1994) A striking similarity in the organization of the E-selectin and beta interferon gene promoters. *Mol Cell Biol* **14**, 6464-6475
109. Vermeulen, L., De Wilde, G., Van Damme, P., Vanden Berghe, W., and Haegeman, G. (2003) Transcriptional activation of the NF-kappaB p65 subunit by mitogen- and stress-activated protein kinase-1 (MSK1). *EMBO J* **22**, 1313-1324
110. Rothmeier, A. S., Ischenko, I., Joore, J., Garczarczyk, D., Fürst, R., Bruns, C. J., Vollmar, A. M., and Zahler, S. (2009) Investigation of the marine compound spongistatin 1 links the inhibition of PKCalpha translocation to nonmitotic effects of tubulin antagonism in angiogenesis. *FASEB J* **23**, 1127-1137
111. Smale, S. T. (2010) Selective transcription in response to an inflammatory stimulus. *Cell* **140**, 833-844
112. Gorovoy, M., Niu, J., Bernard, O., Profirovic, J., Minshall, R., Neamu, R., and Voyno-Yasenetskaya, T. (2005) LIM kinase 1 coordinates microtubule stability and actin polymerization in human endothelial cells. *J Biol Chem* **280**, 26533-26542
113. Gorovoy, M., Han, J., Pan, H., Welch, E., Neamu, R., Jia, Z., Predescu, D., Vogel, S., Minshall, R. D., Ye, R. D., Malik, A. B., and Voyno-Yasenetskaya, T. (2009) LIM kinase 1 promotes endothelial barrier disruption and neutrophil infiltration in mouse lungs. *Circ Res* **105**, 549-556
114. Gorovoy, M., Koga, T., Shen, X., Jia, Z., Yue, B. Y., and Voyno-Yasenetskaya, T. (2008) Downregulation of LIM kinase 1 suppresses ocular inflammation and fibrosis. *Mol Vis* **14**, 1951-1959
115. Singh, N. N., and Ramji, D. P. (2008) Protein kinase CK2, an important regulator of the inflammatory response? *J Mol Med* **86**, 887-897
116. Lerner-Marmarosh, N., Yoshizumi, M., Che, W., Surapisitchat, J., Kawakatsu, H., Akaike, M., Ding, B., Huang, Q., Yan, C., Berk, B. C., and Abe, J. (2003) Inhibition of tumor necrosis factor-[alpha]-induced SHP-2 phosphatase activity by shear stress: a mechanism to reduce endothelial inflammation. *Arterioscler Thromb Vasc Biol* **23**, 1775-1781
117. Fürst, R., Zahler, S., and Vollmar, A. M. (2008) Dexamethasone-induced expression of endothelial mitogen-activated protein kinase phosphatase-1

- involves activation of the transcription factors activator protein-1 and 3',5'-cyclic adenosine 5'-monophosphate response element-binding protein and the generation of reactive oxygen species. *Endocrinology* **149**, 3635-3642
118. Altman, A., and Villalba, M. (2002) Protein kinase C-theta (PKC theta): a key enzyme in T cell life and death. *J Biochem* **132**, 841-846
 119. Knockaert, M., Greengard, P., and Meijer, L. (2002) Pharmacological inhibitors of cyclin-dependent kinases. *Trends Pharmacol Sci* **23**, 417-425
 120. Nonomura, Y., Nagasaka, K., Hagiya, H., Sekine, C., Nanki, T., Tamamori-Adachi, M., Miyasaka, N., and Kohsaka, H. (2006) Direct modulation of rheumatoid inflammatory mediator expression in retinoblastoma protein-dependent and -independent pathways by cyclin-dependent kinase 4/6. *Arthritis Rheum* **54**, 2074-2083
 121. Liu, L., Schwartz, B., Tsubota, Y., Raines, E., Kiyokawa, H., Yonekawa, K., Harlan, J. M., and Schnapp, L. M. (2008) Cyclin-dependent kinase inhibitors block leukocyte adhesion and migration. *J Immunol* **180**, 1808-1817
 122. Elmlund, H., Baraznenok, V., Lindahl, M., Samuelsen, C. O., Koeck, P. J., Holmberg, S., Hebert, H., and Gustafsson, C. M. (2006) The cyclin-dependent kinase 8 module sterically blocks Mediator interactions with RNA polymerase II. *Proc Natl Acad Sci U S A* **103**, 15788-15793
 123. Donner, A. J., Ebmeier, C. C., Taatjes, D. J., and Espinosa, J. M. (2010) CDK8 is a positive regulator of transcriptional elongation within the serum response network. *Nat Struct Mol Biol* **17**, 194-201
 124. Tassan, J. P., Jaquenoud, M., Leopold, P., Schultz, S. J., and Nigg, E. A. (1995) Identification of human cyclin-dependent kinase 8, a putative protein kinase partner for cyclin C. *Proc Natl Acad Sci U S A* **92**, 8871-8875
 125. Brasier, A. R. (2008) Expanding role of cyclin dependent kinases in cytokine inducible gene expression. *Cell Cycle* **7**, 2661-2666
 126. Wang, S., and Fischer, P. M. (2008) Cyclin-dependent kinase 9: a key transcriptional regulator and potential drug target in oncology, virology and cardiology. *Trends Pharmacol Sci* **29**, 302-313
 127. Luecke, H. F., and Yamamoto, K. R. (2005) The glucocorticoid receptor blocks P-TEFb recruitment by NFkappaB to effect promoter-specific transcriptional repression. *Genes Dev* **19**, 1116-1127
 128. Medlin, J. E., Uguen, P., Taylor, A., Bentley, D. L., and Murphy, S. (2003) The C-terminal domain of pol II and a DRB-sensitive kinase are required for 3' processing of U2 snRNA. *EMBO J* **22**, 925-934
 129. Caldwell, R. L., Lane, K. B., and Shepherd, V. L. (2006) HIV-1 Tat interaction with cyclin T1 represses mannose receptor and the bone morphogenetic protein receptor-2 transcription. *Arch Biochem Biophys* **449**, 27-33
 130. Meinhart, A., Kamenski, T., Hoepfner, S., Baumli, S., and Cramer, P. (2005) A structural perspective of CTD function. *Genes Dev* **19**, 1401-1415
 131. Nowak, D. E., Tian, B., Jamaluddin, M., Boldogh, I., Vergara, L. A., Choudhary, S., and Brasier, A. R. (2008) RelA Ser276 phosphorylation is required for activation of a subset of NF-kappaB-dependent genes by recruiting cyclin-dependent kinase 9/cyclin T1 complexes. *Mol Cell Biol* **28**, 3623-3638
 132. Perkins, N. D., Felzien, L. K., Betts, J. C., Leung, K., Beach, D. H., and Nabel, G. J. (1997) Regulation of NF-kappaB by cyclin-dependent kinases associated with the p300 coactivator. *Science* **275**, 523-527

133. Nissen, R. M., and Yamamoto, K. R. (2000) The glucocorticoid receptor inhibits NFkappaB by interfering with serine-2 phosphorylation of the RNA polymerase II carboxy-terminal domain. *Genes Dev* **14**, 2314-2329
134. Amir-Zilberstein, L., Ainbinder, E., Toubé, L., Yamaguchi, Y., Handa, H., and Dikstein, R. (2007) Differential regulation of NF-kappaB by elongation factors is determined by core promoter type. *Mol Cell Biol* **27**, 5246-5259
135. Hargreaves, D. C., Horng, T., and Medzhitov, R. (2009) Control of inducible gene expression by signal-dependent transcriptional elongation. *Cell* **138**, 129-145

8 Appendix

8.1 Abbreviations

ANOVA	Analysis of variance between groups
AP-1	Activator protein 1
AML	Acute myelogenous leukemia
APS	Ammonium persulfate
ATP	Adenosine -5'- triphosphate
BSA	Bovine serum albumin
CAK	Cdk-activating kinase
CAM	Cell adhesion molecule
CAPS	3-(Cyclohexylamino)-1-propanesulfonic acid
Cdk	Cyclin dependent kinase
CKI	Cdk inhibitor
CLL	Chronic lymphocytic leukemia
ConA	Concanavalin A
CTD	C-terminal domain
DHR	Dihydrorhodamine
DNA	Deoxyribonucleic acid
DRB	5,6-Dichloro-1- β -D-ribofuranosylbenzimidazole
DTT	Dithiothreitol
ECGM	Endothelial cell growth medium
ECL	Enhanced chemiluminescence
ECM	Extracellular matrix
ECs	Endothelial cells
EDTA	Ethylenediaminetetraacetic acid
EGTA	Ethylene glycol-bis(2-aminoethylether) tetraacetic acid
ELISA	Enzyme-linked immunosorbent assay
ER	Endoplasmatic reticulum
FACS	Fluorescence-activated cell sorter
FCS	Fetal calf serum
FL	Fluorescence
FP	Flavopiridol
FSC	Forward scatter
GAPDH	Glycerin aldehyde 3 phosphate dehydrogenase

GTP/GDP	Guanosine-5'-tri/diphosphate
h	Hour(s)
H&E	Hematoxylin and eosin
HEPES	N-(2-hydroxyethyl)piperazine-N'-(2-ethanesulfonic acid)
HIV-1	Human immune deficiency virus 1
HRP	Horseradish peroxidase
HUVEC	Human umbilical vein endothelial cell
ICAM-1	Intercellular adhesion molecule 1
i.p.	intraperitoneal
IVM	Intravital microscopy
JAM	Junctional adhesion molecule
kDa	Kilo Dalton
LFA1	Lymphocyte function-associated antigen 1
LIMK1	LIM kinase 1
Mac-1	Macrophage antigen 1
MAPK	Mitogen-activated protein kinase
mRNA	Messenger RNA
NCI	National Cancer Institute
NF- κ B	Nuclear factor-kappa B
nt	Non-targeting
p-	Phospho-
PAA	Polyacrylamide
PBS	Phosphate buffered saline
PBS-T	Phosphate buffered saline with Tween
PCR	Polymerase chain reaction
PI	Propidium iodide
PIPES	Piperazine-1,4-bis(2-ethanesulfonic acid)
PKC	Protein kinase C
PMN	Polymorphonuclear leukocyte
PMSF	Phenylmethylsulphonylfluoride
qRT-PCR	Quantitative real-time polymerase chain reaction
RIPA	Radio Immuno Precipitation Assay
RNA	Ribonucleic acid

ROS	Reactive oxygen species
SDS	Sodium dodecyl sulfate
SDS-PAGE	Sodium dodecyl sulfate polyacrylamide gel electrophoresis
SEM	Standard error of mean
Ser	Serine
shRNA	Short hairpin RNA
siRNA	Small interfering RNA
T/E	Trypsin/EDTA
TEMED	N,N, N' N' tetramethylethylene diamine
TNF α	Tumor necrosis factor α
Tris	Trishydroxymethylaminomethane
VCAM-1	Vascular cell-adhesion molecule 1
VEGF	Vascular Endothelial Growth Factor

8.2 Publications

8.2.1 Original publication

Ulrike K. Schmerwitz, Gabriele Sass, Alexander G. Khandoga, Jos Joore, Bettina A. Mayer, Nina Berberich, Frank Totzke, Fritz Krombach, Gisa Tiegs, Stefan Zahler, Angelika M. Vollmar, Robert Fürst

Flavopiridol protects against inflammation via Cdk9

(2010) in preparation

8.2.2 Oral communication

Ulrike Schmerwitz, Alexander G. Khandoga, Bettina A. Mayer, Nina Berberich, Fritz Krombach, Stefan Zahler, Angelika M. Vollmar, Robert Fürst

Novel effects of the Cdk inhibitor flavopiridol: restraint of leukocyte-endothelial cell interactions by downregulation of endothelial cell adhesion molecules

50. Jahrestagung der Deutschen Gesellschaft für Pharmakologie und Toxikologie, 10-12 March 2009, Mainz, Germany. Naunyn Schmiedeberg's Arch Pharmacol. 2009; 379 Suppl 1:39

Ulrike Schmerwitz

Novel aspects of the Cdk inhibitor flavopiridol

Interdisziplinäres Doktorandenseminar

(15. Januar 2009, Ludwig-Maximilians-University, Munich, Germany)

8.3 Curriculum vitae

PERSONAL DATA

Name	Ulrike Karla Ilse Schmerwitz
Date of Birth	December 31 st , 1981
Place of Birth	Leipzig
Marital status	Single
Nationality	German

Ph.D.

01/07 – 06/10	Ludwig-Maximilians-University, Munich Department of Pharmaceutical Biology Chair: Prof. Dr. Angelika M. Vollmar
---------------	---

EDUCATION

11/06	Degree as pharmacist, Regensburg
10/00 – 10/05	Study of pharmacy at the University of Regensburg, Regensburg <ul style="list-style-type: none"> • 11/06: 3rd state examination • 10/05: 2nd state examination • 03/03: 1st state examination
10/03 – 02/04	TENOVUS, Welsh School of Pharmacy, Cardiff, UK Project: “Effects of EGFR tyrosine kinase inhibitor on the motility related proteins in prostate cancer cell lines”
09/92 – 07/00	Wilhelm-Ostwald-Schule, secondary school, Leipzig
09/90 – 07/92	Pablo-Neruda-Schule, primary school, Leipzig
09/88 – 07/90	Erich-Weinert-Schule, primary school, Leipzig

WORK EXPERIENCE

Since 01/07	Implerapotheke, Munich
05/06 – 10/06	Bienen Apotheke OHG, Munich
11/05 – 04/06	Merz Pharmaceuticals GmbH, Frankfurt/M.

8.4 Acknowledgements

First and foremost, I would like to thank Prof. Dr. Angelika M. Vollmar for giving me the opportunity to perform my Ph.D. studies in her laboratories. Her expert and excellent supervision and mentorship were a constant incentive to me. I am seriously grateful to Dr. Robert Fürst for his permanent professional and skilful supports throughout this work. I want to thank PD Dr. Stefan Zahler for his strong intellectual support and experience.

The encouragement and inspiring discussions of these three persons mentioned above were outstanding helpful and motivating for the successful creation of this work. Thank you!

Further I would like to thank all members of the thesis committee. Special thanks go to Prof. Dr. Christian Wahl-Schott for his time and effort as second advisor for this thesis.

I would like to thank the National Cancer Institut (NCI) for providing flavopiridol. Special thanks go to PD Dr. Gabriele Sass and Prof. Dr. Gisa Tiegs for their collaboration in the concanavalin A induced liver injury model, to Dr. Alexander Khandoga and Prof. Dr. Fritz Krombach for their collaboration in the cremaster muscle model, to Dr. Jos Joore for performing PepChip analysis, and to Dr. Frank Totzke for his support in the ³³PanQinase[®] Activity Assay.

I would especially like to thank all my colleagues and lab members for their helpfulness and warm and friendly atmosphere. For the good times we spent in “our box”, numerous discussions, helpful advices and friendship I want to thank Nina. I would also like to express my gratitude to the entire technical staff, in particular Jana and Bianca for helpful technical assistance and personal support. Gratitude goes as well to Dr. Johanna Liebl and Dr. Robert Fürst for proof-reading the manuscript.

I want to use this opportunity to thank all the voluntary blood donors!

I am especially indebted to my family, my friends and my boyfriend Bolko who gave me encouragement and strength to work during the last years. I am sincerely grateful for their blessings and constant moral support!